

Molecular determinants for the subcellular distribution of the synapto-nuclear protein messenger Jacob

**Der Fakultät für Naturwissenschaften
der Otto-von-Guericke-Universität Magdeburg
zur Erlangung des akademischen Grades**

**doctor rerum naturalium
(Dr. rer. nat.)**

am: 15.10.2009

eingereichte Dissertation,

vorgelegt von: MSc. (Molecular Biology) Jale Şahin

Molecular determinants for the subcellular distribution of the synapto-nuclear protein messenger Jacob

Dissertation

zur Erlangung des akademischen Grades

doctor rerum naturalium

(Dr. rer. nat.)

**Genehmigt durch die Fakultät für Naturwissenschaften
der Otto-von-Guericke-Universität Magdeburg**

von Msc. Jale Şahin

Geb am. 30.04.1979 in Ankara, Turke

Gutachter: Prof. Dr. Eckart D. Gundelfinger

Prof. Dr. Britta Qualmann

Eingereicht am: 15.10.2009

Verteidigt am: 15.02.2010

To my mother, Sevinç Şahin.

“The truth is rarely pure and never simple.”

Oscar Wilde

Acknowledgements

This thesis is a result of almost four years of work at the Leibniz Institute for Neurobiology, Magdeburg in the group of Michael R. Kreutz (Project Group Neuroplasticity) and it is supported by graduate school, DFG-Graduiertenkolleg 1167: "Zell-Zell-Kommunikation in Nerven- und Immunsystem: Topologische Organisation von Signalwegen". Here, I would like to express my gratitude and thanks to my colleagues, friends and family for their endless support and help.

First of all, I would like to thank to my supervisor, Dr. Michael R. Kreutz for his constant support and patience. I sincerely appreciate his help and suggestions.

I want to address my special thanks to my second supervisor Prof. Oliver Stork for his help and encouragement.

I am grateful to Dr. Karl-Heinz Smalla for having time for me and helping me to solve the technical problems I had.

I owe special thanks to Dr. Peter Landgraf for being a good friend. The discussions we had and his suggestions were very helpful.

My appreciation goes to Dr. Anna Karpova and Marina Mikhaylova, for their help in this work and friendship.

I am grateful to Dr. Christina Spilker for reading this thesis carefully and her suggestions and also to Dr. Daniela C. Dieterich for her helpful comments.

My many thanks to Prof. Eckart D. Gundelfinger and Prof. Michael Naumann for their guidance and support.

I would like to thank to my colleagues in the GRK1167, Neuroplasticity Group for the nice atmosphere they provide in the last four years.

My special thanks goes to Corinna Borutzki, Monika Marunde and Stefanie Hochmuth for providing us always a clean and organized working place, their technical help and friendship.

Many thanks to all people working in the Department of Neurochemistry and Molecular Biology at the IfN for their technical support and friendship.

I owe special thanks to my friends Nicole Reichenbach, Holger Lison, Christoph Möller, Ayse Ozge Sungur and Miriam Happel for their valuable support.

I am particularly grateful to my very good friend Mehmet Büge, for his constant support and optimism that gave me strength and courage to continue. I also want to thank to my devoted friend Zekiye Engez for her love and encouragement.

I would like to thank to my dad, Mehmet Şahin who always had and will have a great influence in whatever I do something useful.

Finally, I would like to express my deepest appreciation to my mum, Sevinç Şahin, my best friend and sister Şule Şahin and my brother Tolgahan Şahin. Whatever I have achieved in my life would not be possible without their love and support.

Erklärung

Hiermit erkläre ich, dass ich die von mir eingereichte Dissertation zum dem Thema **”Molecular determinants for the subcellular distribution of the synaptonuclear protein messenger Jacob ”** selbständig verfasst, nicht schon als Dissertation verwendet habe und die benutzten Hilfsmittel und Quellen vollständig angegeben wurden.

Weiterhin erkläre ich, dass ich weder diese noch eine andere Arbeit zur Erlangung des akademischen Grades doctor rerum naturalium (Dr. rer. nat.) an anderen Einrichtungen eingereicht habe.

(Ort, Datum)

(Jale Şahin)

Index

| | |
|---|-----------|
| Summary | 10 |
| 1. Introduction | 13 |
| 1.1 Synapse to nucleus communication | 13 |
| 1.1.1 Activity-dependent synapse to nucleus signaling | 13 |
| 1.1.2 Activity-dependent cAMP-responsive element-binding protein (CREB)-mediated gene transcription | 14 |
| 1.1.3 Activity-dependent retrograde transport mechanisms | 15 |
| 1.1.4 Jacob shuttles to the nucleus after NMDA receptor activation | 17 |
| 1.2 Neuronal cytoskeleton: moderator of the subcellular distribution of proteins | 20 |
| 1.2.1 Intermediate filaments | 20 |
| 1.2.1.1 α -Internexin | 21 |
| 1.2.1.2 Intermediate filaments are involved in signal transduction pathways | 23 |
| 1.3 Calpain-mediated proteolysis in neurons | 25 |
| 1.4 Objectives | 27 |
| 2. Materials and Methods | 28 |
| 2.1 Materials | 28 |
| 2.1.1 Chemicals | 28 |
| 2.1.2 Antibodies | 28 |
| 2.1.2.1 Primary antibodies | 28 |
| 2.1.2.2 Secondary antibodies | 29 |
| 2.1.3 Bacterial and yeast media | 29 |
| 2.1.4 Animals | 30 |
| 2.2 Methods | 30 |
| 2.2.1 Molecular biology | 30 |
| 2.2.1.1 Polymerase chain reaction (PCR) | 30 |
| 2.2.1.2 Restriction enzyme digestion | 31 |
| 2.2.1.3 Agarose gel electrophoresis and isolation of DNA fragments from agarose gel | 31 |
| 2.2.1.4 Cloning of DNA fragments into a specific plasmid vector | 32 |
| 2.2.1.5 Transformation into electrocompetent bacteria E.coli XL1- blue MRF | 32 |
| 2.2.1.6 Amplification of plasmid DNA (mini, midi and maxi preparations) | 32 |
| 2.2.1.7 Production of expression constructs | 33 |
| 2.2.1.8 Yeast two hybrid (Y2H) system | 33 |
| 2.2.1.8.1 Transformation by LiAc/ SS-carrier DNA/ PEG | 34 |
| 2.2.1.8.1.1 Preparation of the competent yeast cells | 34 |
| 2.2.1.8.1.2 Transformation of the plasmids into the competent yeast cells | 34 |
| 2.2.2 Biochemical methods | 35 |
| 2.2.2.1 Protein concentration determination | 35 |
| 2.2.2.2 Sodium dodecyl sulfate- polyacrylamide gel electrophoresis (SDS-PAGE) | 35 |
| 2.2.2.3 Western blotting (immunoblotting) | 36 |
| 2.2.2.4 Expression and purification of protein fused to maltose binding protein (MBP) | 36 |
| 2.2.2.4.1 Induction of MBP-fusion protein | 37 |

| | |
|---|----|
| 2.2.2.4.2 Purification of MBP-fusion protein | 37 |
| 2.2.2.5 Homogenization and subcellular fractionation of rat brain and extraction of protein from rat brain tissue | 37 |
| 2.2.2.5.1 Homogenization of rat brain tissue and extraction of proteins from S1 fraction | 37 |
| 2.2.2.6 Subcellular fractionation of postsynaptic density (PSD) | 38 |
| 2.2.2.7 Protein extraction from transfected HEK 293 and COS7 cell lines | 39 |
| 2.2.2.8 Pull-down assays | 39 |
| 2.2.2.9 Co-immunoprecipitation (Co-IP) experiments | 40 |
| 2.2.2.9.1 Co-IP Performed by using protein extracts of S1 rat brain fraction | 40 |
| 2.2.2.9.2 Heterologous Co-IP performed by using the protein extracts of transfected HEK 293 and COS7 cell lines | 40 |
| 2.2.2.10 Calpain cleavage of Jacob <i>in vitro</i> | 41 |
| 2.2.3 Cell culture | 41 |
| 2.2.3.1 Culturing and transfection of HEK 293 and COS7 cell lines | 41 |
| 2.2.3.2 Primary cultures | 42 |
| 2.2.3.2.1 Hippocampal primary neuronal culture preparation | 42 |
| 2.2.3.2.2 Transfection of hippocampal primary cultures | 43 |
| 2.2.3.2.3 Immunocytochemistry | 43 |
| 2.2.3.2.4 Stimulation of hippocampal primary cultures | 44 |
| 2.2.3.2.5 Quantitative immunocytochemistry | 44 |
| 2.2.4 Statistical Analysis | 45 |
| 3. Results | 46 |
| 3.1 Jacob interacts with α-Internexin | 46 |
| 3.1.1 Subcellular distribution of Jacob in neurons | 46 |
| 3.1.2 Distribution of α -Internexin immunoreactivity in subcellular fractions of rat brain | 47 |
| 3.1.3 Subcellular distribution of α -Internexin in cultured hippocampal primary neurons | 48 |
| 3.1.3.1 α -Internexin does not localize at synapses of hippocampal primary neurons | 50 |
| 3.1.4 Jacob and α -Internexin co-localize in the soma and dendrites of hippocampal primary neurons | 51 |
| 3.1.5 Characterization of the Jacob- α -Internexin interaction | 53 |
| 3.1.5.1 Biochemical characterization of the Jacob- α -Internexin interaction | 53 |
| 3.1.5.2 Molecular characterization of the Jacob- α -Internexin interaction | 55 |
| 3.1.5.2.1 α -Internexin possesses potential Calpain cleavage sites | 55 |
| 3.1.5.2.2 Mapping the Jacob- α -Internexin binding region using the yeast two-hybrid system | 57 |
| 3.1.5.2.3 α -Internexin is cleaved by Calpain <i>in vitro</i> | 59 |
| 3.1.6 α -Internexin does not accumulate in the nucleus after NMDA receptor activation | 60 |
| 3.1.7 Full-length α -Internexin does not co-immunoprecipitate with Dynein intermediate chain, Importin- α 1 or Importin- β 1 in S1 fraction of adult rat brain tissue | 62 |
| 3.1.8 α -Internexin and Importin- β 1 do not co-localize in hippocampal primary neurons after NMDA bath application | 63 |

| | |
|--|------------|
| 3.2 Jacob-induced PSD-like protrusions are preferentially formed in discontinuities of α-Internexin immunostaining | 65 |
| 3.2.1 Co-over-expression of GFP- α -Internexin-wt abolishes the formation of Δ exon9-Jacob-Myc-induced PSD-like protrusions in transfected hippocampal primary neurons | 67 |
| 3.2.2 The presence or absence of α -Internexin has no influence on the formation of synapses in hippocampal primary neurons | 68 |
| 3.2.3 Possible molecular mechanisms underlying the formation of Jacob-induced PSD-like protrusions | 70 |
| 3.2.3.1 Biochemical characterization of Jacob homo-dimer formation | 70 |
| 3.2.3.2 Mapping of Jacob's dimerization sequence | 72 |
| 3.2.4 Possible effects of phosphorylation of Jacob at serine 180 on Jacob homo-dimer formation | 73 |
| 3.3.4.1 Phospho-mimicking (S180D) and non-phospho (S180A) forms of Jacob are found in the same immune complex as wt-Jacob | 73 |
| 3.3.4.2 EGF stimulation of HEK 293 cells enhanced Jacob homo-dimer formation | 75 |
| 3.3 Activity-dependent Calpain-mediated N-terminal truncation of Jacob is required for its nuclear translocation | 76 |
| 3.3.1 Nuclear transport of Jacob is blocked in hippocampal primary cultures after NMDA stimulation in the presence of Calpain inhibitors | 76 |
| 3.3.2 Nuclear trafficking of Jacob from distal dendrites is prevented in hippocampal primary cultures after NMDA stimulation in the presence of the Calpain inhibitor calpeptin | 78 |
| 3.3.3 Jacob is cleaved by Calpain <i>in vitro</i> | 79 |
| 4. Discussion | 81 |
| 4.1 The α-Internexin-Jacob interaction | 82 |
| 4.1.1 α -Internexin is a potential docking site for Jacob in the somato-dendritic compartment of neurons of rat brain | 82 |
| 4.1.2 The possible roles of α -Internexin in retrograde transport of Jacob after NMDA-receptor activation | 84 |
| 4.1.3 The presence of α -Internexin has a negative influence on the formation of Jacob induced PSD-like protrusions in rat hippocampal primary neurons | 87 |
| 4.2 Identification of the Jacob dimerization sequence | 88 |
| 4.2.1 The role of ERK kinase phosphorylation at serine 180 in Jacob homo-dimer formation | 89 |
| 4.3 N-terminal truncation of Jacob by Calpain is a prerequisite for its nuclear translocation after NMDA receptor activation in rat hippocampal primary neurons | 90 |
| 4.4 Concluding remarks | 91 |
| 5. References | 93 |
| 6. Supplementary information | 101 |
| 7. Abbreviations | 109 |

Curriculum Vitae
Scientific publications

Summary

Jacob is a novel PSD protein component identified as an interaction partner of the neuronal calcium sensor protein Caldendrin in rat brain. Similar to Caldendrin, Jacob is found in the PSD, and somato-dendritic compartments of neurons, but different from Caldendrin it is also found in neuronal nuclei. It was previously shown by our lab that after stimulation of N-methyl-D-aspartate (NMDA) receptors, Jacob translocates to the nucleus resulting in a rapid stripping of synaptic contacts and a drastically altered morphology of the dendritic tree. Nuclear translocation of Jacob from distal dendrites requires the classical Importin pathway and is mediated by Importin- α binding to nuclear localization signal (NLS) of Jacob. The NLS sequence of Jacob is located in the central α -helical region of the protein and includes an incomplete IQ domain- a region for Caldendrin binding. At elevated calcium (Ca^{2+}) levels Caldendrin controls extranuclear localization of Jacob by competing with Importin- α binding. Under high Ca^{2+} concentrations, which can only be achieved by activation of synaptic NMDA receptor activation, Caldendrin binds to the IQ domain of Jacob, masks the NLS sequence and subsequent Importin- α binding, thereby prevents the nuclear translocation of Jacob. In addition N-myristoylation of Jacob, which attaches the protein to membranous structures in the cell, is another way to regulate the extranuclear localization of Jacob.

In this PhD thesis further determinants for the subcellular distribution of Jacob and its transport to the nucleus were investigated. In the first part of the thesis, the interaction of Jacob with a neurofilament protein, α -Internexin was characterized. Furthermore, α -Internexin was proposed to provide a docking site for Jacob in the somato-dendritic compartment of neurons. In order to test this hypothesis, the Jacob- α -Internexin interaction was further characterized and found that α -Internexin possesses two different interaction sites for Jacob.

Over-expression of extranuclear Jacob in young hippocampal primary neurons results in the formation of huge dendritic PSD-like protrusions. These protrusions can recruit various Jacob-interaction partners and PSD components. In the second part of the thesis, mechanisms of how Jacob induces dendritic protrusions and recruitment of other proteins into these protrusions were addressed. It was shown that α -Internexin is not found in these protrusions. Instead it has a negative influence on the formation of these processes. It was also shown before by our lab that Jacob can form homo-dimers. Here, it was asked whether Jacob dimers, potentially oligomers, can initiate the formation of these processes. Prior to investigate this hypothesis, Jacob dimer formation was investigated in detail and the minimal dimerization sequence was identified.

As noted before, Jacob is N-myristoylated and has to be cut-off from the N-terminus, prior to its nuclear translocation after NMDA receptor activation. Therefore, at last, mechanisms of how Jacob is released from the docking sites were addressed. Role of Calpain, a cysteine protease, in N-terminal truncation and subsequent nuclear trafficking of Jacob were investigated. It was shown that nuclear translocation of endogenous Jacob is blocked after NMDA stimulation in the presence of Calpain inhibitors *in vitro*. Furthermore, *in vivo* results indicate that translocation of green-fluorescent-protein (GFP)-tagged wt-Jacob from distal dendrites of transfected neurons is completely attenuated after NMDA bath application in the presence of a Calpain inhibitor. Finally, *in vitro* Calpain cleavage assays revealed that Jacob is a novel Calpain substrate in neurons.

Zusammenfassung

Jacob ist ein neues Mitglied der PSD-Proteine und wurde als Interaktionspartner des neuronalen Kalzium-Sensorproteins Caldendrin im Rattenhirn identifiziert. Ähnlich wie Caldendrin ist Jacob in der PSD und im somato-dendritischen Kompartiment von Neuronen lokalisiert, befindet sich darüber hinaus aber zusätzlich in deren Zellkernen. Bereits in früheren Untersuchungen wurde durch unser Labor gezeigt, dass nach Stimulation des N-Methyl-D-Aspartat (NMDA) Rezeptors eine Translokation von Jacob in den Zellkern stattfindet, was eine sehr schnelle Reduzierung synaptischer Kontakte zur Folge hat und zu einer drastischen, morphologischen Veränderung dendritischer Fortsätze führt. Die Translokation von Jacob aus den distalen Bereichen der Dendriten in den Zellkern verläuft über den klassischen „Importin-Pathway“ und wird durch eine Bindung von Importin- α an das Kernlokalisierungssignal (nuclear localization signal, NLS) von Jacob vermittelt. Die NLS-Sequenz von Jacob befindet sich in der zentralen α -helikalen Region des Proteins, welche außerdem eine unvollständige IQ-Domäne, den Bereich für die Caldendrin-Bindung, enthält. In Abhängigkeit von der jeweiligen Kalzium- (Ca^{2+}) Konzentrationen kontrolliert Caldendrin die Lokalisation Jacobs außerhalb des Zellkerns, indem es kompetitiv die Bindung an Importin- α verhindert. Bei hohen Ca^{2+} -Konzentrationen, welche nur durch Aktivierung synaptischer NMDA-Rezeptoren erreicht werden können, bindet Caldendrin an die IQ-Domäne von Jacob, maskiert die NLS-Bindungsstelle und verhindert somit durch Blockierung der Importin- α -Bindung den Kerntransport von Jacob. Zusätzlich stellt die N-Myristoylierung von Jacob, welche das Protein an Membranstrukturen der Zelle bindet, einen weiteren Weg zur Regulation der Lokalisation von Jacob außerhalb des Zellkerns dar.

Die vorgelegte Doktorarbeit beschäftigt sich mit der Untersuchung weiterer Determinanten, die die subzelluläre Verteilung von Jacob und seinen Transport in den Zellkern beeinflussen. Im ersten Teil dieser Arbeit wurde erstmalig die Interaktion zwischen α -Internexin, einem Protein des Neurofilaments und Jacob nachgewiesen und charakterisiert. In diesem Zusammenhang wurde vorgeschlagen, dass α -Internexin eine Bindungsstelle für Jacob im somato-dendritischen Kompartiment von Neuronen darstellt. Um diese Hypothese zu überprüfen, wurde die Jacob- α -Internexin-Interaktion detaillierter charakterisiert, mit dem Resultat, dass α -Internexin offensichtlich über zwei Bindungsdomänen für Jacob verfügt. Überexpression von Jacob Δ NLS in jungen Primärneuronen des Hippokampus führt in den Dendriten zu einer Bildung großer, PSD-artiger Protrusionen. In diese können verschiedene Jacob-Interaktionspartner und PSD-Komponenten rekrutiert werden. Der zweite Teil dieser Arbeit beschäftigte sich mit der Frage, durch welche Mechanismen Jacob die Entstehung von Protrusionen induziert sowie andere Proteine in diesen Bereich rekrutiert. α -Internexin selbst konnte nicht in den Protrusionen nachgewiesen werden. Anstatt dessen scheint es die Bildung dieser Bereiche negativ zu beeinflussen. Da in unserem Labor auch gezeigt werden konnte, dass Jacob Homodimere bildet, wurde in diesem Zusammenhang zusätzlich untersucht, ob Jacob-Dimere (möglicherweise auch Oligomere) die Bildung der Protrusionen initiieren können. Zur Überprüfung dieser Hypothese wurde die Jacob-Dimer-Bildung detaillierter analysiert und die kleinste erforderliche Dimerisierungssequenz identifiziert.

Wie eingangs beschrieben, ist Jacob N-myristoyliert und muss vom N-Terminus gespalten werden, bevor dessen Translokation durch Aktivierung des NMDA-Rezeptors

stattfinden kann. Abschließend wurden daher Mechanismen untersucht, in deren Folge Jacob von den jeweiligen Bindungsstellen freigesetzt wird. Die Rolle von Calpain, einer Cystein-Protease, bei der Spaltung des N-Terminus sowie anschließendem Kerntransport von Jacob stand dabei im Mittelpunkt weiterer Untersuchungen. Dabei konnte gezeigt werden, dass der Kerntransport von endogenem Jacob nach Stimulation durch NMDA in Gegenwart von Calpain-Inhibitoren blockiert wurde. Darüberhinaus zeigen Ergebnisse von Experimenten *in vivo*, dass die Translokation von „green-fluorescent-protein“ (GFP)-markiertem Jacob-wt in distalen Dendriten transfizierter Neurone nach NMDA-Applikation vollständig durch die Gegenwart eines Calpain-Inhibitors verhindert wird. Letztendlich konnte durch Spaltungs-Assays mit Calpain *in vitro*, erstmalig Jacob als dessen Substrat innerhalb von Neuronen beschrieben werden.

1. Introduction

The human brain consists of billions of neurons that establish a complex network of cell-to-cell communication during neuronal development and throughout adulthood. The intercellular communication which enables the transfer of information from one part of the nervous system to another is the basis for proper brain function. For this purpose, neurons have evolved a unique and highly specialized structure called the synapse. The term “synapse” is derived from the Greek word “synaptein” meaning union or association. In order to understand how the brain works, it is crucial to understand the structure and function of synapses. It has been shown that neuronal activity results in long-term changes in synaptic strength via synaptic plasticity, a process that results in changes of synaptic function depending on the incoming signal. Regulation of gene expression after synaptic activity is an important component of synaptic plasticity and is known to be part of the basis for the storage of information, namely, learning and memory formation, in the mammalian brain.

1.1 Synapse to nucleus communication

1.1.1 Activity-dependent synapse to nucleus signaling

Long-lasting changes in neuronal excitability and synapto-dendritic cytoarchitecture require gene transcription, and it is thought that synaptic activity by itself triggers signaling pathways to the nucleus that will eventually control transcriptional regulation. Signaling from the synapse to the nucleus might therefore directly control the making of proteins involved in processes broadly referred to as synaptic plasticity. At present, relatively little is known about the exact role of plasticity-related genes and how their expression is regulated at the cellular level. Moreover, it is largely unclear how this process affects synaptic transmission and whether there is any specific feedback between the nucleus and activated synapses that drive transcriptional regulation. These questions carry critical importance for understanding how the wiring of the brain is brought about during development and how long-term, use-dependent changes of synaptic efficacy are mediated at the molecular level. In general, incoming signals are carried to the nucleus via two different signaling pathways: one is mediated by Ca^{2+} -ion as the principal messenger, and the other is driven by synapto-nuclear protein messengers (Jordan and Kreutz, 2009). In the first pathway, the Ca^{2+} ion is itself considered as the key regulator of plasticity-related

gene expression (Hardingham *et al.*, 2001). It has been shown that stimulation of NMDA receptors, L-type voltage dependent calcium channels (VDCC) can increase the dendritic Ca^{2+} levels which in turn are integrated in the soma by yet unknown mechanisms (Bito and Takemoto-Kimura, 2003). On the other hand, the second way in which the signal is carried by a synapto-nuclear protein messenger is proposed to be considerably slower (Jordan and Kreutz, 2009). In principle, these synapto-nuclear protein messengers are translocated to the nucleus in response to synaptic Ca^{2+} influx and in the end involved in the regulation of nuclear gene transcription. In an activated synapse, the initial Ca^{2+} influx is generated by either NMDA receptors and L-type VDCC or as a consequence of action potential propagation, those in turn induce secondary responses in the endoplasmic reticulum (ER) and the Golgi complex resulting in an increase in the Ca^{2+} levels and enable the Ca^{2+} ion spread throughout the neuron and eventually reaches to nucleus and involve in various transcription events which result in growth, cell survival, synaptic and neuronal plasticity (Yeckel *et al.*, 2007)

1.1.2 Activity-dependent cAMP-responsive element-binding protein (CREB)-mediated gene transcription

CREB-dependent gene transcription induced by neuronal activity has been shown to be important for synaptic plasticity, neuronal survival, learning, and memory formation (Bailey *et al.*, 1996; Silva *et al.*, 1998; Ahn *et al.*, 2000). Two calcium-regulated signaling pathways – the mitogen-activated protein kinase (MAPK)/extracellular signal-regulated kinase (ERK1/2) cascade (Ginty *et al.*, 1994; Impey *et al.*, 1994; Chawla *et al.*, 1998), and the calcium/calmodulin (CaM)-dependent protein kinase cascade, specifically the activation of the nuclear CaM kinase IV – can cause phosphorylation of CREB on serine 133, which renders the protein transcriptionally active (Sheng *et al.*, 1991; Matthews *et al.*, 1994). Activated or phosphorylated CREB (pCREB) is involved in the transcriptional regulation of genes that are controlled by CRE elements. Many of these genes have been shown to be involved in neuronal survival and plasticity, e.g., BDNF, Fos, Jun, CAMK IV (Sassone-Corsi *et al.*, 1995; Shieh *et al.*, 1998; Tao *et al.*, 1998).

It has been shown that NMDA-receptor- induced calcium influx results in the phosphorylation of CREB at serine 133 in immature neurons and the dephosphorylation of CREB at the same residue in mature neurons (Sala *et al.*, 2000). This discrepancy of

NMDA receptor function comes from the fact that, during development, a switch in the NMDA receptor subunit composition occurs. It is proposed that in immature neurons, NMDA receptor stimulation activates the CREB-dependent gene expression because there is a relative lack of phosphatase activity during early development, and the phosphorylation of CREB at serine 133 is persistent (Sala *et al.*, 2000). Moreover, Hardingham *et al.* (2002) shed more light on this matter by demonstrating that synaptic and extra-synaptic NMDA receptors have opposing effects on CREB-dependent gene transcription and neuronal fate. Thus, it has been shown that in hippocampal neurons there are two functionally distinct NMDA receptor signaling pathways (Hardingham *et al.*, 2002). Using different stimulation protocols, Hardingham *et al.* (2002) revealed that the synaptic stimulation of the NMDA receptor complex containing NR2B subunit initiates phosphorylation of nuclear CREB and induces BDNF gene expression which results in cell survival and growth. However, extra-synaptic stimulation of the NMDA receptor complex containing the NR2B subunit has been shown to activate the CREB shut-off pathway which results in dephosphorylation of CREB at serine 133, the blocking of BDNF gene expression, mitochondrial dysfunction, and subsequent neuronal cell death (Hardingham *et al.*, 2002).

1.1.3 Activity-dependent retrograde transport mechanisms

The identity of the carrier molecule(s) transmitting the signals to the nucleus and their retrograde transport mechanisms are important aspects of activity-dependent synapse-to-nucleus communication. It has been shown that many types of synaptic stimulation induce depolarization and electrochemical signaling as well as rapidly alter transcription in the nucleus (Deisseroth *et al.*, 2003). However, as mentioned above, studies have also revealed a slower retrograde transport mechanism which results in more specific gene transcription events, involving the transport of soluble molecules from stimulated synapses to the nucleus (Otis *et al.*, 2006; Heusner *et al.*, 2008; Jordan and Kreutz, 2009). Furthermore, recently it has been demonstrated that many components of synaptic junctions show a nuclear localization upon synaptic stimulation, suggesting that they may shuttle between synaptic and nuclear compartments after synaptic activity. Several of these proteins have been found to possess a Nuclear Localization Signal (NLS), and it has also been shown that nuclear transport of some of

these proteins requires the active nuclear import pathway driven by Importins (Hanz *et al.*, 2003; Thompson *et al.*, 2004; Jordan and Kreutz, 2009).

In the classical Importin pathway, the nuclear import adaptor molecule Importin- α binds to its cargo via NLS. Importin- β binds to the Importin- α -cargo complex and facilitates transport across the nuclear pore. In the nucleus, the small GTP-binding protein Ran (RanGTP) dissociates the heterotrimeric complex by interacting with Importin- β . Finally, Importin- α and - β are separately shuttled back out into the cytoplasm (Otis *et al.*, 2006). In addition to the role of Importins in the transport of cargo through the nuclear pore, in neurons, they have also been implicated in the transport of signals from distal processes to the soma and into the nucleus (Hanz *et al.*, 2003; Thompson *et al.*, 2004; Perlson *et al.*, 2005; Dieterich *et al.*, 2008). Further, in rodent hippocampal and Aplysia sensory neurons, it has been shown that during activity-dependent synaptic plasticity, Importins translocate from distal dendrites to the nucleus (Thompson *et al.*, 2004). In the same paper, it was shown that in dissociated rodent hippocampal neuronal cultures, NMDA receptor stimulation was the trigger for the translocation of Importins from the dendrites to the nucleus (Thompson *et al.*, 2004).

Moreover, Hanz *et al.* (2003) characterized the interaction between Importin- α and the Dynein motor complex in the motor neuron axon (Hanz *et al.*, 2003). Additionally, Perlson *et al.* (2005) described the interaction between Vimentin and Importin- β 1 by showing that Vimentin serves to couple Importin- β 1 bound to phosphorylated MAPK to the Dynein motor complex (Perlson *et al.*, 2005). Since the transport mechanism involves Importins, interaction with the cargo occurs via the binding of Importin- α to the NLS sequence of the cargo protein. Other NLS sequence-bearing proteins transported via Importin-mediated nuclear transport during activity-dependent signaling are: The nuclear factor-kappa b (NF- κ B) (Meffert *et al.*, 2003; Mikenberg *et al.*, 2007), and nuclear factor-activated T-cells (NFATc4) (Graef *et al.*, 1999; Groth *et al.*, 2003). In summary, the finding that Importin- α localizes to synapses and translocates to the nucleus after synaptic stimulation suggest that synapse-to-nucleus trafficking of NLS-containing cargoes might underlie long-term synaptic plasticity in the adult brain (Thompson *et al.*, 2004).

1.1.4 Jacob shuttles to the nucleus after NMDA receptor activation

As outlined above, activity-dependent synaptic plasticity requires Ca^{2+} ion-dependent signaling from dendrites to the nucleus (Kreutz *et al.*, 2006). The ubiquitously expressed Ca^{2+} sensor protein Calmodulin (CaM) is found to be the major mediator that triggers synapto-dendritic Ca^{2+} transients to downstream effectors (Kreutz *et al.*, 2006). However, recent studies revealed that there are many other neuronal Ca^{2+} sensor (NCS) proteins that are suggested to serve more specific functions in neuronal cells (Braunewell and Gundelfinger, 1999; Burgoyne and Weiss, 2001; Burgoyne *et al.*, 2004). For example, Caldendrin/ CaBP1 is an NCS protein that is specifically expressed in the nervous system and exhibits a high homology to CaM at the C-terminus region (Seidenbecher *et al.*, 1998; Haeseleer *et al.*, 2000). Like CaM, Caldendrin possesses 4 EF-hands located at the C-terminus. Unlike CaM, the second EF-hand of Caldendrin is cryptic and hence unable to bind to Ca^{2+} (Seidenbecher *et al.*, 1998; Seidenbecher *et al.*, 2002). The nonfunctional EF-hand of Caldendrin is highly conserved in various species during vertebrate evolution, whereas the N-terminal half is unique to the protein and exhibits no similarity to other known proteins (Seidenbecher *et al.*, 1998). Caldendrin is predominantly found in the somato-dendritic compartment of neurons, enriched in the post-synaptic density (PSD) fractions of rat brains, and is present only in a subset of synapses (Seidenbecher *et al.*, 1998; Laube *et al.*, 2002). Moreover, the synaptic association of Caldendrin is found to be stimulus dependent. Smalla *et al.*, (2003) showed that Caldendrin is highly recruited to the PSD after kainate-induced epileptic seizures, a model of human temporal lobe epilepsy (Smalla *et al.*, 2003).

Jacob is a PSD protein that was recently identified in our lab as a binding partner of Caldendrin in a yeast two-hybrid (Y2H) screen (Dieterich *et al.*, 2008) (Fig. 1). The Jacob mRNA is almost exclusively expressed in cortical and limbic brain regions. At the subcellular level, Jacob is like Caldendrin found in the PSD, dendritic spines and dendrites. However, in contrast to Caldendrin, it is also found in neuronal nuclei (Dieterich *et al.*, 2008). This non-homogenous distribution of Jacob in neurons suggests that Jacob could be associated with distinct binding partners in different neuronal compartments. Additionally, Jacob possesses an N-myristoylation site anchoring it to membranous structures in the cell and more importantly has to be removed before its nuclear translocation.

Jacob is recruited to neuronal nuclei after activation of NMDA receptors. This results in a rapid stripping of synaptic contacts and a drastically altered morphology of the dendritic tree (Dieterich *et al.*, 2008). Nuclear trafficking of Jacob from distal dendrites crucially requires the classical Importin pathway (Dieterich *et al.*, 2008). A bi-

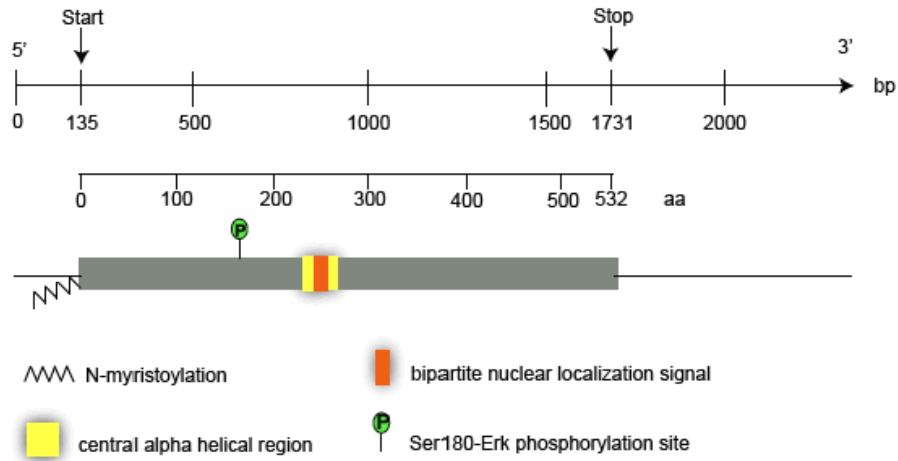


Figure 1. Schematic drawing of the primary structure of Jacob and Jacob cDNA. Depicted are the main sequence features including an ERK phosphorylation site at Ser180, N-myristoylation site, central α -helical region, and bipartite nuclear localization signal (NLS).

partite NLS sequence located in Jacob's central α -helical region is responsible for the retrograde transport of Jacob to the nucleus via the classical Importin pathway. Caldendrin controls the extra-nuclear localization of Jacob by a Ca^{2+} -dependent competition with the binding of Importin- α to the NLS of Jacob (Dieterich *et al.*, 2008). This competition requires sustained synapto-dendritic Ca^{2+} -levels, which presumably cannot be achieved by the activation of extra-synaptic NMDA receptors, but are confined to Ca^{2+} -microdomains such as postsynaptic spines.

As stated before, opposed to their synaptic counterparts, extra-synaptic NMDA receptors trigger the CREB shut-off pathway, and subsequent cell death (Hardingham *et al.*, 2002). It has been also shown that nuclear knockdown of Jacob prevents CREB shut-off after extra-synaptic NMDA receptor activation, while nuclear over-expression of Jacob induces CREB shut-off without NMDA receptor stimulation (Dieterich *et al.*, 2008). Importantly, nuclear knockdown of Jacob attenuates NMDA-induced loss of synaptic contacts, and neuronal degeneration. This defines a novel mechanism of synapse-to-nucleus communication via a synaptic Ca^{2+} -sensor protein, which links the activity of NMDA receptors to nuclear signaling events involved in modeling synapto-

dendritic input and NMDA receptor-induced cellular degeneration (Dieterich *et al.*, 2008).

Interestingly, however, it was also found that targeting Jacob outside of the nucleus has dramatic consequences for the synapto-dendritic complexity of a neuron (Zdobnova, Ph.D. thesis, 2008). Over-expression of certain Jacob splice isoforms, as well as mutants that do not contain the bipartite NLS sequence, in hippocampal primary cultures (DIV5 and DIV10) results in the formation of very large PSD-like structures (larger than 4 μ m in width) that eventually transform into dendritic protrusions (Zdobnova, Ph.D. theis, 2008) (Fig 2). At later stages of development, time-lapse imaging revealed that over-expression of Jacob outside the nucleus in hippocampal primary cultures caused the enlargement of existing synapses (Marina Mikhaylova, unpublished data). Immunocytochemistry performed with primary hippocampal cultures revealed that these protrusions recruit various PSD-scaffolding proteins such as PSD-95 and ProSAP2. Furthermore, NMDA- and α -amino-3-hydroxyl-5-methyl-4-isoxazole-propionate (AMPA)-receptors are recruited and clustered in these protrusions at later stages (Zdobnova, Ph.D. thesis, 2008). It has also been shown that Jacob is enriched in these protrusions and can form homo-dimers (Pöll, Diploma thesis, 2005). Jacob homo-dimer formation might have important consequences such as potentiating the formation of the PSD-like dendritic protrusions in hippocampal primary neurons.

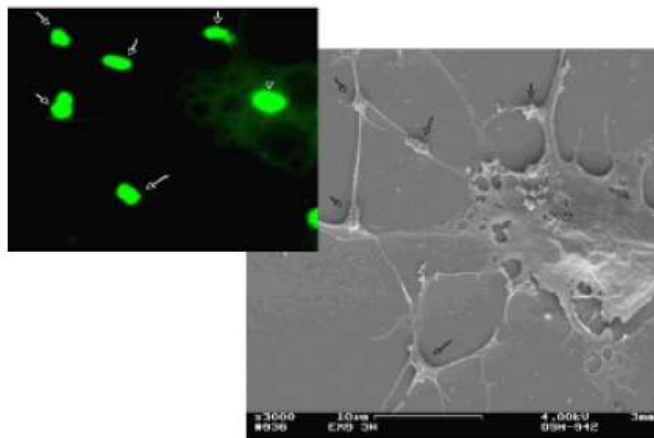


Figure 2. Electron micrograph of PSD-like protrusions. The extra-nuclear Jacob GFP-construct was over-expressed in primary hippocampal cultures at DIV5. Fixation of the transfected cells was performed 24 h after transfection. The size of PSD-like protrusions (arrows) is approximately 4 μ m. (Adapted from Zdobnova, Ph.D. thesis, 2008)

1.2 Neuronal cytoskeleton: moderator of the subcellular distribution of proteins

The neuronal cytoskeleton is composed of microfilaments (MFs), intermediate filaments (IFs), microtubules (MTs) and plays an important structural role for the integrity of dendrites. Each of these structures is formed by a major protein: actin, neurofilament and tubulin, respectively. All of them also have various associated proteins that modify their physical properties and molecular functions (Kaufmann *et al.*, 2000). The major cytoskeletal components and their associated proteins have important roles in the localization and function of many other proteins in neurons. Although all major cytoskeletal proteins are found throughout the neuron, to some extent, they differ in their somatic and dendritic localization from those found in axons (Kaufmann *et al.*, 2000). For example, α -Internexin, a neuronal intermediate filament protein, is predominant in the dendrites and soma of neurons in comparison to other neurofilament (NF) proteins (Benson *et al.*, 1996; Ratzliff and Soltesz, 2000). Previously, a Y2H screen performed by using the C-terminus Jacob as bait disclosed α -Internexin as an interaction partner of Jacob (Daniela C. Dieterich and Michael R. Kreutz, unpublished data). Like many proteins anchored to cell compartments via cytoskeletal components, α -Internexin is mostly localized in the dendrites and soma of the neuron. It was therefore hypothesized that the Jacob- α -Internexin interaction might be important for the localization of Jacob in the somato-dendritic compartment of neurons.

1.2.1 Intermediate filaments

Intermediate filaments form a large protein family in mammalian cells. This family consists of over 65 different genes encoding six different classes of IF proteins. Type I-IV and type VI IF proteins are localized in the cytoplasm, whereas type V IF proteins are found in the nucleus. The reason for the diversity and large number of IF genes in the mammalian genome are questions that have yet to be completely answered. Each major cell type expresses a distinct set of IFs, and this provides them with a relatively specific “fingerprint” of IF proteins (Paramio & Jorcano, 2002; Helfand *et al.*, 2004). They have a rod-shaped structure and can self-assemble *in vitro* into 10-12 nm filaments in one complex. In contrast to the globular subunits of MFs and MTs, G-actin and tubulin, respectively, the assembly of IFs does not require ATP or GTP, and they

remain insoluble under conditions where MFs and MTs are soluble (Helfand *et al.*, 2004; Xiao *et al.*, 2006; Kim *et al.*, 2007). Although this feature contributes to the fact that IF proteins are less flexible in comparison to MFs and MTs, recent evidence has revealed that IF proteins and their precursors are quite dynamic molecules and show a complex array of motile activities related to their subcellular assembly and organization. For instance, it has been shown that Vimentin, a type-III IF protein, exists in several organizational states in a cell, including non-filamentous particles, short filaments (squiggles), and longer filaments (Chang *et al.*, 2004; Helfand *et al.*, 2004). These three different structural forms of IFs are assembled in a highly regulated process to form the extensive cytoskeletal networks in cells (Helfand *et al.*, 2004). Furthermore, in addition to the structural role of IFs in cellular integrity, recent findings indicate that IFs participate in the targeting of proteins to specific locations in polarized cells, in the transport and distribution of organelles, and in the regulation of cell-cell and cell-matrix adhesion (Kim *et al.*, 2007).

In mammals, the cells of the central and peripheral nervous system (CNS and PNS) express brain-specific IFs, also known as the neurofilaments. Together with the neurofilament triplet proteins (NFTPs), NF light chain (NF-L), NF medium chain (NF-M) and NF heavy chain (NF-H), α -Internexin is a member of the type IV IF family, and all of them have been extensively studied in the mammalian brain (Lee *et al.*, 1993; Lariviere and Julien, 2003). It is known that neuronal differentiation is accompanied by changes in neuronal IF composition. During neuronal development type III Vimentin and type VI Nestin IF proteins are replaced by a series of type IV proteins beginning with α -Internexin. As the development continues, α -Internexin is largely replaced by the other neurofilaments: NF-L, NF-M, and finally NF-H (Steinert *et al.*, 1990; Steinert *et al.*, 1999).

1.2.1.1 α -Internexin

α -Internexin, or NF-66, is a type IV IF with high homology to NFTPs which is characterized as their fourth subunit (Chiu *et al.*, 1989; Fliegner *et al.*, 1990; Kaplan *et al.*, 1990; Yuan *et al.*, 2006). Initially, α -Internexin was found as an intermediate filament-associated protein (IFAP) by Patcher and Liem (Patcher and Liem, 1985). However, in 1989, Chiu *et al.* purified NF-66 from the triton-insoluble fraction of rat

spinal cord and characterized it as a novel member of mammalian NFs (Chiu *et al.*, 1989). A year later, based on the cDNA sequence, polymerization *in vitro* and distribution *in vivo*, two independent groups, Fliegner *et al.* and Kaplan *et al.*, revealed that NF-66 protein was indeed the α -Internexin protein, identified as an IFAP by Patcher and Liem (Fliegner *et al.*, 1990; Kaplan *et al.*, 1990; Patcher and Liem, 1985). Like other NFTP, α -Internexin consists of a central α -helical rod domain of about 310 amino acids which is involved in the formation of coiled-coil structures. The globular head and tail segments of α -internexin contain short stretches that are highly homologous to NF-M (Levavasseur *et al.*, 1999) (Fig. 3).

α -Internexin is the first NF protein expressed in postmitotic neurons of the developing CNS and PNS (Ching *et al.*, 1999). The NFTP's expression is preceded by the expression of α -Internexin during mammalian nervous system development. In mature neurons, α -Internexin mRNA level declines, but the protein level remains the same (Ching and Liem, 1993). It is present at lower levels in large neurons, but is highly abundant in cerebellar granule cells (Kaplan *et al.*, 1990; Ching and Liem, 1993; Ching *et al.*, 1999). One of the unique features of α -Internexin in comparison to NFTP is that it can self-assemble and form homo-polymers *in vivo*, i.e. its own filamentous network. It is known that NF-L can also form homo-polymers *in vitro*, but *in vivo* studies revealed that all NFTP including NF-L are obligate hetero-oligomers (Lee *et al.*, 1993). Similarly, α -Internexin can co-assemble with the other IFs and NFTP *in vitro* and in transfected cells (Ching and Liem, 1993; Ching *et al.*, 1999, Levavasseur *et al.*, 1999). It has been shown that both α -Internexin and NFTP can co-assemble with Vimentin *in vitro* (Ching *et al.*, 1999; Steinert *et al.*, 1999), and was also shown to be associated predominantly with NF-M and peripherin *in vivo* (Levavasseur *et al.*, 1999).

Due to its early expression during neuronal development and its ability to form homopolymeric networks in the developing neuron, it has been suggested that α -Internexin provides a scaffold for the co-assembly of the other neuronal IFs during early development (Ching and Liem, 1993). Regeneration studies in amphibians and fish revealed that the lower vertebrate homologues of α -Internexin, Xefiltin (in *Xenopus laevis*) and Gefiltin (in zebrafish), are highly upregulated within developing and regenerating optic nerve axons (Undamatla *et al.*, 2001; Yuan *et al.*, 2006).

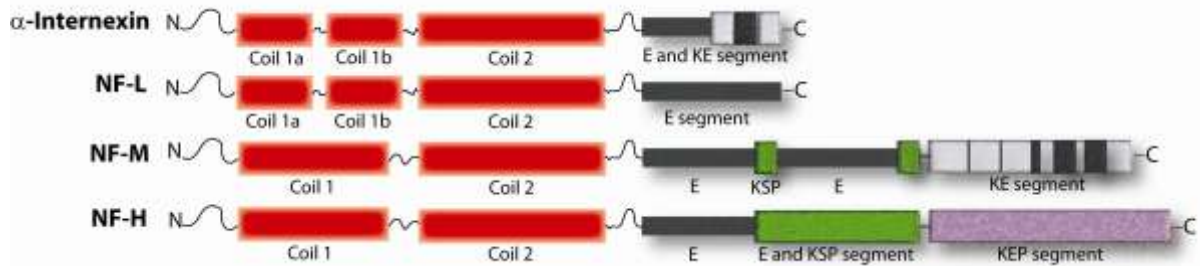


Figure 3. Structure of neuronal intermediate filaments. NFTPs (NF-L, NF-M and NF-H) and α -internexin share an α -helical rod domain responsible for the formation of coiled-coil structures. Flanking amino- and carboxy terminals are the most variable regions among these IFs. NF-M and NF-H carboxy terminal regions consist of multiple repeats of phosphorylation sites Lys-Ser-Pro (KSP). (NF-L; neurofilament light chain, NF-M; neurofilament medium chain, NF-H; neurofilament heavy chain) (Adapted from Lariviere and Julien, 2003)

In contrast, α -internexin-deficient mice showed no gross abnormalities of their nervous system (Levavasseur *et al.*, 1999). They have normal pre- and postnatal development, reach adulthood, reproduce normally and show no signs of neurological disorders (Levavasseur *et al.*, 1999). The loss of α -internexin is not compensated by increased levels of other NFs (Levavasseur *et al.*, 1999).

On the other hand, over-expression of α -Internexin causes motor coordination deficits in transgenic mice in a dose-dependent manner (Ching *et al.*, 1999). The α -internexin over-expression results in the formation of cerebellar torpedoes, which are characterized as abnormal swellings of Purkinje cell axons frequently seen in neurodegenerative diseases involving the cerebellum (Ching *et al.*, 1999).

1.2.1.2 Intermediate filaments are involved in signal transduction pathways

Investigation of the signaling functions of IFs is an increasingly important field in molecular cell biology. IF proteins have several interaction partners which are known to be involved in cellular signaling (Paramio & Jorcano, 2002). It has been shown that Vimentin interacts with Cdc42, Rac1, and phospholipase A2, all of which have been demonstrated to play roles in various signaling pathways in cells (Meriane *et al.*, 2000; Murakami *et al.*, 2000). Another fascinating study demonstrating the role of IFs in signaling came from the field of neurobiology. Perlson *et al.* (2005) showed that Vimentin particles are involved in the retrograde transport of MAP kinases such as

ERK1 and ERK2 in the injured sciatic nerve axon (Perlson *et al.*, 2005) (Fig 4). They introduced an axonal lesion to the sciatic nerve and showed that at the axonal lesion site, Vimentin and Importin- β expression were upregulated. Upon Calpain cleavage of Vimentin, soluble particles of the protein were formed. These newly formed Vimentin particles have been shown to interact with the phosphorylated ERK (pERK) on one side and Importin- β on the other side, and transported pERK to the nucleus with the help of a Dynein motor complex (Perlson *et al.*, 2005).

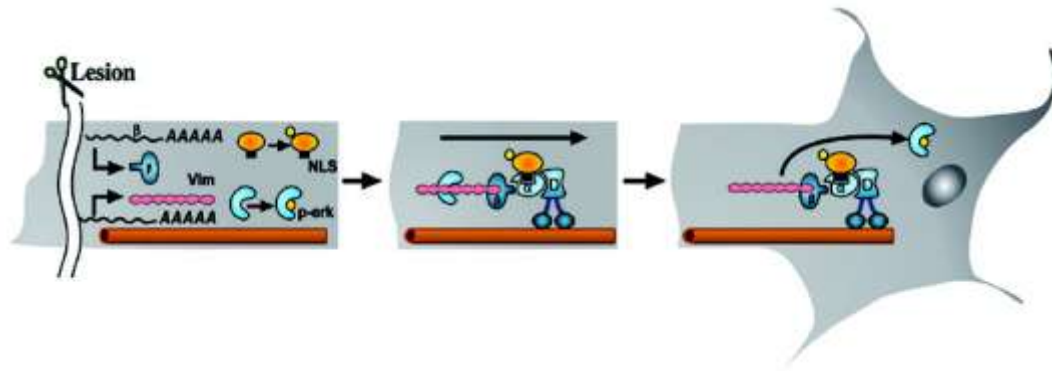


Figure 4. A Model for retrograde transport of phosphorylated MAP kinases mediated by Vimentin. Upon axonal lesion (left), local translation of Vimentin and phosphorylation of ERK (yellow) increases. Vimentin, interacting with pERK on one side and Importin- β on the other side, carries pERK to the nucleus with the help of the Dynein motor complex. (Adapted from Perlson *et al.*, 2005).

Interestingly, α -Internexin has structural and functional similarities to Vimentin (Fliegner *et al.*, 1990; Styers *et al.*, 2004). Therefore, similar to the Vimentin-pERK interaction in lesioned axons, the Jacob- α -Internexin association might have a role in the regulation of Jacob's subcellular localization in neurons after neuronal activity.

Moreover, Perlson *et al.* (2005) also showed that Calpain, a cysteine protease, is important in the regulation of the retrograde transport of pERK by cleaving Vimentin (Perlson *et al.*, 2005). Similarly, over-expression of Δ Myr-Jacob-GFP in COS7 cells and in primary neuronal cultures resulted in nuclear localization of the recombinant protein, indicating that N-terminal truncation of Jacob was a prerequisite for its nuclear translocation (Dieterich *et al.*, 2008). Furthermore, incubation of a Triton X-100 soluble P2 fraction of rat brain with Ca^{2+} in the presence and absence of the Calpain inhibitor ALLN demonstrated that Jacob was sensitive to Ca^{2+} / Calpain-mediated degradation

(Daniela C. Dieterich, unpublished observations), suggesting a plausible role for Calpain in the regulation of the nuclear translocation of Jacob.

1.3 Calpain-mediated proteolysis in neurons

The cysteine protease Calpain was first identified in extracts of skeletal muscles as a phosphorylase kinase-activating factor, and nearly simultaneously in rat brain as a Ca^{2+} -dependent protease (Meyer *et al.*, 1964; Guroff *et al.*, 1964; Huston and Krebs, 1968). Due to its unique action on its substrates, Calpain immediately attracted the attention of biochemists. Unlike most proteases, Calpain hydrolyzes its substrates in a limited manner, i.e. Calpain cleavage results in a modification of the substrate protein's function, rather than abolishing it completely (Sorimachi and Suzuki, 2001).

Calpain, which stands for *calcium-activated papain-like* cysteine protease, exists ubiquitously in organisms ranging from humans to microorganisms (Pinter *et al.*, 1992; Siddiqui *et al.*, 1993). It is also involved in various cellular processes, including cell division, differentiation, platelet activation, and apoptosis (Lu *et al.*, 2002; Goll *et al.*, 2003). The conventional Calpains consist of two subunits: the catalytically active or large subunit, and a regulatory or small subunit, with respective molecular weights of 80 kD and 30 kD (Fig. 5).

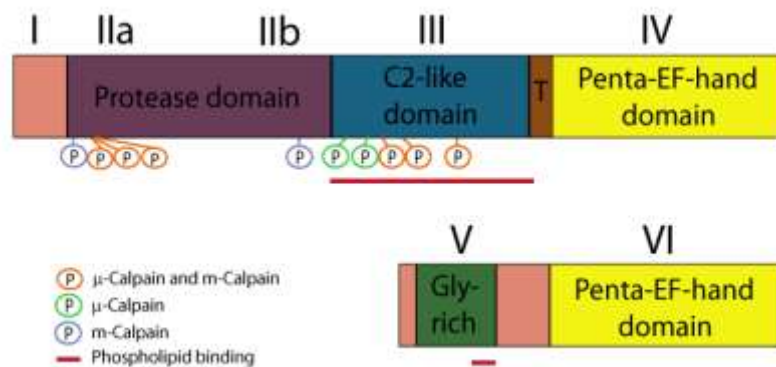


Figure 5. Schematic drawing of the domain structure of conventional Calpains. The large subunit (80 kD) is composed of four domains. Protease activity is contained in domain II (IIa and IIb make up the two halves of the active site). The C2-like domain consists of phosphorylation sites and enables Calpain to bind phospholipids. Domain IV is involved in calcium binding by its EF-hands and dimerization with the small subunit (30 kD). Domain VI of the small subunit has a similar arrangement; the first 4 EF-hands participate in calcium binding, and the last EF-hand enables dimerization with the large subunit. The Gly-rich domain V of the small subunit is highly flexible and also contributes to binding to phospholipids. (Adapted from Franco *et al.*, 2005)

In mammals, the calpain superfamily consists of 14 genes for the large subunit and 2 genes for the small subunit (Sorimachi and Suzuki, 2001). Ubiquitously expressed isoforms, μ - and m-Calpain are named based on their *in vitro* calcium requirements, ranging from 3 to 50 μ M for μ -Calpain (Calpain I), and from 0.4 to 0.8 mM for m-Calpain (Calpain II) (Goll *et al.*, 2003). Both Calpain I and II are expressed in mammalian tissues.

Studies revealed that knockdown of μ -Calpain resulted in no overt phenotype in the deficient mice (Azam *et al.*, 2001). In these mice, it has been shown that m-Calpain compensates for the lack of μ -Calpain activity (Azam *et al.*, 2001). However, when the regulatory subunit (Calpain 4) is knocked down, both μ - and m-Calpains were shown to lose catalytic activity, resulting in the death of knockout mice at embryonic day 11.5 (Arthur *et al.*, 2000).

Substrate protein recognition is another unique feature of members of this protein family. Calpain does not recognize a consensus sequence in its substrates, but prefers sequences associated with tertiary structures of substrate proteins (Suzuki *et al.*, 2004). In the cytoplasm, Calpain is found as a hetero-dimer, composed of small and large subunits. The hetero-dimer form keeps Calpain in an inactive state. Upon an intracellular Ca^{2+} increase, the hetero-dimer translocates to the membrane, the small subunit dissociates, and the catalytically active large subunit binds and cleaves the substrate protein (Sato *et al.*, 2001).

In the nervous system, only μ - and m-Calpain isoforms are expressed and are found both in the soma and synaptic terminals of neurons (Wu and Lynch, 2006; Lynch *et al.*, 2007). The prototypical example of a Calpain substrate in the brain is α -fodrin (α -spectrin) (Stabach *et al.*, 1997; Czogalla *et al.*, 2005). Over the last 20 years, many proteins in neurons were identified as *in vitro* and/or *in vivo* substrates of Calpain. These include the NMDA-receptor subunits, NR2A, NR2B, NR2C (Guttmann *et al.*, 2001; Guttmann *et al.*, 2002), AMPA-receptor subunits, GluR1-3 (Lu *et al.*, 2000; Xu *et al.*, 2007), L-type calcium channel α_{1C} subunit (Hell *et al.*, 1993), the inositol 1,4,5-triphosphate (IP3) receptor (Magnusson *et al.*, 1993), PSD proteins such as PSD-95 and SAP-97 (Lu *et al.*, 2000, Jourdi *et al.*, 2005), enzymes such as Calcineurin A (Liu *et al.*, 2005), CaMKII α , and protein kinase C (PKC) (Kishimoto *et al.*, 1989;

Hajimohammadreza *et al.*, 1997). The proteolytic activity is mostly performed by μ -Calpain activated by a Ca^{2+} influx generated by NMDA receptor activation (Siman *et al.*, 1989; Wu *et al.*, 2005). The fragments of some of these substrates have been shown to be stable *in vivo* and are involved in various signaling pathways in neurons as well (Wu and Lynch, 2006).

1.4 Objectives

Nuclear and extra-nuclear localization of Jacob depends on NMDA receptor-mediated signals, and this has in turn dramatic consequences for neuronal survival and the synapto-dendritic cytoarchitecture of neurons. However, the mechanisms by which Jacob is either transported from dendrites to the nucleus or promotes the growth of PSD-like protrusions are not yet known. Therefore, in this PhD thesis two main questions were addressed:

- What is the somato-dendritic docking site for Jacob in neurons?
- How does Jacob move from the docking site to the nucleus after NMDA receptor activation?

In order to answer the first question, α -Internexin was proposed to serve as the docking site for Jacob in the somato-dendritic compartment. Therefore, the Jacob- α -Internexin interaction was characterized by using co-immunoprecipitations (Co-IPs) and Y2H assays. In order to investigate the mechanisms by which Jacob moves from the docking site to the nucleus, the effect of Calpain proteolytic activity on Jacob nuclear translocation after NMDA receptor stimulation was investigated using pharmacological tools and *in vitro* cleavage assays. Finally, the Jacob homo-dimer, which might have important consequences for Jacob's synaptic and nuclear functions as well as the formation of Jacob-induced PSD-like protrusions, was characterized in detail by Co-IP, pull-down and Y2H assays.

2. Materials and Methods

2.1 Materials

2.1.1 Chemicals

Chemicals used in the experiments of this PhD thesis project were purchased from the following companies: Invitrogen, Calbiochem, Sigma-Aldrich, Merck, Roth, Clontech, Gibco Life Technologies, Abcam, Covance, Roche. Special chemicals and solutions used during the study will be stated in the methods part when it is required. The solutions of the protein biochemistry experiments were prepared by using deionized-double distilled water (Seralpur ProCN[®], Seral); for the molecular biology experiments ultra pure water (Milli-Q[®] System Milipore) was used.

2.1.2 Antibodies

2.1.2.1 Primary antibodies

| Antibody | Specie | Dilution | Company/ Producer |
|----------------------------------|------------------------|-------------------------------|---|
| anti-JB150 | rabbit, polyclonal | WB: 1:2000 IF: 1:100 IP | Dr. Pineda Antibody-Service/ Dipl. – Biochem. B. Hoffmann, Dr. C.I. Seidenbecher |
| anti-Jac2 | guinea pig, polyclonal | WB: 1:2000 | Dr. Pineda Antibody-Service/ Dipl. –Chem. M. Landwehr |
| anti-NJac | rabbit, polyclonal | WB: 1:2000 | Dr. Pineda Antibody- Service/Dipl. Biochem. D.C. Dieterich |
| anti- MAP2 | mouse, monoclonal | IF: 1:1000 | Sigma |
| anti- Myc 9E10 | mouse, monoclonal | IF: 1:1000 WB: 1:1000 | Santa Cruz |
| anti- GFP | rabbit, polyclonal | WB: 1:10000 | Abcam 6556 |
| anti- GFP | mouse, monoclonal | WB: 1:5000 | BABCO |
| anti- MBP | mouse, monoclonal | WB: 1:10000 | NEB |
| anti- ProSAP2 | guinea pig, polyclonal | IF: 1:2000 | Prof. T.M. Böckers |
| anti-Bassoon mAB7f) | mouse, monoclonal | IF: 1:5000 | Dr. S. tom Dieck |
| anti-Bassoon (sap7f) | rabbit, polyclonal | IF: 1:5000 | Dr. W. Altmann |
| anti- α -Internexin (R36) | rabbit, polyclonal | IF: 1: 400 WB: 1:3000 | Abcam 22038 |
| anti- α -Internexin | rabbit polyclonal | IF: 1: 500 WB: 1: 2000 | Chemicon |

| Antibody | Specie | Dilution | Company/ Producer |
|---|--------------------|--------------------------------|--|
| anti- α -Internexin | polyclonal chicken | IF: 1:200 WB: 1:3000 | Chemicon |
| anti- α -Internexin (1D2) | mouse, monoclonal | IF: 1: 400 WB: 1:3000 IP | Covance |
| anti-Neurofilament | rabbit, polyclonal | IF: 1: 400 | Sigma |
| anti- Dynein Light Chain | mouse, monoclonal | WB: 1:1000 | Sigma |
| anti-Importin- α 1/ Karyopherin α /Rch-1 | mouse, monoclonal | IF: 1:200 WB: 1:500 | BD Biosciences, Heidelberg, Germany |
| anti-Importin- β 1/ NTF97 clone E9 | Mouse, monoclonal | IF: 1:400 WB: 1:1000 | Affinity Bioreagents |

2.1.2.2 Secondary antibodies

| Antibody | Specie | Dilution | Company/ Producer |
|---|---------------|-----------------|--------------------------|
| anti-guinepig IgG, HRP-conjugated | rabbit | WB: 1: 4000 | DAKO |
| anti-mouse IgG, HRP-conjugated | goat | WB: 1: 4000 | DAKO |
| anti-rabbit IgG, HRP-conjugated | goat | WB: 1: 5000 | NEB |
| anti-mouse- IgG, Alexa Flour TM 488/568 conjugated | goat | IF: 1:1000 | Molecular Probes |
| anti-rabbit- IgG, Alexa Flour TM 488/568 conjugated | goat | IF: 1:1000 | Molecular Probes |
| anti-guinea pig- IgG, Alexa Flour TM 488/568 conjugated | goat | IF: 1:1000 | Molecular Probes |
| anti-guinea pig IgG, Cy5 TM conjugated | goat | IF: 1:700 | Dianova |
| anti-rabbit IgG, Cy3 TM conjugated | goat | IF: 1:1500 | Dianova |
| anti-mouse IgG, Cy3 TM conjugated | rabbit | IF: 1:1500 | Dianova |

Abbreviations: IF: Immunofluorescence, WB: Western blot, IP: Immunoprecipitation

2.1.3 Bacterial and yeast media

| | |
|----------------------|---|
| LB-Medium | 5 g/l Yeast-extract, 10 g/l Bacto- trypton, 5 g/l NaCl |
| LB-Plates | 1000 ml LB- Medium, 15 g agar |
| SOC-Medium | 20 g/l Bacto- trypton, 5 g/l Yeast-extract, 10 mM NaCl, 2,5 mM KCl, 10 mM Mg ₂ SO ₄ , 10 mM MgCl ₂ , 20 mM Glucose |
| YPD and YPDA- Medium | 50 g/l YPD Media, 30 mg/l adenin hemisulfate (AT; only for YPDA), pH 7.0 |

| | |
|---------------------------|--|
| -L, -W, -LW, -LWH- Medium | 26,7 g/l Minimal SD-Base X g Dropout (DO) Supplement -L: 0.69 g/l –Leu-DO -W: 0.74 g/l –Trp-DO -LW: 0.64 g/l –Leu-Trp-DO -LWH: 0.62 g/l –Leu-Trp-His-DO pH 5.8 |
| Yeast agar plates | 20 gr agar for 1 lt liquid medium |

2.1.4 Animals

Wistar rats from in the Leibniz Institute for Neurobiology (Magdeburg, Germany), were used in all molecular biology, protein biochemistry assays and preparation of primary neuronal cultures.

2.2 Methods

2.2.1 Molecular biology

All molecular biology experiments were performed according to protocols described in detail in *Current Protocols in Molecular Biology* (Ausubel *et al.*, 1990) and *Molecular Cloning* (Sambrook *et al.*, 1989). Therefore, methods used in this work are mentioned briefly and the modifications are stated clearly.

2.2.1.1 Polymerase chain reaction (PCR)

| | |
|--|-------------------|
| PfuTurbo DNA Polymerase: | Stratagene |
| Taq DNA Polymerase: | Qiagen |
| Oligonucleotide (Primer): | Invitrogen |
| Deoxynucleoside-triphosphate Set: | Roche |
| 5x Q solution: | Qiagen |

In order to clone the gene of interest into a vector with specific restriction enzyme site (s), the specific DNA fragment was first amplified by PCR. In each PCR reaction, a pair of specific primer/oligonucleotide sets were used (section 6.1). For a reaction volume of 25 µl, 10-20 ng of plasmid DNA or rat cDNA library were mixed with 0.4 µM of each primer. Together with 12.5 µM of deoxynucleoside triphosphate, 10x Pfu Polymerase buffer was added with a final concentration of 1x. In some cases,

the 5x Q solution was also added to the reaction to increase the efficiency of the PCR reaction. Finally, 0.25 U of Pfu Turbo DNA polymerase was added and the PCR reaction was performed in a thermocycler (TECHNE/PROGENE). Conditions used in each PCR are given below.

| | |
|--------------------------------------|--|
| Initialization step (1 cycle) | 94°C 3 min. |
| 38 cycles | Denaturation: 94°C 45 sec. Annealing: X* °C 30 sec. Elongation: 72 °C 2 min. |
| Final elongation (1 cycle) | 72 °C 10 min. |
| Final hold | 4 °C |

*The T_m of each reaction differs depending on the T_m of each primer pair used per reaction (section 6.1).

2.2.1.2 Restriction enzyme digestion

Restriction enzymes: NEB, Fermentas, Gibco

The specific restriction enzyme(s) (RE) used for each construct is stated in section 6.3. The enzyme-DNA ratio was 1U: 1µg/reaction. Each reaction was performed at the different conditions recommended by the manufacturer(s).

2.2.1.3 Agarose gel electrophoresis and isolation of DNA fragments from agarose gel

| | |
|---|--|
| Agarose: | Ultrapure (Invitrogen) |
| 50x TAE buffer: | 2 M Tris-acetate, 0.05 M EDTA |
| Ethidium bromide solution: | 1 mg/ ml (Roth) |
| 6x DNA loading buffer: | 30% glycerol, 0.25% bromophenol blue, 0.25% xylene cyanol, 50 mM EDTA, pH 8.0 |
| DNA-molecular weight markers: | MBI Fermentas |
| NucleoSpin[®] Extract II: | Macherey-Nagel |

During cloning/subcloning procedures, the DNA fragments (either after PCR reaction or RE digestion) were run on an agarose gel for analysis. The DNA fragments were isolated from the agarose gel using NucleoSpin[®] Extract II based on the protocol provided by the manufacturer.

2.2.1.4 Cloning of DNA fragments into a specific plasmid vector

Alkaline phosphatase (CIP): Roche
T4-DNA-Ligase: Promega

In order to clone/subclone a DNA fragment into a plasmid vector, the vector was first linearized by RE digestion. For every cloning/subcloning, a specific RE site(s) was/were used for inserting the DNA fragments into the vector. If the cloning is an indirect one, i.e., done by using one RE site, the linear vector was dephosphorylated at the 5' end by using CIP (calf intestine phosphatase, Roche) in order to prevent the religation of the plasmid. The insert was also cut by using the same RE. After that, both the insert and vector were run on the agarose gel and finally extracted from the gel. Ligation of the insert and the vector was performed using a T4-DNA-Ligase. The insert-vector ratio used in the reaction was 3:1. Ligation was performed at 23°C for 3 h and held at 16°C overnight.

2.2.1.5 Transformation into electrocompetent bacteria *E.coli* XL1-blue MRF

Electroporation-cuvettes: 0.2 cm electrode gap (Equibio)

Electrocompetent *E.coli* XL1-Blue MRF was prepared by using the protocol from Sambrook *et al.* (1989). The electroporation was performed as described in Dieterich *et al.* (2002). After that, the transformed bacteria were plated on an LB-agar media including appropriate antibiotics and incubated at 37°C overnight.

2.2.1.6 Amplification of plasmid DNA (mini, midi and maxi preparations)

P1 buffer: 50 mM Tris-HCl, pH 8.0, 10 mM EDTA, 100 µg/ml RnaseA
P2 buffer: 200 mM NaOH, 1% (w/v) SDS
P3 buffer: 3 M Potassium acetate (CH₃COOK), pH 5.5

After transformation, for mini preparation of the plasmid DNA, single positive colonies were picked up and inoculated into a 2 ml LB-broth medium containing the appropriate antibiotic(s) and incubated at 37°C overnight. The plasmid isolation was executed using a protocol modified from Birnboim and Doly *et al.*, 1979. According to this protocol, the overnight cultures were spun at 3,000 rpm for 5 min. The bacterial pellet was resuspended with 300 µl P1 buffer. To lyse the cells, 300 µl of P2 buffer was

added and incubated on ice for 5 min. To neutralize the suspension, 300 µl of P3 buffer was added and incubated on ice for 5 min. Afterwards the samples were centrifuged at 20,000 xg for 15 min. 800 µl of the supernatant was transferred to a new 1.5 ml eppendorf tube. In order to precipitate the nucleic acids, 550 µl of isopropanol was added to each sample and incubated at room temperature (RT) for 10 min. The samples were then centrifuged at 20,000 xg for 15 min. At last, each DNA pellet was washed with 1 ml 70% (v/v) Ethanol in order to remove the salts and precipitate the DNA. The pellets were dried out and plasmid DNA was eluted into 40 µl 10 mM Tris with pH 7.4. However, the midi and maxi preparations of plasmid DNA were done by using plasmid DNA purification kits of Qiagen (Qiagen Plasmid Purification Kit or Qiagen Endofree™ Plasmid Maxi Kit).

2.2.1.7 Production of expression construct

Expression constructs used in experiments are given in section 6.3. In order to verify whether the inserted cDNA is inframe with the vector sequence or not, all constructs were sequenced by SEQLAB (Göttingen) and the “Basic Local Alignment Search Tool” (BLAST) search engine was used for the sequence alignment of clones (<http://www.ncbi.nlm.nih.gov/BLAST>).

2.2.1.8 Yeast two hybrid (Y2H) system

Yeast strain: **AH109 (Clontech)**

The Matchmaker™ GAL4 Two Hybrid System from Clontech, which was first introduced by Fields and Song in 1989, is a well-established genetic tool used to identify and characterize protein-protein interactions. This technique is based on the properties of a transcriptional activator, the GAL4 protein of yeast (*Saccharomyces cerevisiae*). The GAL4 protein is required for the expression of genes encoding the enzymes of galactose utilization in yeast. It has two functionally essential separable domains. The N-terminal domain binds to specific DNA sequences (UAS_G), while the acidic C-terminal domain is necessary to activate the transcription. In this system, one of the proteins of interest (X) is expressed as a fusion protein of DNA binding domain (BD-X); also known as the “bait” protein. While the other protein (Y) is expressed as a fusion protein of the activation domain (AD-Y); also known as the “prey” protein. The fusion vectors are introduced to the yeast by the Lithium acetate/ single-stranded carrier

DNA/polyethylene glycol (LiAc/SS-Carier DNA/PEG) transformation method (Gietz and Woods, 2002). Only after expression of these two chimeras, and the subsequent physical interaction of the proteins X and Y, will the gene for the galactose utilization be expressed and the yeast grow in a certain auxotrophic agar media.

2.2.1.8.1 Transformation by LiAc/ SS-carier DNA/ PEG

| | |
|--|--|
| PEG 3350: | 50% w/v, Sigma |
| 10x TE buffer: | 0.1 M Tris-HCl, 10 mM EDTA, pH 7.5 |
| 10x LiAc buffer: | 1.0 M Lithium acetate, pH 7.5 |
| PEG/ LiAc/ TE buffer: | 8 ml PEG 3350 (50% w/v) / 1 ml 10x LiAc / 1ml 10x |
| TE Single-stranded carrier DNA: | Clontech (10 mg/ml) |

2.2.1.8.1.1 Preparation of the competent yeast cells

Yeast strain AH109, obtained in a glycerol stock (Clontech), was inoculated into a YPDA agar plate and incubated at 30°C for 3-4 days. A single colony from this plate was inoculated into 25 ml of YPDA broth and incubated overnight at 30°C with agitation. The next day, the starting culture was diluted into 100 ml of YPDA broth medium with a final OD₆₀₀ 0.2-0.4. 3-4 h after inoculation, i.e. when the OD₆₀₀ reached 0.8-1.0, the cells were spun at 500 xg at RT for 2 min. The cell pellet was then washed with 1x TE washing buffer at RT for 2 min, and spun at 500 xg at RT for 2 min. After that, the cell pellet was washed in 1x LiAc washing buffer for 10 min and centrifuged at 500 xg at RT for 2 min. Finally, the competent yeast cells were resuspended into 1.5-2.0 ml 1x TE/ LiAC buffer.

2.2.1.8.1.2 Transformation of the plasmids into the competent yeast cells

| <u>Components</u> | <u>Amount</u> |
|------------------------|---------------|
| Carrier DNA | 10 µl |
| BD-plasmid | 3-5 µg |
| AD-plasmid | 3-5 µg |
| Competent yeast | 50 µL |
| PEG/ LiAc/ TE | 300 µl |

The components were mixed by a vortex at medium speed for a short time (~10 sec). Then, the samples were incubated in a water bath at 42°C for 50-60 min. After that, the samples were chilled on ice for 2 min, centrifuged at 500 xg for 2 min at RT, and resuspended in 200 µl of ultra-pure water. Finally, 100 µl of each sample was

inoculated on a specific auxotrophic agar media (All media were prepared by using minimal SD base media lacking certain amino acids. TDO: -L, -H, -W; QDO: -L, -H, -W, -A), and incubated at 30°C for 3-5 days.

2.2.2 Biochemical methods

2.2.2.1 Protein concentration determination

BCA protein assay kit **Pierce®**

Protein concentration of the samples was determined by using the Pierce® BCA protein assay kit based on a protocol provided by the manufacturer. The OD of the color reaction was measured with a microplate reader (Molecular Devices) at 562 nm.

2.2.2.2 Sodium dodecyl sulfate- polyacrylamide gel electrophoresis (SDS-PAGE)

| | |
|--|--|
| 4x SDS-loading buffer: | 250 mM Tris-HCl (pH 6.8), 1% (w/v) SDS, 40% (v/v) Glycerol, 20% (v/v) β-mercaptoethanol, 0.004 % Bromophenol Blue |
| Electrophoresis buffer: | 192 mM Glycine, 0.1% (w/v) SDS, 25 mM Tris-base, pH 8.3 |
| Molecular weight marker: | Pageruler, prestain marker (Fermantas) |
| Coomassie Brilliant Blue staining solution: | 0.125% (w/v) Coomassie Brilliant Blue R250, 50% (v/v) methanol, 10% (v/v) acetic acid |
| Coomassie destaining solution: | 7% (v/v) acetic acid |
| Drying solution: | 50% (v/v) methanol, 5% (v/v) glycerol |

Protein gel electrophoresis was performed according to a protocol adapted from Laemmli (1970). According to this protocol, proteins were separated according to their size in a one-dimensional sodium dodecyl sulphate polyacrylamide gel (SDS-PAGE) system under fully denaturing and reducing conditions. At first, protein samples were incubated with an SDS-sample loading buffer at 95°C for 5 min, spun at 18,000 xg for 1 min and then loaded into a 5-20% gradient gel. 1x electrophoresis buffer was used to run the gels at a constant current strength of 12 mA per gel in an electrophoresis chamber (Hoefer Mighty Small System SE 250 from Amersham Biosciences). After that, these gels were either stained with Coomassie Brilliant Blue or were used for immunoblotting. The Coomassie Brilliant Blue stained gels were kept for documentation.

2.2.2.3 Western blotting (immunoblotting)

| | |
|---------------------------------|--|
| Blotting buffer: | 192 mM Glycine, 0.2% (w/v) SDS, 20% (v/v) ethanol, 25 mM Tris-base (pH 8.3) |
| Ponceau S solution: | 0.5% (w/v) Ponceau S in 3% (v/v) acetic acid solution |
| 10x TBS: | 1.4 M NaCl, 0.25 M Tris-HCl (pH 7.6) |
| TBS-A: | 0.02 % (w/v) Sodium azide in 1x TBS |
| TBS-T: | 0.1 % (v/v) Tween-20 in 1x TBS |
| TBST-A: | 1x TBS-T, 0.02% NaN₃ |
| Blocking solution: | 5% (w/v) non-fatty milk powder in 1x TBS-T |
| 10x PBS: | 1.4 M NaCl, 83 mM Na₂HPO₄, 17mM NaH₂PO₄, pH 7.4 |
| Nitrocellulose membrane: | Whatman (ProtRan[®]) |

The transfer of proteins onto the nitrocellulose membrane was done according to the protocol by Towbin *et al.* (1979). The transfer was performed in a blotting chamber from Hoefer at a constant current of 200 mA at 4°C for 1.5 h. In order to visualize the transferred proteins on nitrocellulose membrane, the blots were stained with Ponceau S solution. Blocking of the membrane was done at RT for 1.5 h by using a non-fatty milk powder dissolved in 1x TBS-T. Subsequently, the blots were briefly washed with 1x TBS and the primary antibody, diluted TBST-A, was applied onto the blots, and incubated at 4°C overnight. The next day, blots were washed at RT as follow: First washing step: 1x TBS for 10 min; second: 1x TBS-T for 10 min; third: 1xTBS for 5 min; fourth: 1x TBS-T for 5 min. Finally, the HRP-conjugated secondary antibody, diluted in blocking solution, was applied onto blots and incubated at RT for 1.5 h. After secondary antibody incubation, the blots were washed as described above. Detection was performed using the ECL-detection system. A chemoluminescence sensitive film (Hyperfil Amersham Life Science) and a developing machine from AGFA curix were used for visualization of the protein bands on the film.

2.2.2.4 Expression and purification of protein fused to maltose binding protein (MBP)

| | |
|-------------------------------------|--|
| LB medium: | 100 µg/ml Ampicillin, 2 g/L Glucose |
| Amylose resin: | NEB |
| Elution buffer: | 10 mM Maltose in PBS |
| Protease inhibitor cocktail: | Complete Mini Roche |

2.2.2.4.1 Induction of MBP-fusion protein

E.coli BL21 Gold strain was transformed with the pMAL-Jacob-N₁₋₂₃₀ construct, and the transformants were grown in a 50 ml LB-ampicillin medium at 37°C with agitation for overnight. The next day, the starting culture was inoculated into 1 liter of LB-ampicillin medium and grown till mid-log phase (OD₆₀₀~ 0.6- 0.7) at 37°C with agitation. The culture was induced by addition of 1 mM IPTG to the growth medium and incubated at 37°C with agitation for 4 h. Finally, the cells were spun at 6,000 xg for 20 min.

2.2.2.4.2 Purification of MBP-fusion protein

The bacterial pellet was resuspended in 30 ml PBS buffer including the protease inhibitor cocktail. The cells were disrupted by a Constant Cell Disruption System (Constant System, UK) with a force of 15,000 psi (1350 bar) and spun at 12,000 xg at 4°C for 20 min. After that, the supernatant was incubated with amylose resin, which was washed 3x with ice cold 1x PBS, for 10 min at 4°C. Finally, the amylose resin, coupled to the fusion protein, was washed 6x with ice cold 1x PBS and stored at -20°C until use.

2.2.2.5 Homogenization and subcellular fractionation of rat brain and extraction of protein from rat brain tissue

2.2.2.5.1 Homogenization of Rat Brain Tissue and Extraction of Proteins from S1Fraction

Homogenization-Extraction

buffer (HOM-EX-buffer):

20 mM Tris-HCl (pH 8.0), 1% Triton X-100, 140 ml NaCl with 2x protease inhibitor cocktail (Complete Mini, Roche)

10 ml of HOM-EX-buffer was applied to 1.2 g of brain tissue (without cerebellum) from adult rat and homogenized with a homogenizer at 900 rpm for 12 strokes. The homogenate was centrifuged at 1000 xg at 4°C for 10 min. The pellet that contained the cell debris and nuclei was discarded and the supernatant was spun at 12,000 xg at 4°C for 30 min. The supernatant, S1 was taken out and kept at -80°C until further use.

2.2.2.6 Subcellular fractionation and postsynaptic density (PSD) preparation

The PSD-preparation from adult rat brains was done by using a sucrose gradient dependent protocol, described in detail in the protocol Smalla *et al.* (2003). Briefly, 10 ml/g homogenization buffer including protease inhibitors was mixed with adult rat brain tissue and homogenized at 900 rpm for 12 strokes, spun at 1000 xg for 10 mins. The resulting supernatant is named S1 and pellet is called P1. The P1 fraction was resuspended in homogenization buffer including protease inhibitor (10 ml/g) and homogenized again at 900 rpm for 12 strokes and spun at 1000 xg for 10 min. The resulting supernatant S1' combined with S1 and named as S1 only. The P1' includes now cell debris and nucleus. The S1 mix was taken and spun at 12,000 xg for 15 min. The resulting fractions were S2 and P2. The P2 fraction was taken and the pellet was washed in homogenization buffer (10 ml/g), homogenized again at 900 rpm for 6 strokes and spun at 12,000 xg for 20 min. The resulting P2' fraction is also known as crude membrane fraction. S2 and S2' fractions were combined and put into a specific 1.5 ml sucrose gradient solution and added on top of the sucrose gradient (step gradient 0.85/1.0/1.2 M sucrose) that is prepared before. The samples were spun at 85,000 xg for 2h. The resulting fractions from top to bottom are; myelin, light membranes, synaptosomes and mitochondria. After this step the synaptosomal fraction which is also called S3 fraction was harvested and mixed with 1 mM Tris-HCl (pH 8.1) solution (1/5 volume)-Tris-HCl addition will subject the S3 fraction to a hypo-osmotic shock-, stirred for 30 min at 0°C, and spun at 33,000 xg for 30 min. After this step the resultant supernatant and pellet are called as S3 and P3, respectively. The P3 contains synaptosomal membranes. The P3 fraction was resuspended in 5mM Tris-HCl and added on top of another sucrose gradient (step gradient 0.85/1.0/1.2 M sucrose) prepared before. The samples were spun at 85,000 xg for 2h. The interphase, also called synaptic junctions was harvested and mixed with solution A (60 ml/10 g of brain tissue) and solution B (60 ml/10 g of brain tissue) were added on top. Then the mixture was stirred, incubated at 0°C for 15 min, and spun at 33,000 xg for 30 min. The resultant supernatant and pellet, S4 and P4, respectively were collected. The P4 fraction is also called as PSD1. P4 was mixed with solutions A (60 ml/10 g of brain tissue) and B (60 ml/10 g of brain tissue), spun at 33,000 xg for 30 min. The resulting pellet, P5 contains the PSD fraction.

2.2.2.7 Protein extraction from transfected HEK 293 and COS7 cell lines

Extraction buffer: 50 mM Tris (pH 8.0), 1% Triton X-100, 150 mM NaCl, 2x protease inhibitor cocktail (complete, Roche), 2 mM EGTA

Transfected HEK 293 or COS7 cells were removed from the flasks with the help of a scraper collected into a 15 ml falcon tube and spun at 1,500 xg at 4°C for 3 min. The cell pellets were washed with 1x PBS and transferred into a 1.5 ml eppendorf tube for lysis. Depending on the cell pellet, 400-800 µl of extraction buffer was added to each sample and the cells were subjected to freezing (in liquid nitrogen) and thawing steps twice. The cells were incubated with the lysis buffer at 4°C for 30- 50 min depending on the type of the recombinant protein expressed in HEK 293 or COS7 cells. Finally, the cell lysates were centrifuged at 20,000 xg for 20 min, and the supernatant was used in further experiments.

2.2.2.8 Pull-down assays

Extraction buffer: 50 mM Tris (pH 8.0), 1% Triton X-100, 150 mM NaCl, 2x protease inhibitor cocktail (complete, Roche), 2 mM EGTA
DTT (dithiothreitol): (Roth) stock 100 mM in water

The COS7 cells were transfected with Myc-Jacob-wt construct and recombinant proteins were extracted by using extraction buffer containing freshly added 2 mM DTT, according to the protocol described at section 2.2.2.7. Equimolar amounts of MBP fusion protein, MBP-Jacob₁₋₂₃₀ and MBP-coupled sepharose beads were washed with ice cold extraction buffer three times and spun at 300 xg at 4°C for 3 min after each wash. After that 500 µl of COS7 cell extracts were added to the prewashed MBP-Jacob₁₋₂₃₀ and MBP-coupled amylose resin and each of the reaction mixtures was completed to 1 ml by the addition of extraction buffer. The reaction mixtures were incubated at RT with rotation for 1 h. Afterwards, the samples were spun at 300 xg at 4°C for 3 min and washed with the extraction buffer three times and spun at 300 xg at 4°C for 3 min after each wash. The bound fraction was resuspended in 40 µl 2x SDS-sample loading buffer, and analyzed by western blotting.

2.2.2.9 Co-immunoprecipitation (Co-IP) experiments

2.2.2.9.1 Co-IP performed by using protein extracts of S1 rat brain fraction

| | |
|---|---|
| anti-α-Internexin (monoclonal mouse) (1D2) | Covance |
| anti-JB150 (polyclonal rabbit) | Dieterich <i>et al.</i>, 2008 |
| anti-IgG (mouse): | Santa Cruz |
| anti-IgG (rabbit): | Santa Cruz |
| Protein-G Plus Agarose: | Santa Cruz |
| Protein-A Plus Agarose: | Santa Cruz |
| Washing buffer(HOM-EX-buffer): | 20 mM Tris-HCl (pH 8.0), 1% Triton X-100, 140 ml NaCl with 2x protease inhibitor cocktail (complete mini, Roche) |

The protein extracts of S1 fraction of rat brain, prepared according to the protocol, which was explained in detail at section 2.2.2.5.1, were used in the Co-IP experiments. 2 μ g of polyclonal JB150 rabbit or monoclonal α -Internexin mouse antibodies (anti-IgG (rabbit) and anti-IgG (mouse) for control) were incubated with 1 ml of protein extracts of S1 fraction at 4°C overnight. The next day, 20 μ l of Protein-A or -G agarose beads were washed with the washing buffer three times at 300 xg at 4°C for 3 min after each wash and then added to the antibody-S1 mixture, incubated at 4°C for 2 h. Afterwards, the samples were spun at 300 xg at 4°C for 3 min. The pellets were washed with the washing buffer three times at 300 xg at 4°C for 3 min after each wash. Finally, 40 μ l of 2x SDS-sample loading buffer was added onto the pellets, cooked at 95°C for 5 min, and loaded onto the SDS gels for further western blot analysis.

2.2.2.9.2 Heterologous Co-IP performed by using the protein extracts of transfected HEK 293 and COS7 cell lines

| | |
|--------------------------------|--|
| anti- Myc 9E10 (mouse): | Santa Cruz |
| anti-GFP (rabbit): | Abcam 6556 |
| anti-IgG (mouse): | Santa Cruz |
| IgG (rabbit): | Santa Cruz |
| Protein-G Plus Agarose: | Santa Cruz |
| Protein-A Plus Agarose: | Santa Cruz |
| Washing buffer: | 50 mM Tris (pH 8.0), 1% Tx, 150 mM NaCl, 2x protease inhibitor cocktail (complete, Roche) , 2 mM EGTA |

The HEK 293 and COS7 cells were co-transfected with different Myc- and GFP- tagged constructs depending on the purpose of the experiment. Recombinant proteins were extracted from the transfected cells according to the protocol described in section 2.2.7. The protein extracts were incubated with 2 µg of either a monoclonal Myc mouse or a polyclonal GFP rabbit antibody at 4°C for 4 h. Anti-IgG (rabbit) and anti-IgG (mouse) were used as controls. After that, 20 µl of Protein-G or -A agarose beads, washed with the washing buffer three times at 300 xg at 4°C for 3 min after each wash, added onto these samples and incubated at 4°C for 2 h. Then, they were spun at 300 xg at 4°C for 3min. The pellets were washed with washing buffer three times at 300 xg at 4°C for 3 min after each wash. Finally, 30 µl of 2x SDS-sample loading buffer was added onto the pellets, cooked at 95°C for 5 min and loaded onto the SDS gels for further Western Blot analysis.

2.2.2.10 Calpain cleavage of Jacob *in vitro*

µ-Calpain : **From Porcine Erythrocytes, 1.3 mg/ml, 5591.0 units/mg (Calbiochem)**
Reaction buffer: **1x TBS (pH 7.6)**

MBP-Jacob₁₋₂₃₀ fusion protein was produced based on the protocol described in section 2.2.2.4.2. Samples containing 5 nM MBP-Jacob₁₋₂₃₀ or 5 nM MBP alone, 2mM Ca⁺² or 2mM EGTA and µ-Calpain (specific activity 0.195 units) were incubated in Calpain reaction buffer. Reactions were brought to 20 µL and incubated at 30°C for 10 sec, 30 sec and 1 min. The reactions were terminated by addition of 5 µl of 4x SDS sample buffer. MBP-Jacob₁₋₂₃₀ protein degradation was visualized on immunoblots.

2.2.3 Cell culture

2.2.3.1 Culturing and transfection of HEK 293 and COS7 cell lines

DMEM (+): **DMEM (-), 10% fetal calf serum (FCS), 2 mM L-Glutamine, 100 U/ml Penicillin, 100 µg/ml Streptomycin (Gibco)**
DMEM (-): **(Gibco)**
1x Trypsin/EDTA: **(Gibco) stock solution diluted to 1:10 in HBSS**
Poly-D-Lysin: **(Qiagen) Transfection reagent**

The African Green Monkey SV40-transformed kidney fibroblast (COS7) and Human Embryonic Kidney 293 (HEK 293) cell lines were used for protein over-

expression studies. For transfection experiments, splitting of the COS7 cells was accomplished as follows: First, the cells were washed with pre-warmed HBSS and then incubated with 500 μ L trypsin solution at RT for 5 min. Cells were collected into a 15 ml falcon tube, spun at 500 xg for 5 min at 4°C, and diluted to 1:5 with DMEM (+) into a new culture flask (75 cm²) and kept in a Heraeus Incubator at 37°C with 5% CO₂ and 95% humidity. Splitting of the HEK 293 cells was similar to the splitting of the COS7 cells with some modifications. For instance, after trypsin application, HEK 293 cells were incubated at 37°C for 2.5 min, diluted to 1:2.5 and directly inoculated into new culture flasks. 24 h after culturing, the cells were transfected at 80 % confluency with appropriate construct(s) as follows: 12 μ g of plasmid DNA (total) and 40 μ l of polyfect were added into 500 μ l DMEM (-), mixed well by pipetting, and incubated at RT for 10 min. Next, 1 ml of DMEM (+) was added to the transfection mixture and transferred into the 1 day old cultures. The transfected cells were harvested 36-48 h after transfection. However, cultures split into the 24 well plates were prepared as described above. Apart from that, poly-D-lysine was used to attach the cells onto the coverslips. Transfection for 4 wells was performed as follows: 2 μ g of plasmid DNA mixed with 4 μ L polyfect was added into 200 μ L DMEM (-) used for transfection and incubated at RT for 10 min. After incubation, 400 μ L of DMEM (+) were added and 150 μ L of the transfection mixture were transferred into the one day old cultures. 36-48 h after transfection, transfected cells were fixed by 4% PFA for 10 min at RT.

2.2.3.2 Primary cultures

2.2.3.2.1 Hippocampal primary neuronal culture preparation

| | |
|----------------------|---|
| Medium 1: | DMEM (-), 10% FCS, 100 U/ ml Penicillin, 100 μg/ml Streptomycin, 2 mM L-Glutamine |
| Medium 2: | Neurobasal™, 1x B27 (Gibco), 100 U/ ml Penicillin, 100 μg/ml Streptomycin, 0.5 mM L-Glutamine |
| Trypsin: | 0.1 % dissolved in HBSS |
| DNaseI: | (Roche) 0.01 % (200 U) dissolved in HBSS, 2.4 mM MgSO₄ |
| Poly-D-Lysin: | 100 mg/ml in 0.15 M boric acid, pH 8.4 |

The protocol from Goslin and Banker *et al.* (1998) was used with some modifications (Dresbach *et al.* 2003) to prepare the hippocampal primary neuronal cultures. Based on this, hippocampus and/or cortex of rat embryos at embryonic day 19

(E19), were used for culturing. For high-density cultures, 40,000-60,000 cells were used per coverslip. For low density cultures 10,000-15,000 cells per coverslip were plated (Poly-D-Lysin was used to attach the cells onto the coverslips). The cultures were kept in a Heraeus incubator at 37°C with 5% CO₂ and 95% humidity.

2.2.3.2.2 Transfection of hippocampal primary cultures

| | |
|-----------------------------|--|
| Opti-MEM: | (Gibco) |
| Neurobasal (+): | Neurobasal™, 1x B27 (Gibco), 0.5 mM L-Glutamine |
| Lipofectamine™ 2000: | (Invitrogen™) |

The transfection of hippocampal primary cultures was done on day in vitro (DIV) 5 or 9 after plating. The cell densities used for transfections were 50,000 and 60,000. Transfection was performed by using Lipofectamine™ 2000 as the transfection agent. This is based on a protocol provided by the manufacturer. Transfected cultures were kept in a Heraeus incubator at 37°C with 5% CO₂ and 95% humidity for 8-24 h depending on the purpose of the experiment. The transfected cells were fixed with 4% PFA.

2.2.3.2.3 Immunocytochemistry

| | |
|-----------------------------------|--|
| 4% PFA | 4% (w/v) paraformaldehyde in 1x PBS |
| Blocking solution: | 2% (w/v) Glycine, 2% (w/v) BSA (Albumin Factor V, Applichem), 0.2% (w/v) Gelatine, 50 mM NH₂Cl |
| Permeabilization solution: | 0.25% (v/v) Triton X-100 dissolved in PBS |
| Mowiol: | 10% (w/v) Mowiol, 25% (v/v) Glycerol, 100 mM Tris-HCl, pH 8.5, 2.5% (w/v) DABCO |
| Vectashield® (with DAPI): | (Vector Laboratories Inc.) mounting medium |

The fixation of the primary neuronal cultures and cell lines was accomplished by the incubation of these cells with 4% PFA for 10 min at RT (for cell lines) and at 37°C (for neuronal cells). After fixation, the cells were washed 3x with 1x PBS at RT for 10 min. The permeabilization of the cells was performed by using 0.25% Triton X-100 dissolved in 1x PBS at RT for 10 mins. Then, the cells were washed 3x with 1x PBS at RT for 5 min. Afterwards, the cells were blocked with blocking solution at RT for 1,5 h. During this time, the primary antibody was spun at 14,000 at 4°C for 20 min and diluted into the blocking solution. The primary antibody dilutions were applied onto the cells

and incubated at 4°C overnight. The next day, the primary antibody was removed by washing (3x with 1x PBS at RT for 10 min). The secondary antibody (fluorescence-conjugated), diluted in blocking solution, was spun at 14,000 rpm at 4°C for 20 min and applied onto the cells and incubated at RT for 2 h. Next, the cells were washed (3x with 1x PBS at RT for 10 min) and the coverslips were mounted on slides by using either mowiol or Vectashield[®] mounting medium with DAPI, depending on the purpose of the experiment.

2.2.3.2.4 Stimulation of hippocampal primary cultures

| | |
|------------------------|---|
| Neurobasal (-): | (NeurobasalTM) |
| NMDA: | (Sigma) stock 100 mM in milipore water |
| Calpeptin: | (Calbiochem) stock 100mM in DMSO |
| E-64d: | (Sigma) stock 60 mM in DMSO |
| Anisomycin-D | (Sigma) stock 7,5 mM in milipore water |

For stimulation of the cultures with NMDA, primary cultures of hippocampal neurons (DIV 16 or DIV21) were treated with anisomycin-D at 37°C for 5 min. After that, 100 µM NMDA in stimulation buffer (Neurobasal medium with 7.5 µM anisomycin) was applied at 37°C for 5 min. After stimulation, cells were washed twice with stimulation buffer and then incubated at 37°C for 30 min. Cells were fixed with 4% PFA at 37°C for 10 min, immunostained with the appropriate primary and secondary antibodies as stated previously. For inhibition of calpain, primary cultures of hippocampal neurons (DIV16 for calpeptin, DIV21 for E-64d) were incubated with 60 µM calpeptin and 50 µM E-64d, for 30 min at 37°C. 100 µM NMDA in stimulation buffer (Neurobasal medium with 7.5 µM anisomycin) was applied at 37°C for 5 min in the presence of the inhibitors. After stimulation, cells were washed twice with stimulation buffer and then incubated at 37°C for 30 min. Cells were fixed with 4% PFA at 37°C for 10 min and immunostained with the appropriate primary and secondary antibodies as described before.

2.2.3.2.5 Quantitative immunocytochemistry

In NMDA stimulation experiments, with and without calpain inhibitors, the Jacob immunoreactivity in the nucleus was measured according to the following protocol: By utilizing DAPI staining, nuclei were identified and nuclear Jacob levels

were determined by calculating the mean pixel intensity from 2-3 nuclear planes. Differences between groups were described as relative deviations from the control. The nuclear membrane was excluded from the analysis. Images were obtained using a Leica DMRXE microscope equipped with a Krypton-Argon-Ion laser (488/ 568/ 647 nm) and an acousto-optic-tunable filter for selection and intensity adaptation of laser lines. Images were analyzed with ImageJ software (<http://rsb.info.nih.gov/ij>). *In vivo* time-lapse imaging and transfection of hippocampal primary neurons with Jacob-GFP was performed as described (Dieterich *et al.*, 2008). Stimulation was performed with 20 μ M NMDA either in the presence or absence of 60 μ M calpeptin.

2.2.4 Statistical analysis

The paired Student's *t* test and the Mann-Whitney U-test were used for statistical analyses when applicable using Excel software.

3. Results

3.1 Jacob interacts with α -Internexin

3.1.1 Subcellular distribution of Jacob in neurons

As mentioned previously, the subcellular distribution of Jacob in neurons is regulated by several ways. For instance, the myristoylation site at the N-terminus of Jacob attaches the protein to membraneous structures in the cell. Furthermore, the well-conserved bipartite NLS sequence of Jacob is located in the central α -helical region of the protein and the incomplete IQ motif is embedded into this region (Dieterich *et al.*, 2008). After NMDA-receptor activation Jacob translocated to the nucleus and this is mediated by Importin- α binding to its NLS sequence. In contrast, at elevated Ca^{2+} concentrations, Caldendrin binds to the IQ domain of Jacob and masks the NLS sequence of Jacob, thereby preventing the binding of Importin- α and subsequent nuclear translocation of Jacob suggesting that Caldendrin is one of the regulators of the extra-nuclear localization of Jacob.

Moreover, by over-expressing different deletion mutants of Jacob in COS7 cells and in primary neuronal cultures, it was shown that these regions are important for the subcellular localization of Jacob in these cells (Dieterich *et al.*, 2008; Zdobnova, Ph.D. thesis, 2008). It was also demonstrated that over-expression of nuclear Jacob in hippocampal primary cultures resulted in the accumulation of recombinant protein in the nucleus, which eventually leads to stripping of the synaptic contacts and the retraction of dendritic processes (Dieterich *et al.*, 2008). On the other hand, over-expression of certain splice isoforms of Jacob in hippocampal primary cultures resulted in a prominent extra-nuclear localization of Jacob and a more complex dendritic cytoarchitecture with an increased number of synaptic contacts in transfected neurons (Zdobnova, Ph.D. thesis, 2008). It has also been shown that the N-terminus of Jacob is crucial and sufficient to make these changes in the synapto-dendritic morphology of the transfected primary cultures (Zdobnova, Ph.D. thesis, 2008). To test whether the C-terminus of Jacob has any influence on the subcellular localization of the protein, a construct lacking the first 235 amino acids, C-terminal-Jacob-GFP, was overexpressed in hippocampal primary neurons. The recombinant protein accumulated in the nucleus without showing any distinct effects on the synapto-dendritic morphology of the transfected neurons (Dieterich *et al.*, 2008).

In order to unravel the functional significance of the C-terminus of Jacob, potential interaction partners of Jacob were screened in a Y2H screen at which the C-terminus of Jacob was used as bait. In this screen α -Internexin, a type IV IF was disclosed as a potential binding partner of Jacob (Daniela C. Dieterich and Michael R. Kreutz, unpublished data). α -Internexin is one of the components of the neuronal cytoskeleton of the mammalian brain and abundant in the somato-dendritic compartment of neurons (Kaufmann *et al.*, 2000). Based on the hypothesis that α -Internexin might provide a docking site for Jacob in neurons, the characteristics of the Jacob- α -Internexin interaction were analyzed using molecular and biochemical tools as well as with immunocytochemistry.

3.1.2 Distribution of α -Internexin immunoreactivity in subcellular fractions of rat brain

Previously, it was shown that α -Internexin is found in PSD fractions of rat brain (Suzuki *et al.*, 1997). To confirm these results, α -Internexin immunoreactivity (IR) was analyzed in various subcellular fractions prepared from rat brain using the protocol from Smalla *et al.*, (2003). Subsequent western blot analyses of the samples demonstrated that

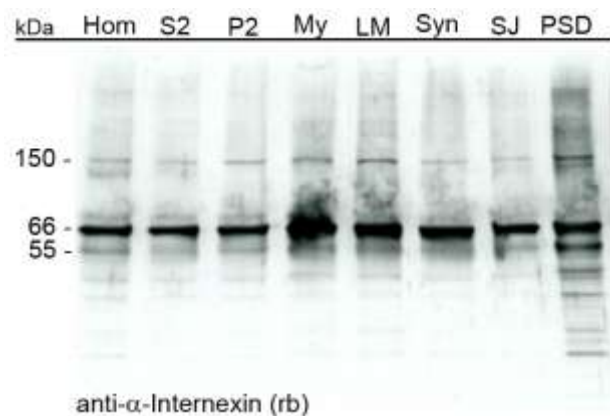


Figure 6. Distribution of α -Internexin immunoreactivity in subcellular fractions of adult rat brain. Different subcellular fractions (20 μ g/lane) obtained by differential centrifugation of homogenates of adult rat brains were analyzed by western blotting. Detection was done using a polyclonal α -Internexin rabbit antibody. (Hom, homogenate; S2, supernatant after removal of cell debris and nuclei; P2, crude membranes; My, myelin fraction; LM, light membranes; Syn, synaptosomes; SJ, synaptic junctions; PSD, postsynaptic density fraction).

α -Internexin IR is present more or less at the same level in all fractions of rat brain, including homogenate, S2, P2 and myelin fractions, light membranes, synaptosomes, synaptic junctions and PSD fractions (Fig. 6). This largely confirms the results of Suzuki *et al.* (1997), who detected α -Internexin IR in P1, synaptosomal, light membrane and myelin fractions (Suzuki *et al.*, 1997). The calculated molecular weight (MW) of full-length α -Internexin is 55 kDa. However, in a SDS-gel system, it migrates as a band at 66 kDa (Kaplan *et al.*, 1990; Fliegner *et al.* 1990). This discrepancy in migration rates is due to the difference between the phosphorylated and non-phosphorylated states of α -Internexin, a typical feature among all neurofilaments (Fliegner *et al.*, 1990). The phosphorylated form of the protein migrates more slowly and therefore is detected at 66 kDa. Similar to Suzuki *et al.*, α -Internexin IR was detected with a polyclonal α -Internexin rabbit antibody recognizing the most variable C-terminus tail domain of the protein. However, unlike Suzuki *et al.*, a lower band at ~55 kDa and a slight band at ~150 kDa are obtained in immunoblots (Fig. 6). These bands might correspond to degradation products and homo-dimers of α -Internexin, respectively (Evans *et al.*, 2002).

3.1.3 Subcellular distribution of α -Internexin in cultured hippocampal primary neurons

Previously, Benson *et al.* (1996) showed that α -Internexin immunostaining is present in all neurons of hippocampal primary cultures at all developmental stages (Benson *et al.*, 1996). It was shown that α -Internexin immunostaining is found as long filaments in axons and short fragments in dendrites which extended into dendritic spines (Benson *et al.* 1996). Moreover, studies revealed that α -Internexin is more abundant in the somata-dendritic compartment of neurons, whereas NFTP are predominantly found in axons of neurons (Kaufmann *et al.*, 2000). Similarly, in the present study, the subcellular distribution of α -Internexin was analyzed in hippocampal neurons at different developmental stages. The immunostainings of hippocampal primary neurons at different time frames were performed with a monoclonal α -Internexin mouse antibody, and the counterstaining was done for NF-H protein with a polyclonal NF200 rabbit antibody targeted to both phosphorylated and non-phosphorylated forms of NF-H protein (Fig. 7A-I). Similar to Benson *et al.* (1996), the results revealed that α -

Internexin is found in all developmental stages of hippocampal primary cultures tested (Fig. 7A-I). Immunofluorescence for NF-H protein shows a continuous distribution throughout the

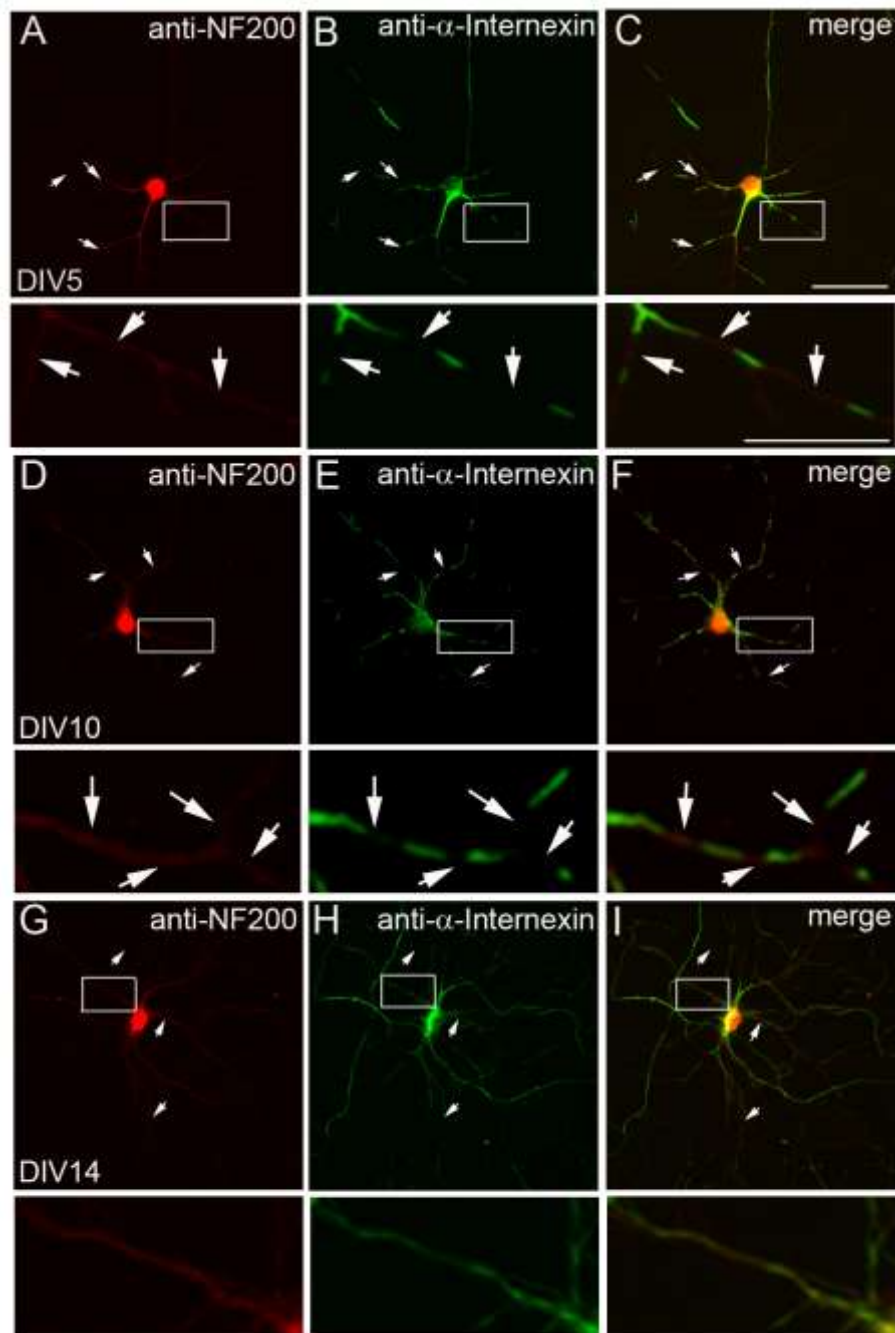


Figure 7. Fragmented immunostaining of α -Internexin was observed in hippocampal primary neurons of rat brain at early stages of development. Confocal laser scans revealed a fragmented distribution of α -Internexin immunostaining in dendrites of hippocampal primary cultures at (A-C) DIV5 and (D-F) DIV10. The α -Internexin immunostaining becomes continuous and overlaps with NF-H immunostaining at DIV14 (G-I). Arrows indicate

discontinuities or fragmented stainings of α -Internexin. Scale bar indicates 20 μm and 10 μm for the magnified pictures. (NF-H, neurofilament heavy chain). (DIV: day *in vitro*).

neuron at all time points investigated (Fig. 7A, D). On the other hand, at early stages of development α -Internexin exhibits a fragmented distribution in the dendrites of cultured neurons (Fig. 7B, E). Moreover, α -Internexin immunofluorescence becomes continuous and overlaps with NF-H immunofluorescence with neuronal maturation (Fig. 7H).

3.1.3.1 α -Internexin is not present at synapses of hippocampal primary neurons

In order to investigate whether α -Internexin is localized at synapses of hippocampal primary neurons, co-localization of α -Internexin with Bassoon, a major component of the presynaptic active zone, was checked using immunocytochemistry. Hippocampal primary cultures were fixed at DIV14 and co-immunostained with a monoclonal α -Internexin mouse antibody (Covance, clone 1D2) and a polyclonal Bassoon rabbit antibody (Fig. 8A-C). Results showed that α -Internexin immunofluorescence does not co-localize with the immunofluorescence of the presynaptic marker Bassoon, indicating that α -Internexin is not found in synapses (Fig. 8C).

In order to confirm that α -Internexin does not localize at synapses, co-localization of α -Internexin with another synaptic protein was tested. For this purpose, ProSAP2, one of the major scaffolding proteins of the PSD, was used. Similarly, hippocampal primary cultures were fixed at DIV14 and co-immunostained with a polyclonal α -Internexin rabbit antibody (Abcam, clone R36) and a polyclonal ProSAP2 guinea pig antibody. Results revealed that α -Internexin immunofluorescence does not overlap with ProSAP2 immunofluorescence in hippocampal primary neurons (Fig. 8D-F). In addition to these, co-immunostainings of pre- and postsynaptic markers were done with polyclonal α -Internexin chicken antibody (Chemicon) or another polyclonal α -Internexin rabbit antibody (Chemicon, clone R36). Similarly, the results showed that α -Internexin does not localize at synapses (Jale Sahin, unpublished data). Taken together, these data suggest that α -Internexin is not present at synapses of hippocampal primary neurons.

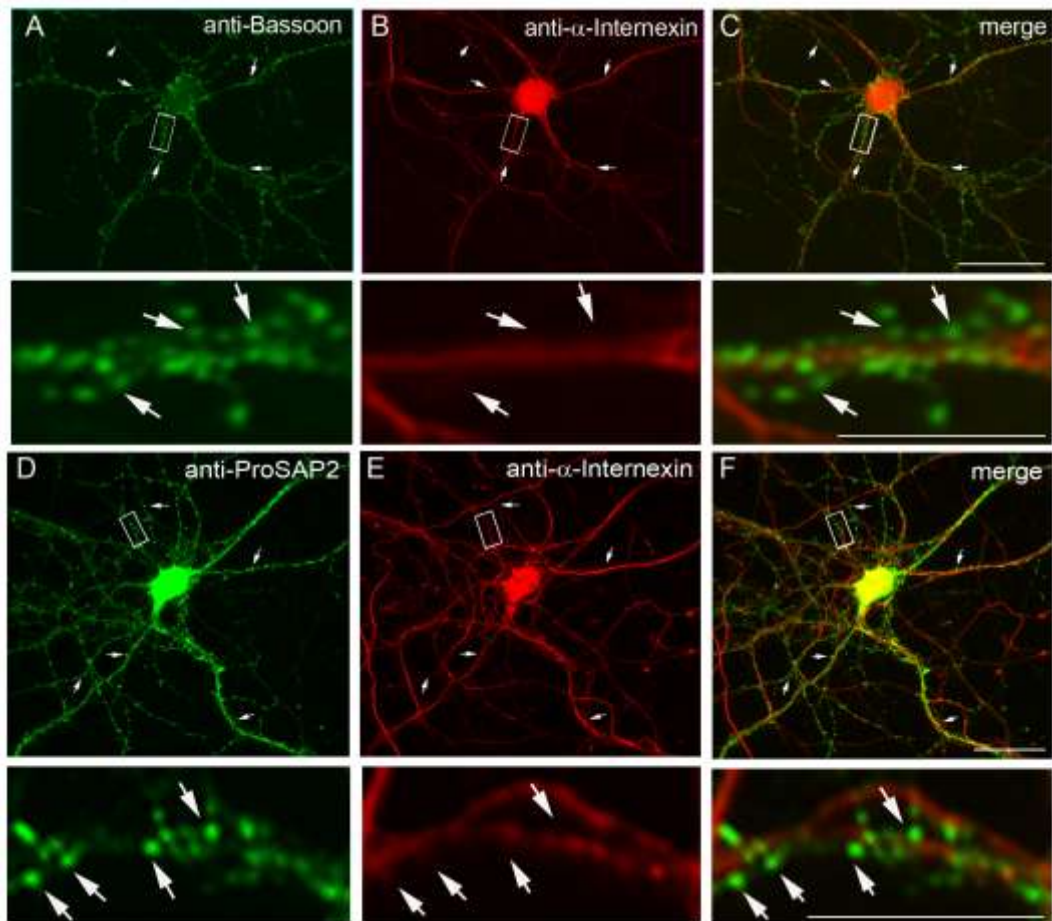


Figure 8. α -Internexin does not co-localize with pre- or postsynaptic markers, Bassoon and ProSAP2, respectively. Co-immunostaining of (B, E) α -Internexin (monoclonal mouse) (red) with (A, C) the presynaptic marker Bassoon (polyclonal rabbit) (green) or of (D, F) α -Internexin (monoclonal rabbit) (red) and the postsynaptic marker ProSAP2 (polyclonal guinea pig) (green) in DIV14 primary hippocampal cultures showed that α -Internexin co-localized with neither (A, B, C) Bassoon nor (D, E, F) ProSAP2. Scale bar indicates 10 μ m.

3.1.4 Jacob and α -Internexin co-localize in the soma and dendrites of hippocampal primary neurons

Previously it was shown that α -Internexin is predominantly found in the somato-dendritic compartment of neurons (Kaufmann *et al.*, 2000). Furthermore, as outlined in the previous section, α -Internexin is not localized at synapses. Therefore, the co-localization of Jacob and α -Internexin was analyzed in hippocampal primary cultures. The primary neurons were fixed at different developmental stages and co-immunostained with a monoclonal α -Internexin mouse antibody (Covance, clone 1D2) and a polyclonal JB150 rabbit antibody (Fig. 9). The confocal laser scan images

revealed that Jacob and α -Internexin co-localize in the dendrites and soma of hippocampal primary neurons at all stages of development tested (Fig. 9A-I).

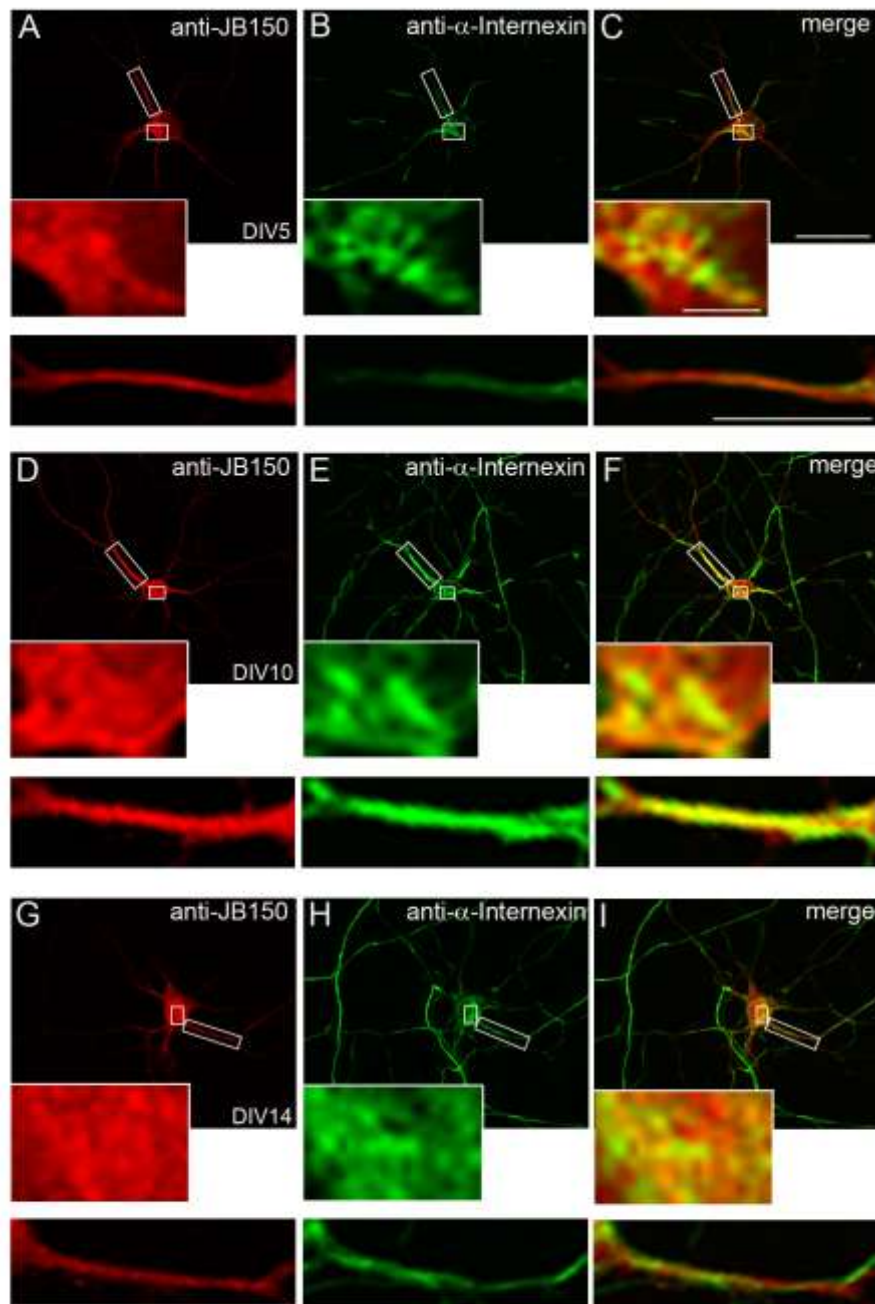


Figure 9. Jacob and α -Internexin co-localize at hippocampal primary neurons. Hippocampal primary cultures were fixed at different developmental stages and co-immunostained with (A, D, G) a polyclonal JB150 rabbit antibody and (B, E, H) a monoclonal α -Internexin mouse antibody. Confocal laser-scan images showed that (C, F, I) α -Internexin and Jacob co-localize in soma and dendrites of hippocampal primary neurons. The degree of co-localization differs depending on the age of the culture used for immunostainings. Scale bar indicates 20 μ m in the complete pictures and 10 μ m in magnified pictures.

3.1.5 Characterization of the Jacob- α -Internexin interaction

As mentioned above, the immunocytochemistry and western blot analysis revealed that the subcellular distribution of Jacob and α -Internexin overlaps. These data suggest that both proteins might interact *in vivo* and that α -Internexin might serve as a docking site for Jacob at the somato-dendritic compartment of neurons. We therefore investigated the putative interaction further using biochemical methods.

3.1.5.1 Biochemical characterization of the Jacob- α -Internexin interaction

To investigate whether both proteins are found in one complex, Co-IP experiments were performed. Adult rat brain tissue was homogenized in a 1% Triton X-100 containing homogenization buffer and then centrifuged at 1000 xg for 10 min. The supernatant obtained was spun at 30,000 xg for 30 min and used to precipitate α -Internexin. Polyclonal JB150 rabbit antibody was incubated with Protein A-agarose beads and the S1 fraction of rat brain overnight, and α -Internexin IR was detected on immunoblots by using a monoclonal α -Internexin mouse antibody (Fig. 10A). Results also demonstrated that on immunoblots α -Internexin IR appeared as two bands at 66 kDa and 55 kDa, showing that the degradation product of α -Internexin, visible as a band at 55 kDa (Evans *et al.*, 2002) also interacts with Jacob in S1 fraction of adult rat brain (Fig. 10A).

Similarly, Jacob was precipitated from protein extract of rat brain obtained by spinning the Triton X-100-treated S1 fraction of rat brain homogenate at 100,000 xg for 1 hr. A monoclonal α -Internexin mouse antibody was incubated with Protein G-agarose beads and the protein extract obtained from rat brain, described above. The polyclonal JB150 rabbit antibody was used to detect Jacob immunoreactivity on immunoblots. The results revealed that Jacob is present as two bands appearing at 60 kDa and 70 kDa, indicating that more than one Jacob isoform interacts with α -Internexin (Fig. 10B).

In addition, the Jacob- α -Internexin interaction was confirmed by performing a heterologous Co-IP from protein extracts of COS7 cells co-transfected with GFP- α -Internexin-wt and wt-Jacob-His-Myc constructs (Fig. 11A). In brief, the transfected COS7 cells were washed with ice-cold 1x PBS two times and incubated with an extraction buffer containing 1% Triton X-100 on ice for 50 min. After that, the cell lysate was centrifuged at 20,000 xg for 20 min and the supernatant was used for the Co-

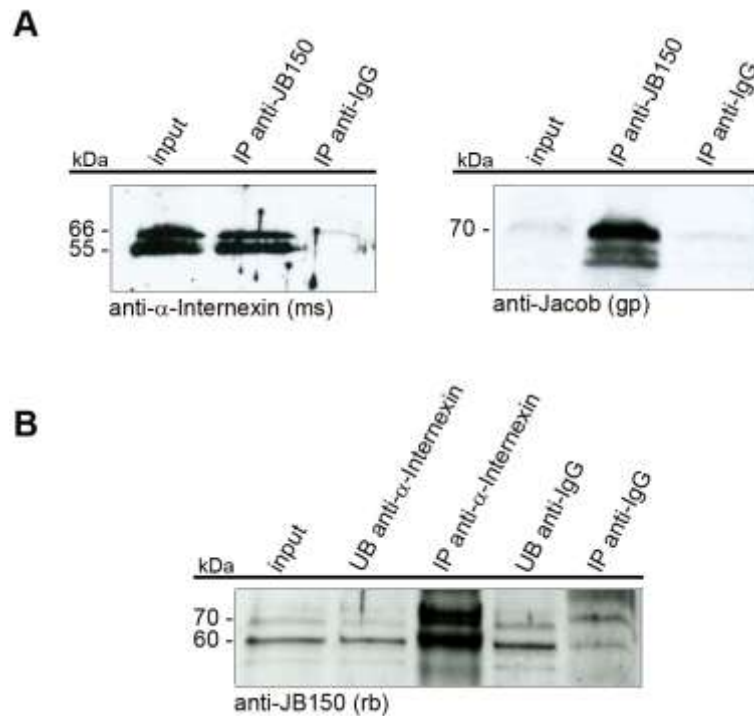


Figure 10. Co-IP of Jacob and α -Internexin from S1 fraction of adult rat brain (A) α -Internexin co-immunoprecipitated with Jacob from protein extract obtained by Triton X-100 extraction of adult rat brain homogenate. Immunodetection of α -Internexin protein was done with a monoclonal α -Internexin mouse antibody. A positive control (right) showed that the Co-IP worked properly. Immunodetection of Jacob protein was done using a polyclonal Jacob guinea pig (gp) antibody. (B) Jacob co-immunoprecipitated with α -Internexin from from protein extract obtained by Triton X-100 extraction of rat brain homogenate. Immunodetection was performed using the polyclonal JB150 rabbit antibody.

IP experiment. The polyclonal JB150 rabbit antibody was incubated with Protein A-agarose beads and the protein extract. The results showed that the GFP- α -Internexin-wt immunoprecipitated and the detection on immunoblot was done using a monoclonal α -Internexin mouse antibody (Fig. 11A). Additionally, a construct of Δ exon9-Jacob isoform (Dieterich *et al.*, 2008) lacking most of the C-terminus region of wt-Jacob protein, and GFP- α -Internexin-wt construct were co-overexpressed in COS7 cells. To immunoprecipitate GFP- α -Internexin-wt, the polyclonal JB150 rabbit antibody was incubated with Protein A-agarose beads and the protein extract obtained from the co-transfected COS7 cells using the same protocol described above. Immunoblotting of samples with a monoclonal α -Internexin mouse antibody showed that α -Internexin IR is present as a faint band (Fig. 11B), suggesting that the interaction of wt- α -Internexin and

Δ exon9-Jacob seems to be less pronounced than the interaction between wt- α -Internexin and wt-Jacob proteins.

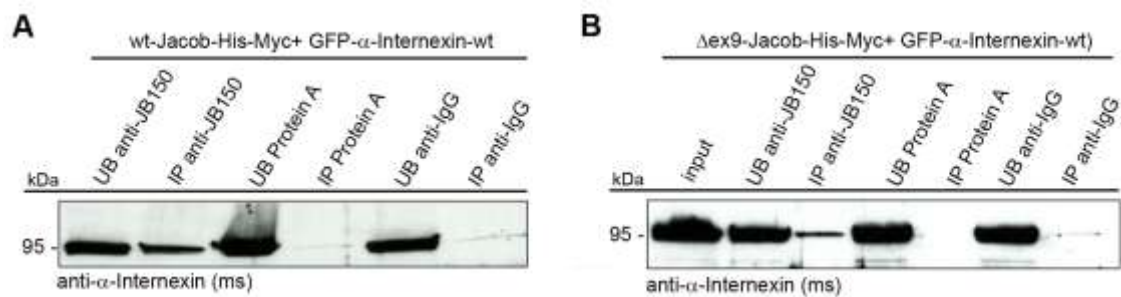


Figure 11. Heterologous Co-IP of Jacob and α -Internexin from cell lysates of COS7 cells co-transfected with different constructs of Jacob and α -Internexin. (A) α -Internexin is co-immunoprecipitated with Jacob from extracts of COS7 cells co-transfected with GFP- α -Internexin-wt and wt-Jacob-His-Myc constructs. (B) α -Internexin is co-immunoprecipitated with Δ exon9-Jacob from extracts of COS7 cells co-transfected with GFP- α -Internexin-wt and Δ exon9-Jacob-His-Myc constructs. Immunodetection was done with a monoclonal α -Internexin mouse antibody.

3.1.5.2 Molecular characterization of the Jacob- α -Internexin interaction

3.1.5.2.1 α -Internexin possesses potential Calpain cleavage sites

Most of the IF proteins as well as NFs are targets of Calpain-mediated limited proteolytic cleavage (Shields *et al.*, 1997; Bernier *et al.*, 1999; Shaw *et al.*, 2004). It has been shown that some of the cleavage products interact with other proteins and most of these interactions were shown to have a role in various signaling pathways in different cell types (Perlson *et al.*, 2005; Wu and Lynch, 2006). For example, Perlson *et al.* (2005) showed that after an axonal lesion of a sciatic nerve, Vimentin and Importin- β 1 local translations were increased at the lesion site. Activated Calpain, a cysteine protease activated by intracellular Ca^{2+} increase, cleaved Vimentin results in the formation of soluble Vimentin particles. These particles were shown to interact with pERK and Importin- β 1 and resulted in the retrograde transport of pERK to the nucleus with the help of the Dynein motor complex (Perlson *et al.*, 2005). Interestingly, amino acid alignment of rat α -Internexin and rat Vimentin showed that these proteins exhibit a high degree of homology in their amino acid sequences (Fig. 12) (Fliegner *et al.*, 1990;

Perlson *et al.*, 2005; Perlson *et al.*, 2006). Additionally, Vimentin was shown to be replaced by α -Internexin during neuronal development, and both proteins were found to have a role in the lysosomal-endosomal sorting machinery by a direct interaction with the AP-3 vesicle complex, suggesting that these two proteins might have similar functions in cells (Styers *et al.*, 2004).

| | | | |
|----------------------|-----|---|-----|
| α -Internexin | 1 | MSFGSEHYLCSASSYRKVFGDGSRLSARLSGPGASGSF-----RSQSLSR | 45 |
| Vimentin | 1 | MSTRS----VSSSSYRRMFG-GSGTSSR---PSSNRSYVTTSTRTYSLGS | 42 |
| α -Internexin | 46 | SNVASTAACSSASSLGLGLAYR----RLPAS-----DGLDLSQAAAR | 83 |
| Vimentin | 43 | ALRPSTSRSLYSSSPGGAYVTRSSAVRLRSMPGVRLQLQDSVDFSLADAI | 92 |
| α -Internexin | 84 | <u>TNEYKIIRTNEKEQLQGLNDRFAVFIKRVHQLETQNRALAEALALRQRH</u> | 133 |
| Vimentin | 93 | NTEFKNTRTNEKVELQELNDRFANYIDKVRPLEQQNKILLAELEQLKQG- | 141 |
| α -Internexin | 134 | <u>AEPSRVGELFQRELRELGELEEASSARAQALLERDGLAEVQRLRARCE</u> | 183 |
| Vimentin | 142 | -GKSRLGDLYEEMRELRRQVDQLTNDKARVEVERDNLAEIDIMRLREKLQ | 190 |
| α -Internexin | 184 | <u>EESRREGAERALKAQQRDVGATLARLDLEKKVESLLDELAFVRQVHDE</u> | 233 |
| Vimentin | 191 | EEMLRQEEAESTLQSFQDQVDNASLARLDLERKVESLQEEAFLKRLHDE | 240 |
| α -Internexin | 234 | <u>EVAELQASSQAA-AEVDVAVAKPDLTSALREIRAQYESLAAKNLQSAEEW</u> | 282 |
| Vimentin | 241 | EIQELQAQIQEQHVQIDVDVSKPDLTAALRDVRRQYESVAAKNLQSAEEW | 290 |
| α -Internexin | 283 | <u>YKSKFANLNEQAARSTEAIRASREEIHEYRRQLQARTIEIEGLRGANESL</u> | 332 |
| Vimentin | 291 | YKSKFADLSEAAANRNDALRQAKQESNEYRRQVQSLTCEVDALKGTNESL | 340 |
| α -Internexin | 333 | <u>ERQILELEERHSAEVAGYQDSIGQLESDLRNTKSEMARHLREYQDLLNVK</u> | 382 |
| Vimentin | 341 | ERQMREMEENFALEAANYQDTIGRLQDEIQNMKEEMARHLREYQDLLNVK | 390 |
| α -Internexin | 383 | <u>MALDIEIAAYRKLLGEETRFSTSGLSISGLNPLPNPSYL-----L</u> | 423 |
| Vimentin | 391 | MALDIEIATYRKLLGEESRISL-----PLPNFSSLNLRRETNLES | 431 |
| α -Internexin | 424 | PPRILSSTTSKVSSAGLSLKKEEEEEEEEGASKEVTKKTSKVGESFEET | 473 |
| Vimentin | 432 | P---LVDTHSKRT---LLIKTVETRD-----GQVINETSQHDDLE | 466 |
| α -Internexin | 474 | LEETVVS TKRTEKSTIEEITTSSSQKM 500 | |

Figure 12. Amino acid alignment of rat α -Internexin and rat Vimentin proteins. The amino acid alignment demonstrated that Coil1 and Coil2 regions of rat α -Internexin protein show high homology to the same regions of rat Vimentin protein (<http://www.ebi.ac.uk/Tools/emboss/align/>).

Previously, it has been reported that α -Internexin is sensitive to Calpain-mediated proteolysis, but neither the cleavage products nor the cleavage sites of α -Internexin were identified (Chan *et al.*, 1998). Therefore, potential Calpain cleavage sites in rat α -Internexin amino acid sequence were checked by aligning the rat α -

Internexin amino acid sequence with known potential Calpain cleavage sites found in rat and mouse Vimentin (Fig. 13). Analysis revealed that there are two potential Calpain cleavage sites located in the tail domain of rat α -Internexin (Fig. 13). There is also a potential PEST (proline (P), glutamate (E), serine (S), threonine (T)) sequence frequently found in proteins that undergo proteolysis (Rechsteiner and Rogers, 1996), and is detected in the tail domain of rat α -Internexin.

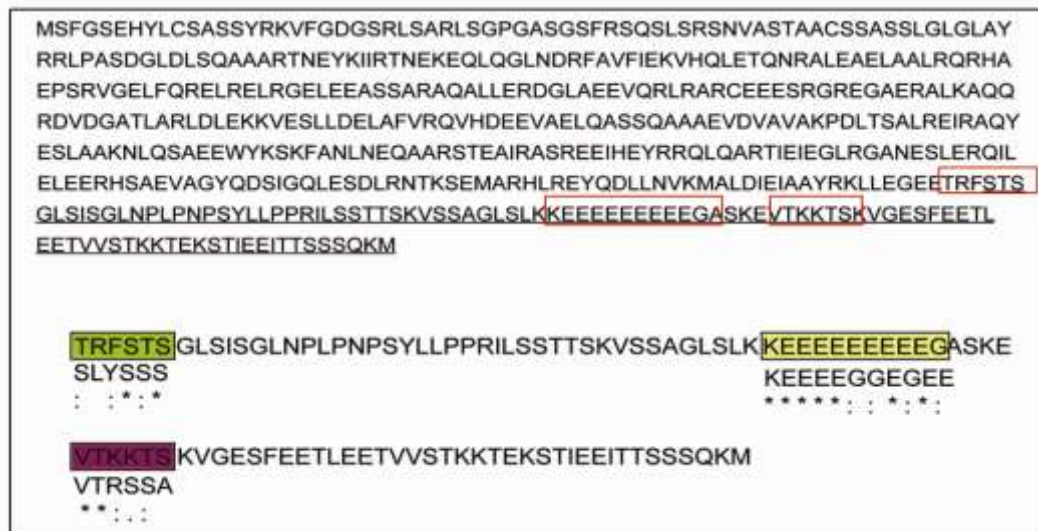


Figure 13. α -Internexin possesses potential Calpain cleavage sites and a potential PEST domain. The amino acid alignments with confirmed Calpain cleavage sites of Vimentin (SLYSSS from mouse and VTRSSA from rat) showed that there are two potential Calpain cleavage sites at the C-terminus of rat α -Internexin, highlighted in green and pink, respectively. Additionally, there is a potential PEST domain (highlighted in yellow) found in the α -Internexin tail domain (underlined). The corresponding amino acid sequence, KEEEEEGEGEE, is the PEST domain of the rat NF-L protein. (NF-L: neurofilament light chain) (<http://www.ebi.ac.uk/Tools/emboss/align/>).

3.1.5.2.2 Mapping the Jacob- α -Internexin binding region using the Y2H system

In this PhD thesis, in order to characterize the binding regions of protein-protein interactions, the Y2H system from Clontech (Matchmaker TM GAL4 Two-Hybrid System) was used. Briefly, based on transcriptional activation, the Y2H system screens for the interacting proteins and also determines the interaction interfaces between two proteins that are known to interact. The protein of interest, denoted as “bait,” is fused to a DNA-binding domain. Protein or protein fragments that bind to the bait, also known

as “prey,” are fused to a transcription activation domain. Any protein that binds to the bait will activate the transcription of an HIS reporter gene. Similarly, here, in order to map the binding region of the Jacob α -Internexin interaction, several constructs of the proteins were cloned into bait-and- prey plasmids (section 6.3). Potential Calpain cleavage sites located in the tail domain of α -Internexin were considered during the preparation of yeast constructs used in interaction assays. The results of several Y2H interaction assays revealed that the smallest α -Internexin fragment responsible for the Jacob interaction was indeed located between two potential Calpain cleavage sites, encompassing a peptide ranging from residues 408 to 442 (α -Internexin₄₀₈₋₄₄₂) (Fig. 14),

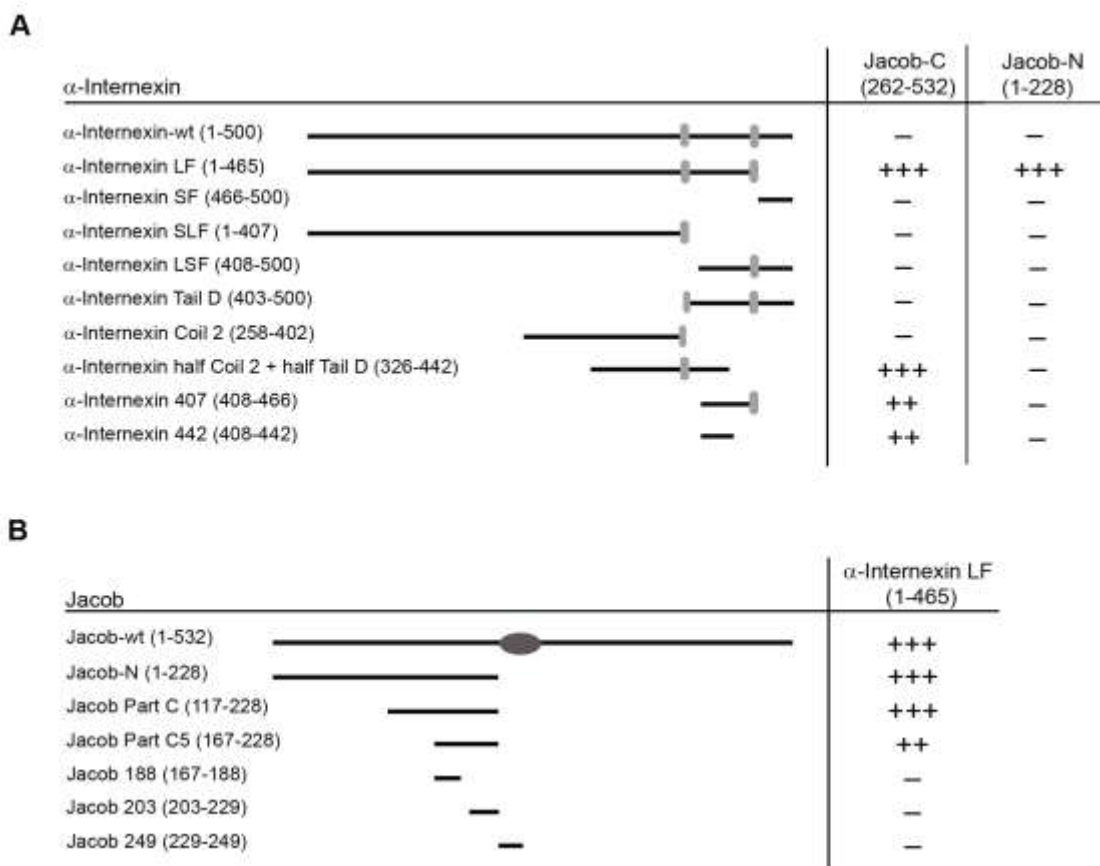


Figure 14. Mapping of the Jacob- α -Internexin interaction region using the yeast two-hybrid system. (A) α -Internexin has two different interaction sites for the N- and C-terminuses of Jacob. α -Internexin 442₄₀₈₋₄₄₂ -Jacob-C₂₆₂₋₅₃₂ interaction is specific. (B) The second interaction interface for Jacob, Jacob C5₁₆₇₋₂₂₈, contains the Ser180 Erk kinase phosphorylation site. (+++ and ++ : yeast growth in TDO media was detected on days 3 and day 4 after plating, respectively, — : no interaction)

Surprisingly, the full length α -Internexin protein did not interact with any of the Jacob proteins used, namely Jacob-C (263-532) and Jacob-N (1-228) (Fig. 14A). Moreover, α -Internexin fragments containing the last few amino acids of the protein from 466 to 500 did not show any interaction with the Jacob C-terminus (Fig. 14A). Interestingly, it was previously shown that the tail domain of NFs can fold back resulting in an intramolecular interaction (Janmey *et al.*, 2003). Similar to this, the very C-terminus of α -Internexin (residues 466-500) might fold back and have a negative influence on the interaction with Jacob. Furthermore, the yeast interaction assays also showed that there is a second interaction site in the rat α -Internexin amino acid sequence that binds to the N-terminus of Jacob (Fig 14B). More importantly, it has been recently shown in our lab that Jacob is phosphorylated by ERK kinases and the phosphorylation site is identified as serine residue 180, located at the N-terminus of the protein (Marina Mikhaylova, unpublished data). Interestingly, here, the minimal interaction region in Jacob N-terminus for α -Internexin was identified as a fragment lying between residues 167 and 228 (Jacob Part C5₁₆₇₋₂₂₈), including the ERK kinase phosphorylation site, serine 180 (Fig. 14B).

3.1.5.2.3 α -Internexin is cleaved by Calpain *in vitro*

Previously, it has been shown that α -Internexin is sensitive to Calpain-mediated degradation, but neither the cleavage products nor the cleavage sites have been identified (Chan *et al.*, 1998) In the present work, it has been shown that the rat α -Internexin amino acid sequence possesses two potential Calpain cleavage sites located on the most variable tail region (Fig. 13). Moreover, the Y2H interaction assays revealed that the α -Internexin fragment located between these two potential cleavage sites interacts with the C-terminus of Jacob (Fig. 14). Additionally, *in vitro* Calpain cleavage assays revealed that a GFP- α -Internexin-wt-Myc recombinant protein is cleaved by μ -Calpain (Fig. 15). In order to differentiate the N- and C-terminal cleavage products of α -Internexin, a construct of α -Internexin having two tags, GFP- in the beginning and Myc-tag in the end of the protein, was used. However, unfortunately no cleavage products were detected, possibly due to the very rapid degradation of the α -Internexin recombinant protein after the μ -Calpain addition to the reaction mixture.

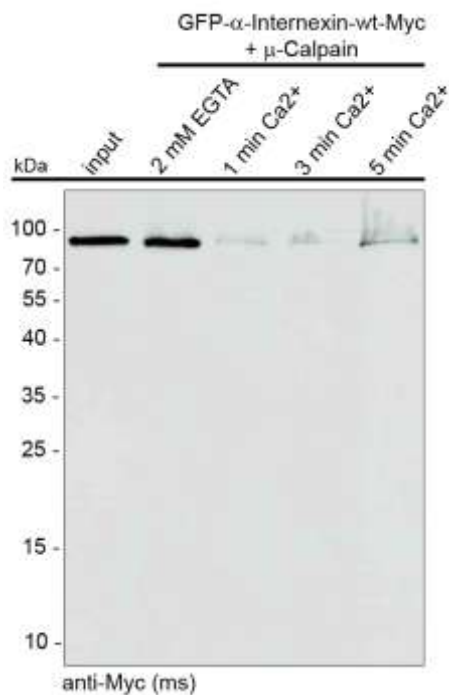


Figure 15. A GFP- α -Internexin-wt-Myc recombinant protein is cleaved by μ -Calpain in vitro. Protein extracts of COS7 cells transfected with GFP- α -Internexin-wt-Myc construct were purified using GFP (ms) antibody-coupled magnetic beads (μ MACS Anti-GFP Starting Kit, Miltenyi Biotec), and the protein elution was used for the in vitro Calpain assay. The eluted GFP- α -Internexin-wt-Myc recombinant protein was cleaved very rapidly in the presence of μ -Calpain and 2mM Ca^{2+} , whereas no cleavage was detected in the presence of 2mM EGTA.

3.1.6 α -Internexin does not accumulate in the nucleus after NMDA receptor activation

Previously, it was shown that Jacob translocates to the nucleus after NMDA receptor activation (Dieterich *et al.*, 2008). It is also known that Calpain can be activated by the Ca^{2+} influx generated by NMDA receptor stimulation (Sato *et al.*, 2001; Croall *et al.*, 2007; Lynch and Glieman, 2007). In addition, it has been shown that Vimentin-mediated retrograde transport of phosphorylated ERK requires Calpain cleavage of Vimentin (Perlson *et al.*, 2005). Therefore, in analogy to Vimentin, the role of α -Internexin in the retrograde transport of Jacob after NMDA receptor activation was investigated.

Hippocampal primary cultures at DIV21 were stimulated with NMDA and checked for α -Internexin IR in the nucleus. An antibody against the C-terminus tail domain of α -Internexin was used to detect α -Internexin fragments that might be formed after Calpain cleavage (Fig. 16M). Results showed that after NMDA bath application, Jacob accumulates to a significant extent in the nucleus (Fig. 16E) but that there is no increase in α -Internexin IR in the nuclei of stimulated neurons (Fig 16D). However, interestingly the nuclear translocation of Jacob is blocked after NMDA receptor stimu-

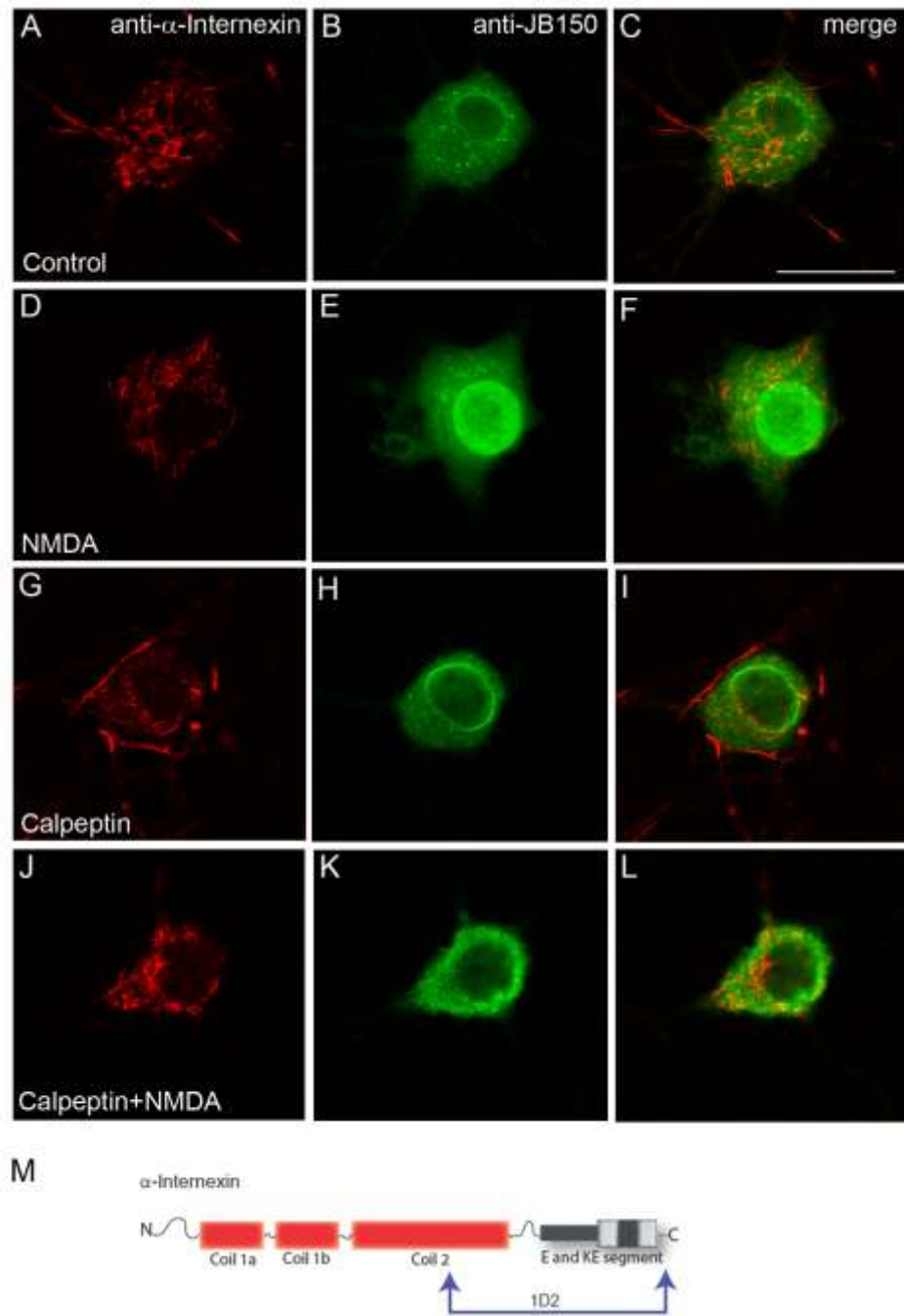


Figure 16. After NMDA bath application, α -Interneixin does not accumulate in the nucleus of stimulated hippocampal primary neurons. (A-L) Hippocampal primary cultures (DIV21) were stimulated with 100 μ M NMDA for 5 min. 30 min after stimulation cultures were fixed and co-immunostained with a monoclonal α -Interneixin mouse and a polyclonal JB150 rabbit antibody to visualize the nuclear localization of both proteins. (E) After NMDA bath application, Jacob IR is detected in the nucleus of stimulated neurons, whereas (D) NMDA stimulation does not cause nuclear accumulation of α -Interneixin in the same primary neurons. (K) After NMDA stimulation, in the presence of a Calpain inhibitor, calpeptin, nuclear translocation of Jacob is prevented. Scale bar indicates 20 μ m. (M) The scheme shows the epitope that is recognized by the monoclonal α -Interneixin mouse antibody (clone 1D2, Evans *et al.*, 2002).

lation in the presence of calpeptin, a Calpain inhibitor (Fig. 16K). In conclusion, these data revealed that α -Internexin does not enter the nucleus after NMDA bath application, and inhibition of Calpain activity has a prominent negative effect on the transport of Jacob to the nucleus upon NMDA receptor activation in the presence of the Calpain inhibitor calpeptin (Fig. 16).

3.1.7 Full-length α -Internexin does not co-immunoprecipitate with Dynein Intermediate Chain, Importin- α 1 or Importin- β 1 in S1 fraction of adult rat brain tissue

It was previously shown that Vimentin is expressed in all neurons of the CNS and PNS at early stages of mammalian nervous system development (Cochard and Paulin, 1984). Moreover, as CNS development proceeds, Vimentin molecules are replaced by type IV intermediate filaments starting with α -Internexin (Steniert *et al.*, 1999). In addition, rat α -Internexin and Vimentin show significant homology in their amino acid sequences (Fig. 12) and are shown to be functionally related to each other (Styers *et al.*, 2004). Furthermore, according to data from Perlson *et al.* (2005), the direct interaction of Vimentin particles with the Dynein motor complex via the Dynein intermediate chain (IC) and Importin- β 1 is important for the retrograde transport of phosphorylated ERK in sciatic nerve axon (Perlson *et al.*, 2005). Similar to Vimentin, it was hypothesized that α -Internexin might interact with the components of the Dynein motor complex. In order to test this hypothesis, an S1 fraction of adult rat brain, obtained by Triton X-100 extraction (section 2.2.2.5.1), was incubated overnight with a polyclonal α -Internexin rabbit antibody and Protein A-agarose beads. The samples were loaded on a SDS-gel and analyzed by western blotting for the presence of Dynein IC, with a monoclonal Dynein IC mouse antibody (Fig. 17A); for Importin- α 1, with a monoclonal Importin- α 1 mouse antibody (Fig. 17B); and for Importin- β 1, with a monoclonal Importin- β 1 (NTF97) mouse antibody (Fig. 17C). The positive control showed that α -Internexin was immuno-precipitated (Fig. 17D). However, immunoblot analysis revealed that α -Internexin does not co-immunoprecipitate with Dynein IC, Importin- α 1 or Importin- β 1 (Fig. 17). Thus, it is questionable whether α -Internexin is associated with Dynein IC, Importin- α 1 or Importin- β 1 at least in adult rat brain.

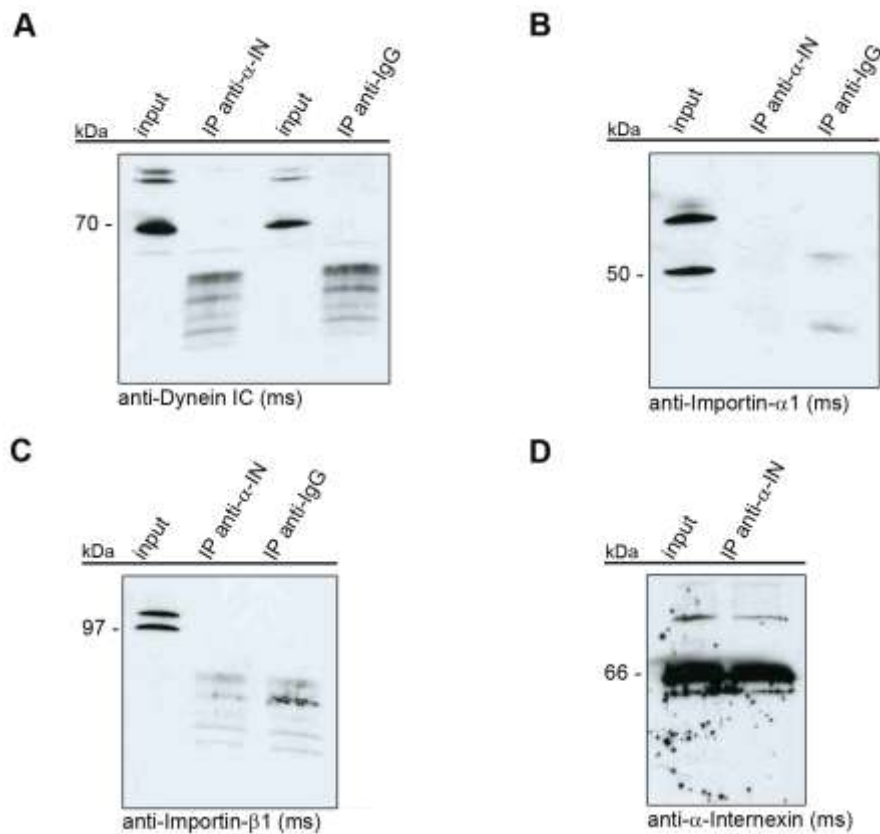


Figure 17. Co-IPs from an S1 fraction of rat brain do not show that α -Internexin in the same complex with the components of Dynein motor complex. The S1 fraction of adult rat brain tissue was obtained by using 1% Triton X-100 in the homogenization buffer, incubated with a polyclonal α -Internexin rabbit antibody. The results showed that α -Internexin don't interact with (A) Dynein IC, (B) Importin- α 1, (C) Importin- β 1. The immunodetections were done using monoclonal mouse antibodies of (A) Dynein IC, (B) Importin- α 1, (C) Importin- β 1, and (D) α -Internexin. (D) Positive control showed that the IP worked properly. (IP: immunoprecipitate, α -IN: α -Internexin).

3.1.8 α -Internexin and Importin- β 1 do not co-localize in hippocampal primary neurons after NMDA bath application

In order to show whether endogenous α -Internexin and Importin- β 1 proteins co-localize in hippocampal primary neurons, the primary cultures were fixed at DIV16 and co-immunostained with a polyclonal α -Internexin rabbit antibody and a monoclonal Importin- β 1 mouse antibody in non-stimulated conditions and after NMDA stimulation (Fig. 18). Results revealed that there is a partial co-localization of α -Internexin and Importin- β 1 in non-stimulated primary neurons (Fig. 18A-C), whereas α -Internexin and

Importin- β 1 do not co-localize in NMDA-treated primary neurons (Fig. 18D-F). Furthermore, in untreated cultures, Importin- β 1 exhibits both a somatic and nuclear distribution (Fig. 18B), though the latter is more prominent after NMDA bath application (Fig. 18E). Moreover, the subcellular distribution of Importin- β 1 at basal conditions and after NMDA stimulation is consistent with the data from Thompson *et al.* (2004), where it was shown that Importin- β 1 translocates from somato-dendritic compartments to the nucleus after NMDA receptor activation (Thompson *et al.*, 2004).

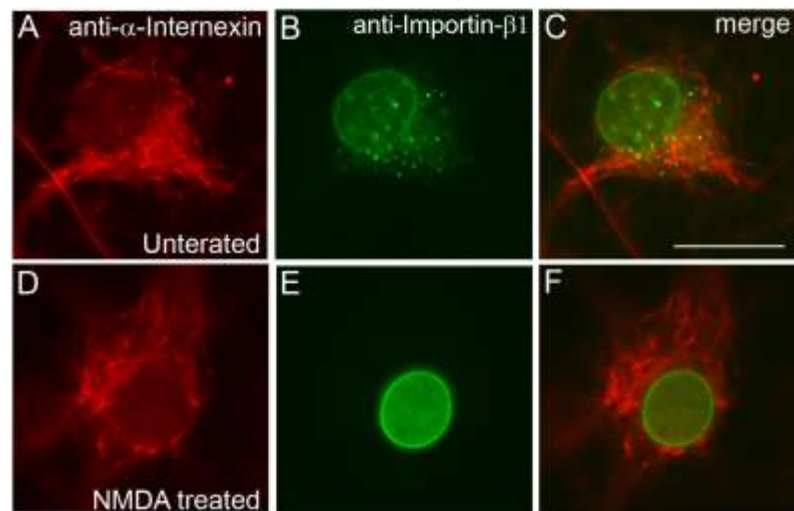


Figure 18. α -Internexin and Importin- β 1 show very little co-localization in hippocampal primary neurons after NMDA stimulation. (A-C) Immunofluorescence images show that at basal conditions (A), α -Internexin has a somatic distribution, whereas (B) Importin- β 1 exhibits both a somatic and nuclear distribution. (C) α -Internexin and Importin- β 1 partially co-localize at basal levels. (D-E) After NMDA stimulation, (D), α -Internexin is not accumulated in the nucleus but is detected in the soma of stimulated neurons, whereas (E) Importin- β 1 translocates to the nucleus and exhibits a prominent nuclear distribution. (F) α -Internexin and Importin- β 1 do not co-localize after NMDA application. Scale bar indicates 10 μ m.

3.2 Jacob-induced PSD-like protrusions are preferentially formed in discontinuities of α -Internexin immunostaining

The Jacob gene is composed of 16 exons, most of them smaller than 120 bp. A number of different Jacob isoforms with different calculated molecular weights are generated by alternative splicing (Dieterich *et al.*, 2008). As mentioned above, one of these isoforms, Δ exon9-Jacob, is formed by the deletion of exon 9, which causes a frame-shift in the coding sequence resulting in an alternative stop codon (Dieterich *et al.*, 2008, Kindler *et al.*, 2009). The resulting protein contains the N-myristoylation site and NLS sequence but lacks a large portion of the C-terminus. Scanning electron micrographs (SEM) showed that neurons transfected with Δ exon9-Jacob-GFP have very large round-shaped structures formed around the cell body and along the dendrites (Zdobnova, Ph.D. thesis 2008). Additionally, immunohistochemical data revealed that the PSD-like protrusions could recruit various PSD proteins such as PSD-95, ProSAP2/Shank3, NMDA- and AMPA-receptor subunits before synaptogenesis takes place (Zdobnova, Ph.D. thesis, 2008). Moreover, the interaction partners of Jacob-like Caldendrin and Kalirin are highly abundant in these protrusions (Zdobnova, Ph.D. thesis, 2008). Previous results indicated that the N-terminus of Jacob (residues 1-228) is required for the formation of PSD-like protrusions (Pöll, Diploma thesis, 2005) and that the N-terminus is sufficient for the morphogenetic effects of Jacob induced by its nuclear accumulation after NMDA bath application (Dieterich *et al.*, 2008). So far, here it has been shown that α -Internexin is abundant in the somato-dendritic compartments of neurons, and the interaction with Jacob was further characterized. Moreover, it has been shown that α -Internexin exhibits a fragmented distribution in dendrites of immature hippocampal primary neurons (Benson *et al.*, 1996, and Fig. 7). Since Jacob-induced protrusions are most pronounced in young neurons, it was asked whether the presence of α -Internexin has a negative influence on the formation process of these protrusions. Thus, to analyze whether there is a correlation between the formation of PSD-like protrusions and the presence of α -Internexin, the Jacob- Δ exon9-GFP construct was over-expressed in hippocampal primary cultures at DIV5. 24h after transfection, the transfected cells were fixed and immunostained with a monoclonal α -Internexin mouse antibody (Fig. 19). Results showed that Jacob-induced PSD-like protrusions are formed preferentially in locations where α -Internexin immunostaining is

either absent or only very faint staining is present (Fig. 19A). Furthermore, quantification of the data revealed that the effect is statistically significant (Fig. 19B).

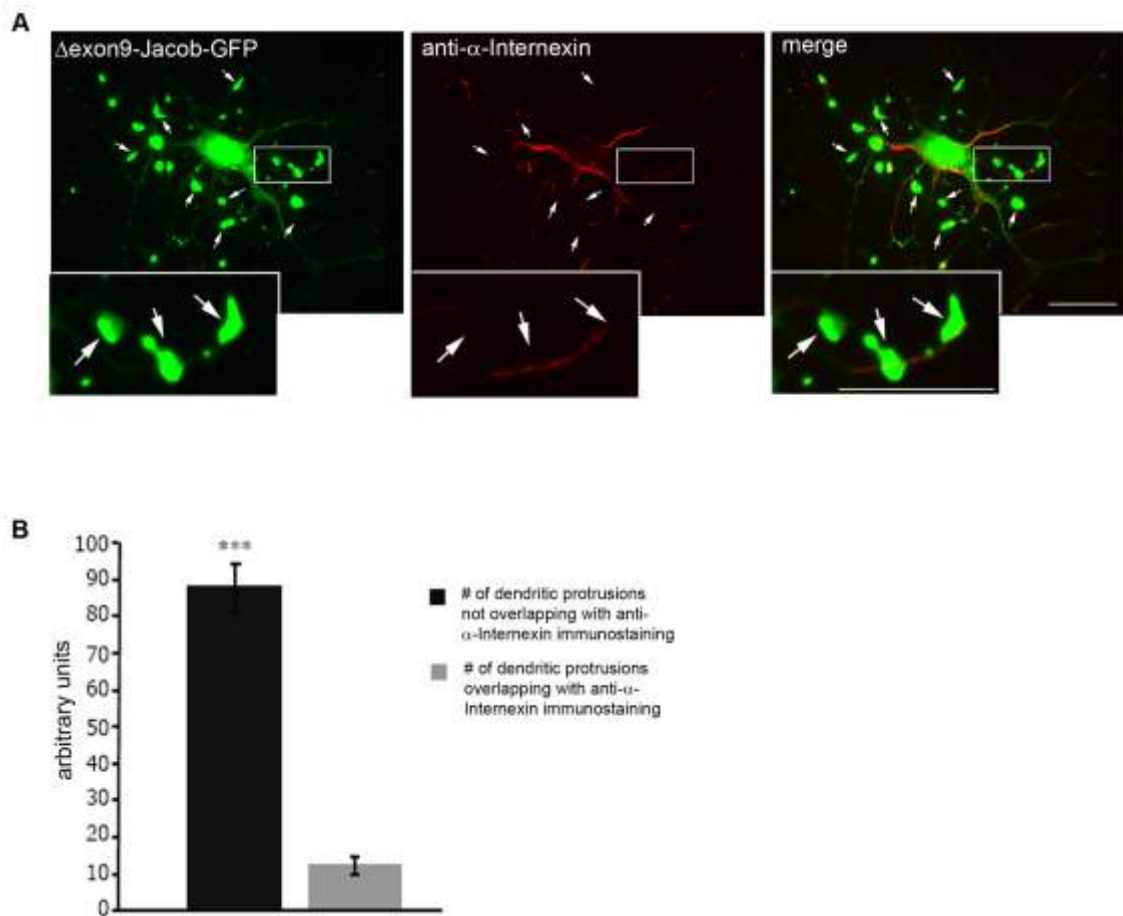


Figure 19. PSD-like protrusions are formed in places where α -Internexin IR was absent or of very low intensity. (A) Primary hippocampal cultures at DIV5 were transfected with a Δ exon9-Jacob-GFP construct. Fixation and immunostaining for α -Internexin (red) of transfected primary neurons was performed 24h after transfection. (B) The protrusions located in the discontinuities and those overlapping with the α -Internexin immunostaining were counted. Statistical analysis of the data indicated that Jacob-induced dendritic protrusions are formed preferentially at the discontinuities of α -Internexin immunostaining. N=20 cells per group ($p < 0.05$; Student t-Test). Scale bar indicates 10 μ m.

3.2.1 Co-overexpression of GFP- α -Internexin-wt abolishes the formation of Δ exon9-Jacob-Myc-induced PSD-like protrusions in transfected hippocampal primary neurons

Over-expression of the Δ exon9-Jacob-Myc construct results in the formation of protrusions in hippocampal primary neurons also at later stages of development as well (Fig. 20A) (Zdobnova, Ph.D. thesis, 2008). On the other hand, the over-expressed GFP- α -Internexin-wt protein accumulates in the soma and dendrites of transfected neurons (Fig. 20B).

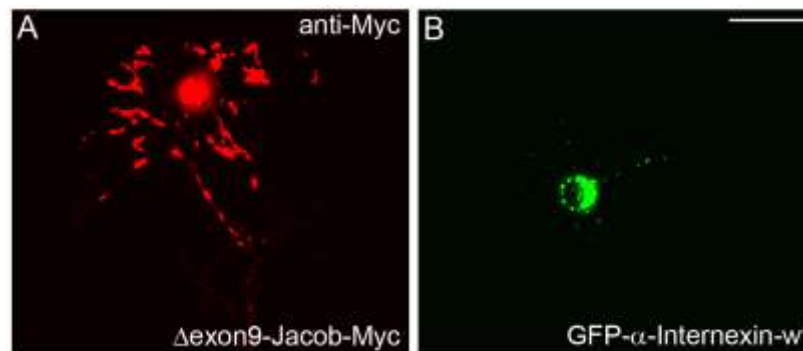


Figure 20. Δ exon9-Jacob-Myc and GFP- α -Internexin-wt exhibit different subcellular localizations in hippocampal primary neurons at DIV9. (A) Over-expression of Δ exon9-Jacob-Myc construct in hippocampal primary neurons at DIV9 results in the formation of PSD-like protrusions in dendrites in the nucleus of the transfected neurons. To visualize the Δ exon9-Jacob-Myc protein in transfected neurons, a monoclonal Myc mouse antibody was used for immunostaining. (B) GFP- α -Internexin-wt over-expression reveals a somato-dendritic distribution of the recombinant protein in transfected hippocampal primary neurons at DIV9. Scale bar 50 μ m.

In order to analyze whether co-over-expression of GFP- α -Internexin-wt and Δ exon9-Jacob-Myc prevents the formation of PSD-like protrusions, hippocampal primary cultures were co-transfected with Δ exon9-Jacob-Myc and GFP- α -Internexin-wt constructs at DIV9. 24h after transfection, transfected neurons were fixed and immunostained with a monoclonal Myc mouse antibody to visualize the Δ exon9-Jacob-Myc protein (Fig. 21C, F). Results revealed that in the presence of GFP- α -Internexin-wt, Jacob-induced protrusions are much less pronounced (Fig. 21D, F). Moreover, in

most of the transfected neurons (~80% of the transfected neurons, Jale Sahin, unpublished observations) protrusions were not formed at all (Fig. 21A, C). Taken together, these results suggest that GFP- α -Internexin-wt has a negative influence on the formation of Jacob-induced PSD-like protrusions when it is co-overexpressed with Δ exon9-Jacob-Myc construct.

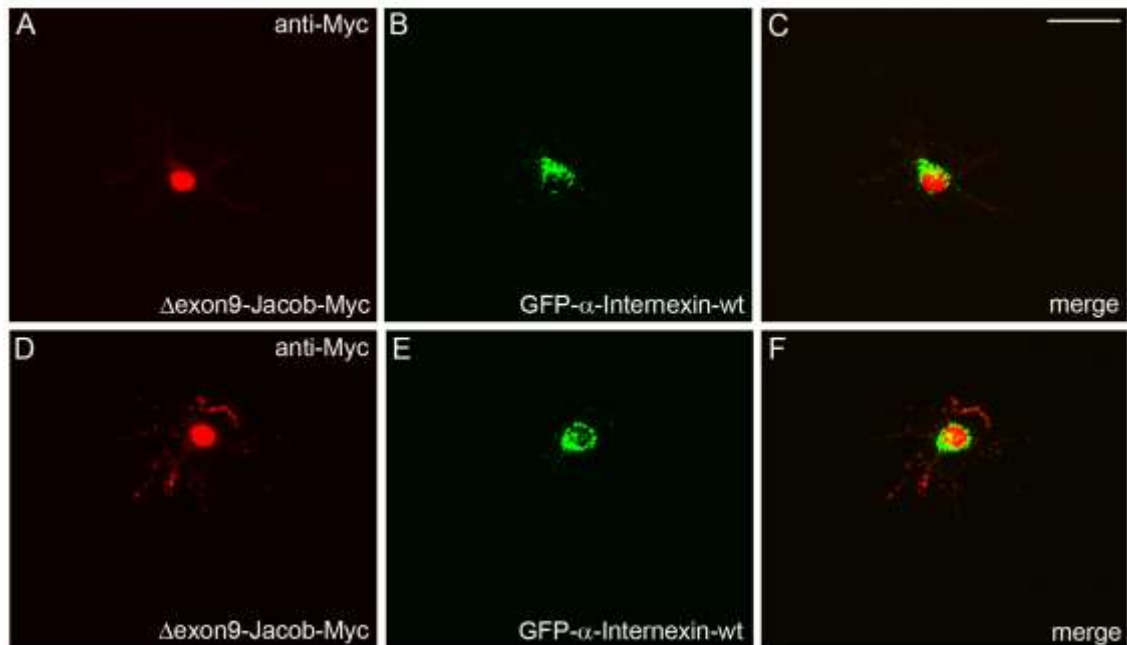


Figure 21. Co-over-expression of GFP- α -Internexin-wt and Δ exon9-Jacob-Myc constructs in hippocampal primary neurons abolishes the effect of extra-nuclear Jacob over-expression that results in the formation of PSD-like protrusions. (A) When it is co-overexpressed with GFP- α -Internexin-wt, the Δ exon9-Jacob-Myc protein is mostly localized in the nucleus of transfected hippocampal primary neurons at DIV9. (D) There are cases (about 20% of the transfected primary neurons) where Jacob-induced PSD-like protrusions are still formed but exhibit a smaller size compared to the protrusions formed in single-transfected primary neurons (Fig. 21A). (B, E) Subcellular distribution of GFP- α -Internexin-wt did not change with co-over-expression. (C, F) The over-expressed recombinant proteins exhibit different subcellular localizations in transfected hippocampal primary neurons. Scale bar 50 μ m.

3.2.2 The presence or absence of α -Internexin has no influence on the formation of synapses in hippocampal primary neurons

Jacob-induced PSD-like protrusions are formed at early stages of development, before synaptogenesis takes place (Zdobnova, Ph.D. thesis, 2008). In the present work,

it has been shown that these protrusions are formed preferentially in places where α -Internexin immunofluorescence was not detected (Fig. 19), and also co-overexpression studies indicated that the presence of GFP- α -Internexin-wt protein seem to negatively affect the formation of Jacob-induced protrusions (Fig. 21). Although these Jacob-induced PSD-like protrusions probably do not reflect a role of the protein in synaptogenesis, we still asked whether the presence or absence of α -Internexin has any influence on the number of synapses in hippocampal primary neurons at DIV10. For this purpose, cultured primary neurons were fixed at DIV10, and the fragmented staining was visualized with a polyclonal α -Internexin rabbit antibody and a polyclonal

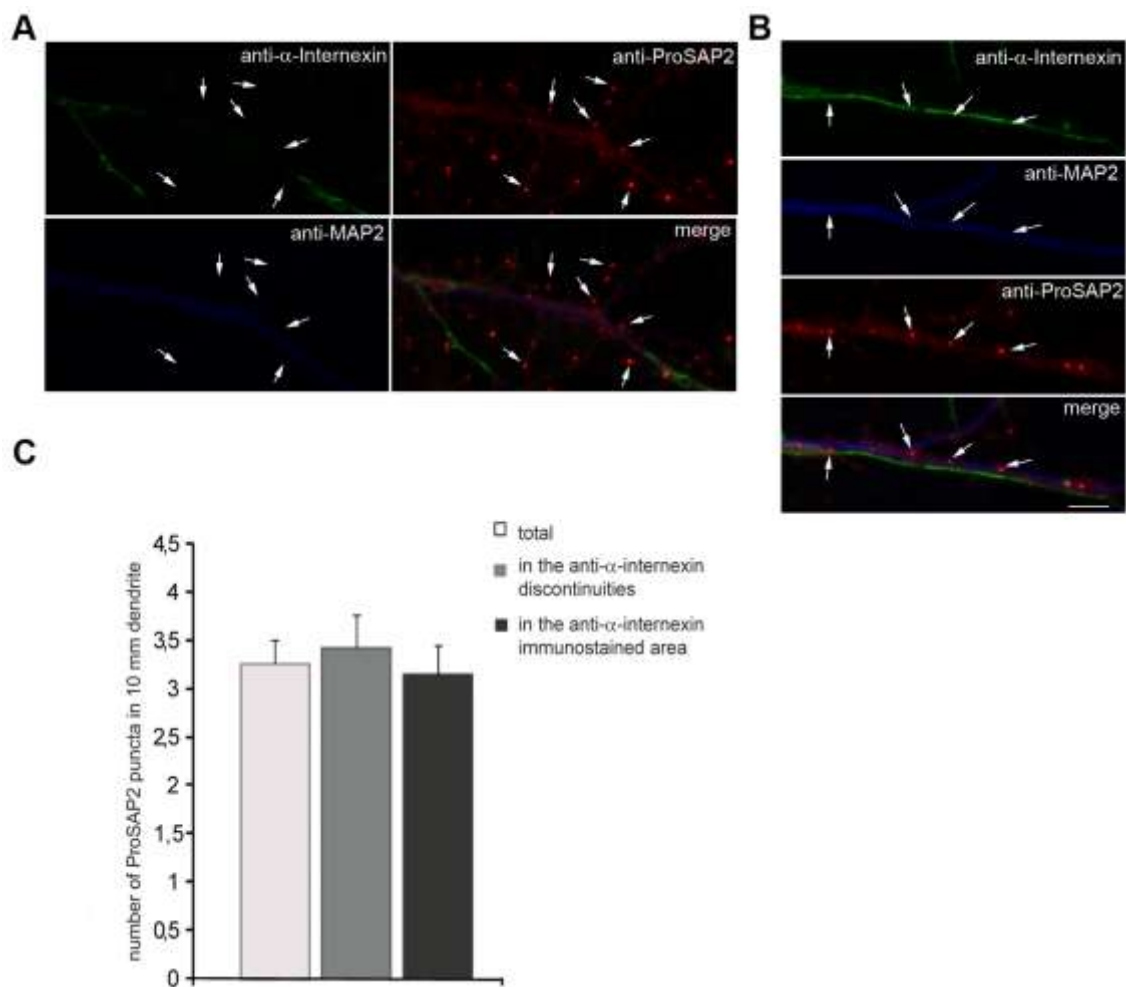


Figure 22. The presence of α -Internexin has no effect on synapse formation. Primary hippocampal neurons (DIV10) were fixed and co-immunostained with α -Internexin (ms) (green), ProSAP2 (gp) (red) and MAP2 (ms) (blue) antibodies. ProSAP2 puncta found in the α -Internexin discontinuities (A) and in α -Internexin immunostaining (B) are indicated with arrows. (C) Quantification of the data showed that the difference in the number of ProSAP2 puncta in 10 μ m of dendrite is not significant. N=48. Scale bar indicates 10 μ m.

ProSAP2 guinea pig antibody as a synaptic marker. A triple MAP2 immunostaining was performed with a monoclonal MAP2 mouse antibody to visualize dendrites (Fig. 22A, B). The results showed that the number of ProSAP2 puncta overlapping, not overlapping with α -Internexin immunostaining, and the total number of synaptic puncta per 10 μ m length of dendrite, remain unchanged (Fig. 22A, B, C).

3.2.3 Possible molecular mechanisms underlying the formation of Jacob-induced PSD-like protrusions

In order to shed more light on the question of how Jacob can induce the formation of PSD-like protrusions in hippocampal primary neurons at early stages of development, the composition of PSD-like protrusions was examined by immunohistochemistry (Zdobnova, Ph.D. thesis, 2008). Results showed that PSD proteins such as PSD-95, ProSAP2/Shank3, and subunits of NMDA- and AMPA-receptors are highly recruited in these protrusions. Moreover, Caldendrin, the interaction partner of Jacob which has been shown to be responsible for its extra-nuclear localization, is also enriched in these protrusions (Zdobnova, Ph.D. thesis, 2008). Since at early stages of development the recruitment of these proteins to the PSD is not very likely, and extra-nuclear Jacob seems to regulate these processes, it was asked whether extra-nuclear Jacob might be the nucleation factor for the formation of PSD-like protrusions. If yes, then which of its properties might enable extra-nuclear Jacob to form these huge PSD-like structures before synaptogenesis takes place?

As previously mentioned, it has been shown that Jacob is enriched in some synapses, clustered in dendrites, and has a patchy distribution in the nucleus (Dieterich *et al.*, 2008), indicating that Jacob exhibits a non-homogeneous distribution in neurons. Moreover, under non-reducing conditions, Jacob IR is detected at high molecular weights, suggesting that Jacob might form dimers (Dieterich Ph.D. thesis 2003). In the present work, Jacob homo-dimer formation was characterized in detail.

3.2.3.1 Biochemical characterization of Jacob homo-dimer formation

To analyze the Jacob homo-dimer formation pull-down and Co-IP assays were performed (Fig. 23). A heterologous Co-IP was performed in which the wt-Jacob-GFP protein is immunoprecipitated from protein extracts of HEK 293 cells co-transfected with wt-Jacob-Myc and wt-Jacob-GFP constructs (Fig. 23A). To precipitate wt-Jacob-

GFP, a monoclonal Myc mouse antibody was incubated with Protein-G agarose beads and the protein extract of co-transfected HEK 293 cells (Fig. 23A). The detection of IR of wt-Jacob-GFP was performed using a polyclonal GFP rabbit antibody. Furthermore, an MBP-tagged Jacob N-terminus (MBP-Jacob₁₋₂₃₀) recombinant protein was expressed in a bacterial expression system and purified based on a protocol described in detail in section 2.2.2.4. The purified MBP-Jacob₁₋₂₃₀ fusion protein was coupled to sepharose beads and incubated with a protein extract of COS7 cells transfected with wt-Jacob-His-Myc construct. The protein extraction was done by using 1% Triton X-100 in the extraction buffer. Immunoblots showed that wt-Jacob-His-Myc is pulled down, whereas no immunoreactivity is detected for the MBP control (Fig. 23B).

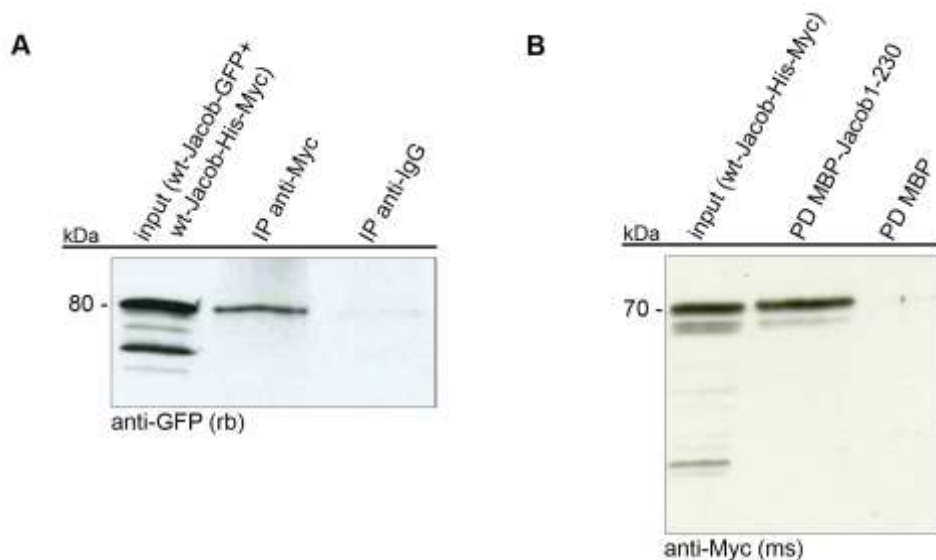


Figure 23. Biochemical assays revealed that Jacob forms homo-dimer. (A) Heterologous Co-IP revealed that wt-Jacob-GFP co-immunoprecipitated with wt-Jacob-His-Myc from protein extracts of HEK 293 cells co-transfected with wt-Jacob-GFP and wt-Jacob-His-Myc constructs. (B) Pull-down assay performed with MBP-Jacob₁₋₂₃₀ revealed that wt-Jacob-His-Myc protein extracted from transfected COS7 cells interacts with MBP-Jacob₁₋₂₃₀, whereas no interaction was detected for MBP control. (IP, immunoprecipitate, PD, pull-down fraction).

3.2.3.2 Mapping of Jacob's dimerization sequence

As stated before, the characterization of the dimerization region was performed using the Y2H system from Clontech (Matchmaker™ GAL4 Two-Hybrid system).

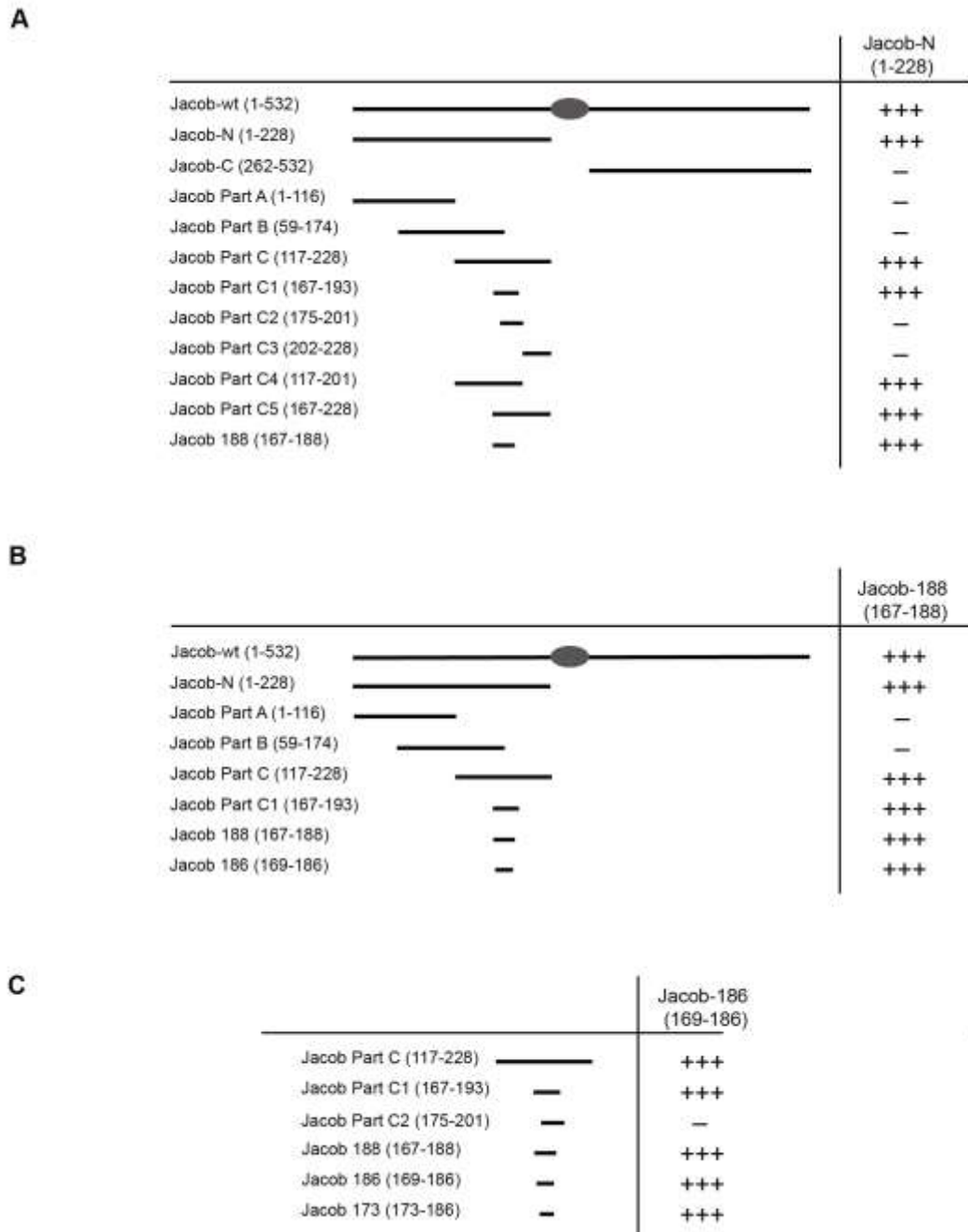


Figure 24. The Jacob dimerization sequence is located at the N-terminus of Jacob. (A, B, C) Yeast two-hybrid technology was used to narrow down the dimerization sequence of Jacob. (C) Results showed that the minimal dimerization sequence of Jacob is located between residues 173 and 186. (+++: yeast growth in TDO media was detected at day 3 after plating, -: no interaction).

The yeast constructs used in the experiments are depicted in section 6.3. The results obtained from several yeast interaction assays revealed that the minimal dimerization region is a fragment composed of residues 173 to 186 (Jacob-173₁₇₃₋₁₈₆) (Fig. 24C). Interestingly, this region contains the ERK kinase phosphorylation site, serine 180. Furthermore, to test whether the ERK kinase phosphorylation is important for Jacob dimer formation, an alanine mutant of Jacob at serine 180 (Jacob-S180A) was used in the interaction assays. The results revealed that the Jacob alanine mutant protein did not interact with either the wild-type Jacob protein or the alanine mutant itself (Fig. 25), suggesting that phosphorylation of Jacob at serine 180 seems to be crucial for Jacob homo-dimer formation.

| | Jacob Part C S180A (117-228) |
|------------------------------|------------------------------------|
| Jacob Part C (117-228) | — |
| Jacob Part C S180A (117-228) | — |

Figure 25. Phosphorylation of Jacob at serine 180 might be crucial for its homo-dimer formation. The alanine mutant of Jacob, Jacob Part C S180A (117-228), shows no interaction with either wild type Jacob Part C (117-228) or itself. (+++: yeast growth in TDO media was detected at day 3 after plating, -: no interaction).

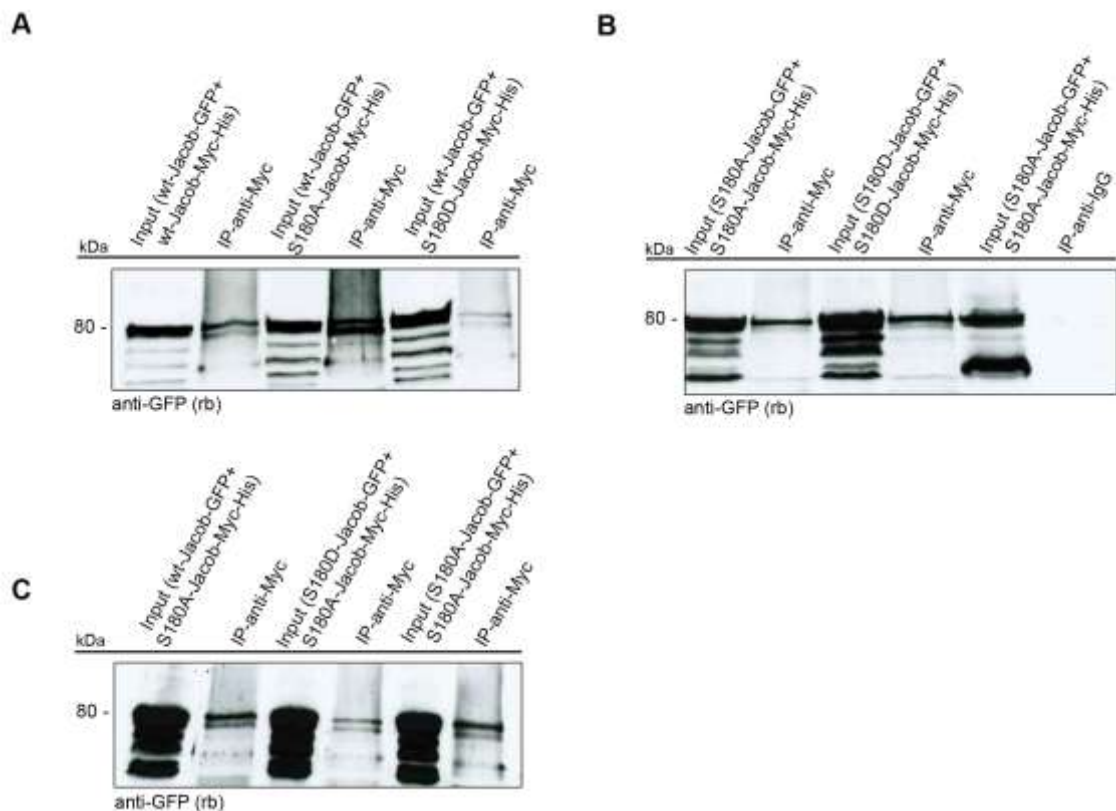
3.2.4 Possible effects of phosphorylation of Jacob at serine 180 on Jacob homo-dimer formation

3.2.4.1 Phospho-mimicking (S180D) and non-phospho (S180A) forms of Jacob are found in the same immune complex as wt-Jacob

To investigate whether phosphorylation of Jacob at serine 180 is required for Jacob homo-dimer formation, Co-IP assays were performed using protein extracts of alanine and aspartate mutants of Jacob at serine 180. GFP- and Myc-tagged Jacob mutant proteins were co-overexpressed in COS7 cells at various combinations as shown below (Fig. 26). The protein extracts were incubated with monoclonal Myc mouse antibody and Protein G-agarose beads. Immunodetections were performed with a polyclonal GFP rabbit antibody. The results showed that wt-Jacob-GFP protein interacts

with both S180A-Jacob-His-Myc and S180D-Jacob-His-Myc mutant proteins (Fig. 26A). Moreover, it was also found that S180A-Jacob-GFP mutant protein interacts with both S180D-Jacob-His-Myc and S180D-Jacob-His-Myc mutant proteins (Fig. 26B). Similarly, it was shown that each of the wt-Jacob-GFP, S180D-Jacob-GFP, and S180A-Jacob-GFP proteins interacts with S180A-His-Myc mutant protein (Fig. 26C). Taken together, these Co-IP experiments indicate that the phosphorylation of Jacob at serine 180 has no prominent positive effect on Jacob homo-dimer formation.

Figure 26. Heterologous Co-IP experiments showed that phospho-mimicking (S180D-



Jacob) and non-phospho (S180A-Jacob) forms of Jacob can immunoprecipitate with wt-Jacob and with each other. (A) wt-Jacob-GFP was co-transfected with either of the His-Myc-tagged wt-Jacob, S180A-Jacob or S180D-Jacob. (left and middle) wt-Jacob-GFP is precipitated from the protein extract of COS7 cells, and (right) a slight band for wt-Jacob-GFP was detected from the Co-IP of protein extracts of COS7 cells co-transfected with wt-Jacob-GFP and S180D-Jacob-His-Myc construct. (B) (left) S180A-Jacob-GFP was precipitated from the protein extract of COS7 cells co-transfected with S180A-Jacob-GFP and S180A-Jacob-His-Myc. (middle) Similarly, S180D-Jacob-GFP was precipitated from the protein extract of COS7 cells co-transfected with S180D-Jacob-GFP and S180D-Jacob-His-Myc construct. (right) the Ig-G control showed that Co-IP is specific. (C) S180A-Jacob-His-Myc construct was co-transfected with one of the GFP- tagged constructs of wt-Jacob, S180D-Jacob and S180A-Jacob. The results showed that the GFP-tagged proteins are immunoprecipitated from the protein extracts of transfected COS7 cells.

It is known that Jacob is an ERK kinase substrate (Marina Mikhaylova, unpublished data) and that Jacob possesses the ERK kinase interaction site at the C-terminus. This suggests that it is very likely that wt-Jacob and the alanine and aspartate mutants of Jacob protein might be only found in the same immune complex bridged by ERK kinase which is also found endogenously in COS7 cells.

3.2.4.2 EGF stimulation of HEK 293 cells enhanced Jacob homo-dimer formation

Heterologous Co-IPs revealed that both non-phospho and phospho-mimicking forms of Jacob protein at serine 180 can be found in the same immune complex (Fig. 26). Moreover, by using a serine 180 phospho-specific antibody of Jacob, it was shown that phospho-Jacob levels increase after epidermal growth factor (EGF) stimulation of HEK 293 cells (Christina Spilker, unpublished data). In order to understand whether enhanced ERK kinase activity by EGF favors Jacob homo-dimer formation, HEK 293 cells were co-transfected with GFP- and His-Myc-tagged wt-Jacob constructs. 24 h after transfection, HEK 293 cells were stimulated with EGF in the presence and absence of the ERK kinase inhibitor, U-0126. Protein extracts of transfected and EGF- or EGF+U-0126-treated HEK 293 cells were used for Co-immunoprecipitation (Fig. 27).

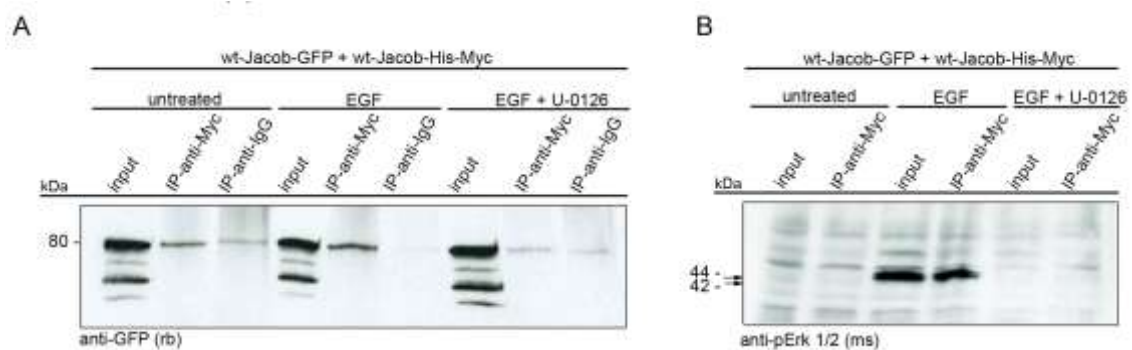


Figure 27. After EGF stimulation of HEK 293 cells, Jacob dimer formation is enhanced. HEK 293 cells, co-transfected with GFP- and His-Myc-tagged wt-Jacob constructs, were stimulated with EGF in the presence and absence of a specific ERK kinase inhibitor, U-0126. The heterologous Co-IP performed from the extracts of transfected and treated or untreated HEK 293 cells revealed that enhanced ERK kinase activity increased the level of Jacob dimers, whereas dimer formation decreased after EGF stimulation in the presence of an ERK kinase inhibitor, U-0126. Immunodetection for wt-Jacob-GFP protein was done with a polyclonal GFP rabbit antibody. (B) Control for ERK kinase activity. Immunodetection performed with a monoclonal ERK 1/2 mouse antibody revealed that active ERK 1/2 levels increase after EGF stimulation and decrease after EGF stimulation in the presence of the ERK kinase inhibitor U-0126.

The results indicated that after EGF stimulation, the Jacob-Jacob interaction increases slightly in comparison to the non-stimulated condition. Moreover, the Jacob-Jacob interaction significantly decreases after EGF stimulation in the presence of the ERK kinase inhibitor, U-0126 (Fig. 27).

3.3 Activity-dependent Calpain-mediated N-terminal truncation of Jacob is required for its nuclear translocation

Using a myristoylation mutant construct of Jacob, Δ Myr-Jacob-GFP, it was shown that the crucial glycine residue in the second position of the Jacob N-terminus is required for N-myristoylation of Jacob (Dieterich *et al.*, 2008), a posttranslational modification known to serve as an anchor for proteins by attaching them to membranes (Boutin *et al.*, 1997). On the other hand, over-expression of Δ Myr-Jacob-GFP resulted in an exclusive nuclear accumulation of the mutant protein in transfected hippocampal primary neurons (Dieterich *et al.*, 2008). Moreover, it was found that Jacob isoforms in the nucleus are 2-3 kDA smaller than the extra-nuclear protein. Therefore it is plausible to assume that before the transport to the nucleus can occur, Jacob has to be cleaved at the N-terminus. Interestingly, previous data demonstrated that Jacob is sensitive to Calpain/ Ca^{2+} mediated proteolysis (Daniela C. Dieterich, unpublished observations).

3.3.1 Nuclear transport of Jacob is blocked in hippocampal primary cultures after NMDA stimulation in the presence of Calpain inhibitors

To initially analyze whether Calpain activity is necessary for the nuclear translocation of Jacob, hippocampal primary cultures were stimulated in the presence of two membrane- permeable Calpain inhibitors, E64-d and calpeptin, at DIV21 and at DIV16, respectively, and the Jacob IR in the nucleus was quantified (Fig. 28). The cultures were pre-incubated with 50 μM E64-d or 60 μM calpeptin for 30 min, and then the cultures were stimulated with 100 μM NMDA for 5 min in the presence or absence of the inhibitors. Moreover, anisomycin, a specific inhibitor of protein synthesis, was added to primary cultures before stimulation and to the stimulation buffer to make sure that de novo protein synthesis would not confuse the data. The stimulated cells were immunostained with polyclonal JB150 rabbit antibody to visualize the Jacob IR in the nucleus (Fig. 28). As demonstrated before, Jacob translocates from the cytoplasm to the

nucleus within a few minutes after NMDA receptor stimulation (Fig. 28A, B, control conditions) (Dieterich *et al.*, 2008). Importantly, addition of the Calpain inhibitor to the stimulation buffer completely blocked the nuclear accumulation of Jacob after NMDA stimulation (Fig. 28A, B, E64d, Calpep). Moreover, quantification of the data showed that the effect is statistically significant (Fig. 28C, D).

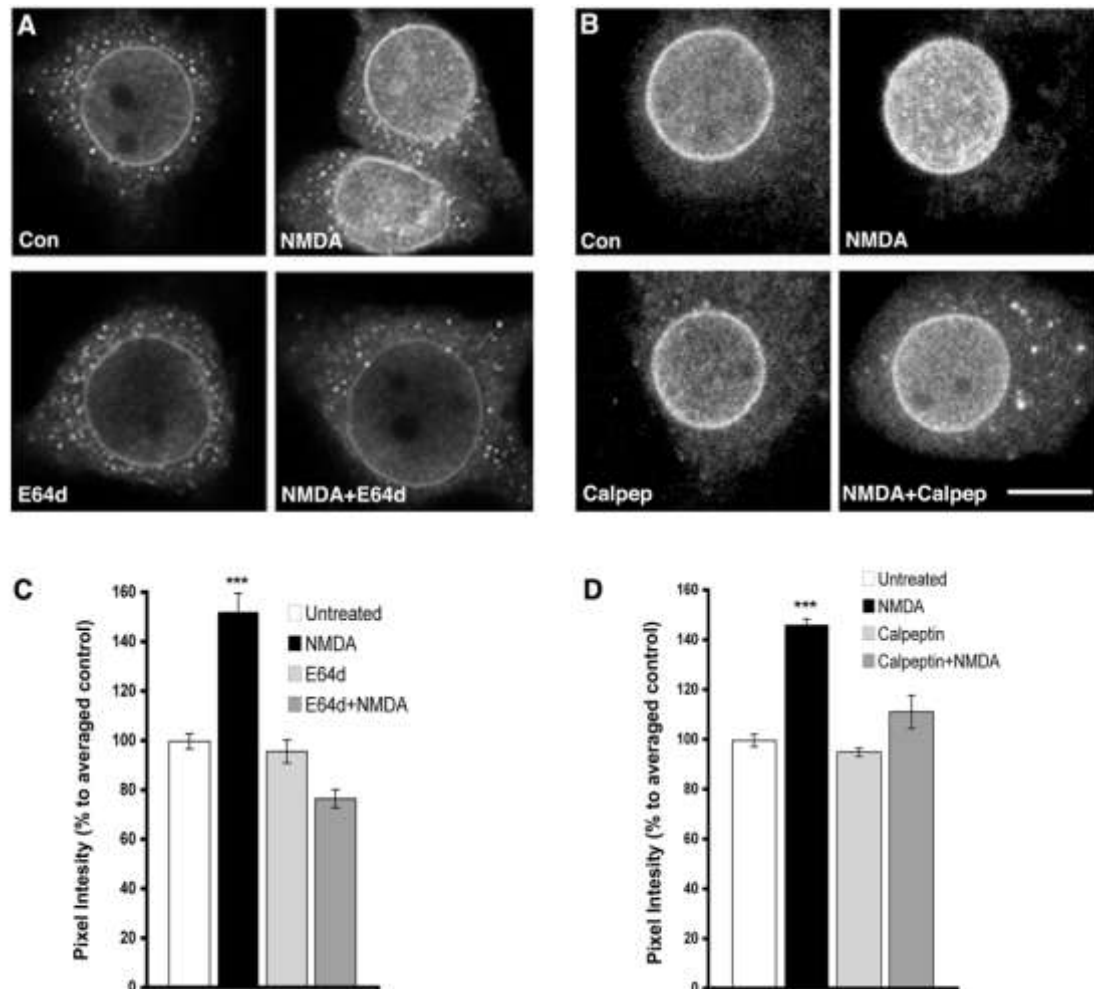


Figure 28. Nuclear translocation of Jacob is blocked in the presence of Calpain inhibitors. DIV21 (left) and DIV16 (right) primary hippocampal neurons were treated with 100 μ M NMDA in the presence and absence of Calpain inhibitors, E64d (left) and calpeptin (right). Cells were fixed and immunostained with a polyclonal JB150 rabbit antibody in order to detect Jacob IR in the nucleus. Confocal images given here were obtained from a single nuclear focal plane. (C and D) Nuclear Jacob immunofluorescence was quantified using ImageJ software. N: 18 for each condition in C, and 20 for each condition in D. ***, $p < 0.001$. Scale bar in A and B is 5 μ m. All experiments were performed in the presence of 7.5 μ M anisomycin.

3.3.2 Nuclear trafficking of Jacob from distal dendrites is prevented in hippocampal primary cultures after NMDA stimulation in the presence of the Calpain inhibitor calpeptin

To investigate whether inhibition of Calpain prevents not only nuclear import but also trafficking of Jacob from distal dendrites, quantitative fluorescence time-lapse microscopy was used. Previously, it was shown that in wt-Jacob-GFP-transfected hippocampal primary neurons, trafficking of Jacob from distal dendrites to the nucleus after NMDA receptor activation occurs (Dieterich *et al.*, 2008). In addition to this, here,

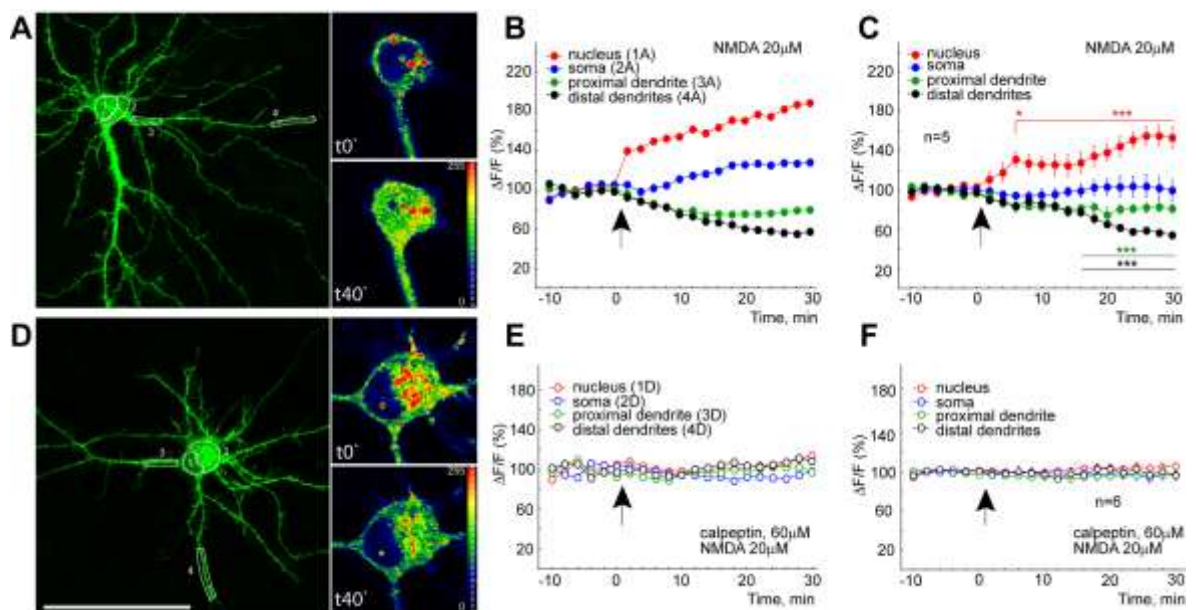


Figure 29. Translocation of Jacob from distal dendrites to the nucleus after NMDA receptor stimulation is prevented by a specific Calpain inhibitor, calpeptin. (A, D) GFP-Jacob-wt was over-expressed in primary hippocampal cultures at DIV10. Confocal images of transfected live cells were taken 10 minutes before (t_0) and 30 minutes after (t_{40}) stimulation with NMDA. In (D) the neuron was preincubated with 60 μM of calpeptin for 5 hours. (B, E) Time course of fluorescent intensity quantified using ImageJ software in depicted ROIs before and after stimulation with 20 μM NMDA. The arrow indicates the time point of NMDA application. Averaged, normalized and bleaching-corrected temporal dynamics of GFP-Jacob-wt fluorescence intensity change after NMDA treatment both with (F) and without calpeptin (C). Without calpeptin pre-treatment, the increase in GFP-Jacob-wt fluorescence in the nucleus is accompanied by a reduction of fluorescence intensity in the dendrites. Statistically significant differences in GFP fluorescence in neuronal nuclei and dendrites after stimulation in comparison to baseline fluorescence are indicated. * $p < 0.05$; *** $p < 0.001$. Scale bar: 40 μm in A and D. All experiments were performed in the presence of 7.5 μM anisomycin.

nuclear translocation of wt-Jacob-GFP was visualized after NMDA receptor stimulation in the presence and absence of the Calpain inhibitor calpeptin (Fig. 29). To analyze the nuclear trafficking of Jacob from distal dendrites, hippocampal primary cultures were transfected with wt-Jacob-GFP at DIV10. 24 h after transfection, the transfected cells were stimulated with 20 μ M NMDA in the presence of 60 μ M calpeptin. *In vivo* time-lapse imaging and quantitative analysis of GFP fluorescence in the nucleus after NMDA stimulation revealed that Jacob moves very rapidly from distal and proximal dendrites to the nucleus (Fig. 29A-C). Within 5 minutes, a statistically significant increase of nuclear GFP-fluorescence was obtained (Fig. 29C). However, in cultures pre-incubated with calpeptin and stimulated in the presence of the inhibitor, the effect of NMDA stimulation is completely blocked (Fig. 29D-F). Moreover, under these conditions Jacob detected is largely immobile (Fig. 29E-F). Therefore, it can be concluded that Calpain-mediated proteolysis of Jacob is a prerequisite for its nuclear translocation from dendrites of transfected hippocampal primary neurons.

3.3.3 Jacob is cleaved by Calpain *in vitro*

In order to further prove that Jacob is a substrate for Calpain, an *in vitro* Calpain cleavage assay was used (Han *et al.*, 1999). The MBP-tagged Jacob N-terminus (MBP-Jacob₁₋₂₃₀) was purified, and incubated the fusion protein with μ -Calpain under EGTA or Ca²⁺ conditions. Jacob degradation was visualized in immunoblots (Fig. 30). The results indicated that MBP-Jacob₁₋₂₃₀ is cleaved by μ -Calpain very rapidly, resulting in the formation of three cleavage products (Fig. 30A). The major fragment appeared with a molecular weight of 2-3 kDa attached to MBP protein (Fig. 30C). Importantly, the MBP control is not cleaved and the cleavage products of Jacob are not detected or significantly attenuated in the presence of EGTA (Fig. 30B, C). Two of the cleavage products were also visualized by using an antibody against the N-terminus of Jacob (Fig. 30D). These data identified Jacob as a Calpain substrate *in vitro*.

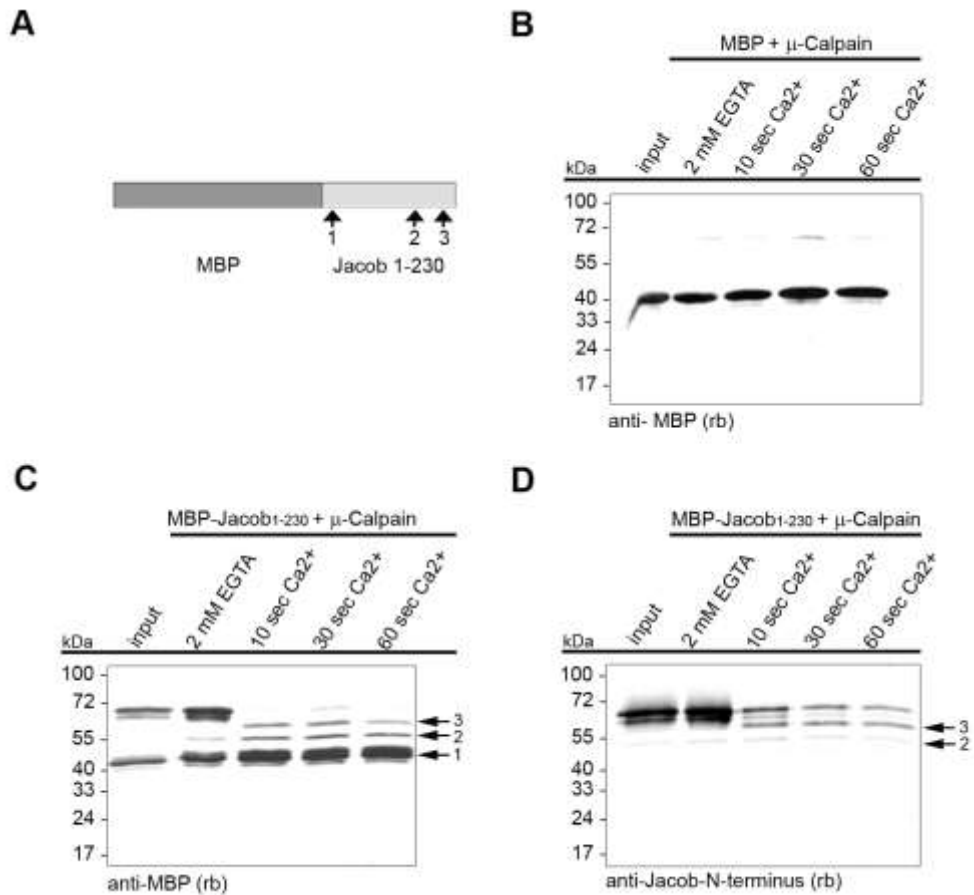


Figure 30. Jacob is cleaved by Calpain *in vitro*. The *in vitro* μ -Calpain assay showed that MBP-Jacob₁₋₂₃₀ fusion protein is cleaved by μ -Calpain. (A) The region for the three potential μ -Calpain cleavage sites as suggested by the *in vitro* Calpain assay is indicated with arrows. (B) The MBP fusion protein is not cleaved by μ -Calpain after adding the enzyme to the cleavage buffer. (C) MBP-Jacob₁₋₂₃₀ is rapidly cleaved after adding μ -Calpain to the cleavage buffer. Three degradation products are shown by arrows. Detection was done with a specific MBP antibody. (D) Two of these bands are also visible when immunoblots were treated with a Jacob-specific antibody directed against the N-terminus of the protein.

4. Discussion

The Jacob-mediated coupling of NMDA receptor signalling to activity-dependent gene transcription events defines a novel mechanism in which Jacob serves as a key nucleocytoplasmic messenger protein (Dieterich *et al.*, 2008). In this study it was also shown that upon activation of NMDA receptors, Jacob translocates to the nucleus via the classical Importin pathway which is mediated by Importin- α binding to the Jacob's NLS sequence. Moreover, at elevated Ca^{2+} levels Caldendrin controls the extra-nuclear localization of Jacob by competing with Importin- α binding (Dieterich *et al.*, 2008). Under high Ca^{2+} conditions, Caldendrin binds to the incomplete IQ domain of Jacob and masks its NLS sequence, thereby preventing Importin- α binding and subsequent nuclear transport of Jacob (Dieterich *et al.*, 2008). In addition, it has been demonstrated that the subcellular localization of Jacob is controlled by N-myristoylation which enables the protein to attach to membranous structures in neurons (Dieterich *et al.*, 2008).

In this PhD thesis further determinants for the subcellular distribution of Jacob and its transport to the nucleus were investigated. It was found that α -Internexin, a neurofilament, interacts with Jacob in rat brain and it was proposed that α -Internexin functions as a docking site for Jacob in the somato-dendritic compartment of neurons in rat brain. Furthermore, mechanisms for how Jacob is released from its docking site after NMDA receptor activation were investigated and it was shown that Calpain, a cysteine protease that is activated upon NMDA receptor stimulation, is required for N-terminal truncation and subsequent release of Jacob from membranes after NMDA bath application.

Finally, possible mechanisms for the formation of PSD-like dendritic protrusions in rat hippocampal primary cultures were investigated and it was shown that α -Internexin has a prominent negative influence on the formation of these processes. It was also proposed that Jacob homo-dimers might serve as a nucleation factor for these processes and prior to testing this hypothesis, Jacob homo-dimer formation was confirmed by biochemical tools and the dimerization region was narrowed down to 14 amino acids.

4.1 The α -Internexin-Jacob interaction

4.1.1 α -Internexin is a potential docking site for Jacob in the somato-dendritic compartment of neurons of rat brain

α -Internexin is a neurofilament characterized as the fourth subunit of neurofilament triplet proteins NF-H, NF-M and NF-L (Fliegner *et al.*, 1990; Kaplan *et al.*, 1990; Yuan *et al.*, 2006). It is highly expressed during mammalian nervous system development and there have been suggested that it might function as a scaffolding for the assembly of the other NFs during development (Kaplan *et al.*, 1990). α -Internexin immunostaining exhibits a fragmented distribution at early stages of development of hippocampal primary cultures (Benson *et al.*, 1996). It was also reported that α -Internexin is found along the dendrites and in dendritic spines of hippocampal primary neurons (Benson *et al.*, 1996). The dendritic localization of the protein was confirmed by confocal microscopy where α -Internexin immunoreactivity colocalizes with MAP2 immunostaining (Benson *et al.*, 1996). In this PhD thesis, this finding was confirmed by immunohistochemistry in which the primary neuronal cultures were co-immunostained with four different α -Internexin antibodies and MAP2 antibody. Moreover, Benson *et al.* (1996) stated that in addition to the dendrites, MAP2 staining was observed in the spine neck whereas α -Internexin immunoreactivity was present in the entire spine (Benson *et al.*, 1996). They also mentioned that a co-immunostaining with an antibody against GluR2/3 showed that α -Internexin immunoreactivity was associated with GluR2/3 positive spines (Benson *et al.*, 1996). However, these data were not shown in the publication. Interestingly, this is the only report claiming that α -Internexin localizes to synapses. Therefore, in this thesis, the synaptic localization of α -Internexin was tested through immunohistochemistry. Co-immunostaining experiments performed with post- and pre-synaptic markers, Bassoon and ProSAP2 respectively, and four different α -Internexin antibodies showed that α -Internexin is not localized at synapses of hippocampal primary cultures at DIV14. Similarly, co-immunostainings done with the primary neuronal cultures at later stages of development show no co-localization between α -Internexin and the presynaptic marker Bassoon or the postsynaptic marker ProSAP2, thus suggesting that α -Internexin is not localized at the synapses of excitatory synapses of mature neurons (Jale Sahin, unpublished data). Taken together these results

make it very unlikely that the report of Benson *et al.* (1996) is more correct and that a large proportion of spines contain α -Internexin.

Previously, α -Internexin was identified as a potential interaction partner of Jacob in a Y2H screen in our lab. Based on data on the subcellular localization of α -Internexin in hippocampal primary neurons, in this PhD thesis, it was proposed that α -Internexin could provide a docking site for Jacob in the dendrites and soma of these neurons. Indeed the immunohistochemistry data revealed that Jacob and α -Internexin co-localize in the dendrites and soma of hippocampal primary neurons at all stages of development tested. Furthermore, the Jacob- α -Internexin interaction was confirmed by Co-IP experiments performed with protein extracts of both rat brain tissue and transfected COS7 cells. Finally, the interaction interface was identified by using Y2H interaction assays and it was found that in fact both, α -Internexin and Jacob, have two different sites for interaction. The interaction interfaces are located at both the N-terminal and C-terminal regions of each protein.

As mentioned before, the N-terminus of Jacob possesses an ERK kinase phosphorylation site at serine 180. Moreover, it has recently been shown that ERK phosphorylation of Jacob at this key serine residue might be important for its nuclear and synaptic function (Anna Karpova and Marina Mikhaylova, unpublished data). More interestingly, it was found in this PhD thesis that the N-terminal binding region of Jacob interacting with α -Internexin includes the serine 180 ERK kinase phosphorylation site. Furthermore, the dimerization sequence of Jacob, characterized in this work, contains the serine residue 180, and that the phosphorylation of Jacob by ERK kinases seems to have a positive effect on Jacob dimer formation. Taken together these data suggest that α -Internexin binding to Jacob might influence the phosphorylation of Jacob and thereby the Jacob dimer formation by rendering the serine phosphorylation site inaccessible to ERK kinases. Therefore, in the future, it would be very interesting to look whether α -Internexin can interact with phospho- and/or non-phospho forms of Jacob protein. To check this hypothesis protein-protein interaction assays such as Y2H system or pull-down assays can be used.

4.1.2 The possible roles of α -Internexin in retrograde transport of Jacob after NMDA receptor activation

Apart from their structural role, IFs have been shown to serve as ‘signaling platforms’ in several signaling pathways (Paramio & Jorcano., 2002). It has been shown that some of the IF proteins can mediate the cellular signaling directly or indirectly via interactions with various proteins (for review Paramio & Jorcano, 2002; Wu and Lynch, 2006). For instance, Vimentin was shown to interact with Cdc42, Rac1, and phospholipase A2, which are in turn involved in various signal transduction pathways (Meriane *et al.*, 2000; Murakami *et al.*, 2000). Moreover, Perlson *et al.* (2005) have shown that after axonal lesions of the sciatic nerve, Vimentin mediates the retrograde transport of phosphorylated ERK (pERK) via a direct interaction with Importin- β 1 and components of the Dynein motor complex (Perlson *et al.*, 2005). It was also shown that the Vimentin interaction with pERK and Importin- β 1 was regulated by Calpain cleavage of the newly formed Vimentin molecules (Perlson *et al.*, 2005). Moreover, this highly complex regulation of retrograde transportation of pERK has been shown to be Ca^{2+} dependent. At high Ca^{2+} concentrations, soluble particles of Vimentin formed by Calpain cleavage, interact with pERK and Importin- β 1, hold the retrograde transport complex intact and prevent the dephosphorylation of pERK during translocation from the lesion site to the nucleus (Perlson *et al.*, 2005; Perlson *et al.*, 2006).

Analogous to the role of Vimentin in pERK retrograde transport, it was hypothesized here that following NMDA receptor activation α -Internexin is cleaved by Calpain and that the cleavage product might still be bound to Jacob and involved in the nuclear translocation of Jacob via a direct interaction with the components of the Dynein motor complex (Fig. 31). In support of this idea, it was confirmed in this study that the α -Internexin fragment, assumed to be formed after Calpain cleavage, interacts with Jacob in the YTH system. Furthermore, the inhibition of Calpain activity by a specific inhibitor, calpeptin, blocked the nuclear transport of Jacob in hippocampal primary cultures after NMDA stimulation. However, contrary to the original hypothesis, α -Internexin immunoreactivity is not detected in the nucleus of primary neurons stimulated by NMDA in the experimental conditions tested. On the other hand, the possibility remains that α -Internexin might be part of the Jacob transport complex up to the nuclear pore without entering the nucleus. To test this hypothesis and investigate

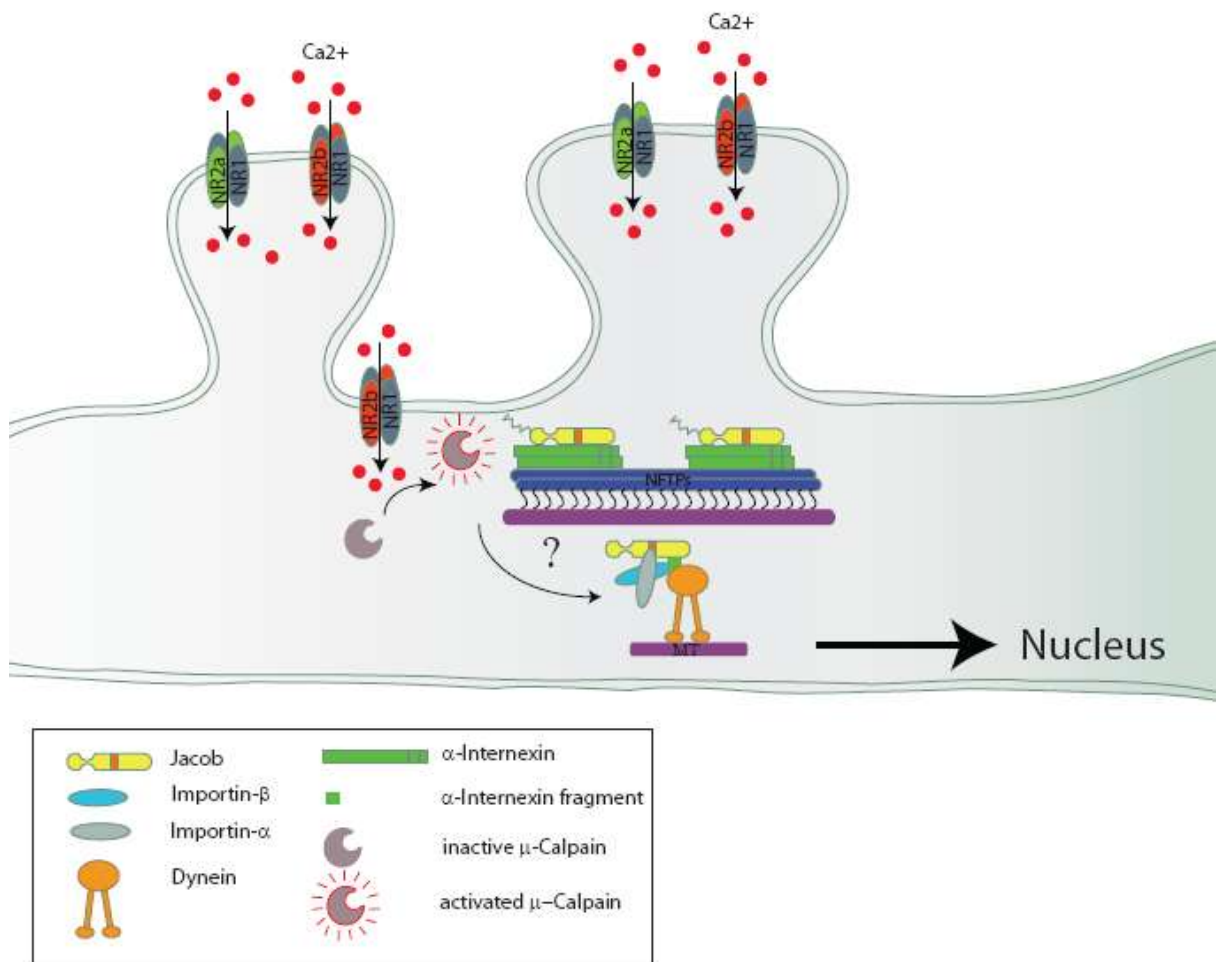


Figure 31. Original hypothesis. α-Internexin fragments assumed to be formed after Calpain cleavage might be part of a Jacob-transport complex that enables the retrograde transport of Jacob via the Dynein motor complex. (CDD: Caldendrin; MT: Microtubules; NFTPs: Neurofilament Triplet Proteins)

whether α-Internexin is important in the nuclear transport of Jacob, future studies could be performed using primary neuronal cultures of α-Internexin KO mice as a model system. Although α-Internexin KO mice have shown no gross abnormalities in nervous system development, and breed normally and have rich adulthoods (Levasseur *et al.*, 1999), to date there has been no study showing what subtle molecular changes might occur in the absence of α-Internexin. Therefore, by looking at the distribution and retrograde transport of Jacob in the primary neuronal cultures of α-Internexin KO mice, possible subtle functional roles of α-Internexin could be revealed.

Additionally, similar to Vimentin, α -Internexin might be associated with the Dynein motor complex and involved in retrograde transport of Jacob to the nucleus upon neuronal activity. To test whether α -Internexin is associated with any of the components of the Dynein motor complex, protein extracts from adult rat brain tissue were used in a number of Co-IP assays. Results revealed that α -Internexin does not co-immunoprecipitate with the Dynein motor complex components Dynein IC, Importin- α 1 or Importin- β 1 in the adult rat brain. Moreover, the immunohistochemistry data revealed that Importin- β 1 and α -Internexin do not co-localize in mature hippocampal primary neurons either at basal conditions or after NMDA stimulation. However, it is important to state that Vimentin-pERK and Vimentin-Importin- β 1 interactions were shown to be prominent only after axonal lesion (Perlson *et al.*, 2005). Moreover, the intensity of the protein interactions increased with time after injury, and this was shown to be directly correlated with the formation of soluble Vimentin particles by Calpain, activated increased Ca^{2+} levels at the lesion site (Perlson *et al.*, 2005). Similarly, α -Internexin might be associated with the components of the Dynein motor complex under different physiological or pathophysiological conditions. Therefore, future interaction studies addressing this issue might help to shed more light on whether α -Internexin is a part of the Dynein-Importins-driven retrograde transport mechanism.

Since α -Internexin is not localized to synapses, however, the data point to the intriguing possibility that the interaction with α -Internexin might be only involved in shuttling of Jacob to the nucleus after extrasynaptic NMDA-receptor stimulation. According to this α -Internexin binding to the N-terminus of Jacob and potential masking of the ERK-phosphorylation site might be part of the mechanism for why Jacob is not phosphorylated at this crucial residue following the activation of extrasynaptic NMDA-receptors. Moreover, if a Calpain-cleaved C-terminal fragment of α -Internexin will be co-released from dendrites with the N-terminal truncated Jacob, this complex will prevent further phosphorylation on the way to the nucleus. This in turn would preserve the information from where this complex originally derived even if in the meantime synaptic NMDA-receptors and ERK kinase are activated in the meantime. Thus, the interaction might also have a signaling function that decodes the synaptic or extrasynaptic position of the activated NMDA-receptor, which is

responsible for the nuclear shuttling of the complex. This possibility clearly deserves further examination.

4.1.3 The presence of α -Internexin has a negative influence on the formation of Jacob induced PSD-like protrusions in rat hippocampal primary neurons

It has been shown previously that over-expression of extra-nuclear Jacob results in the formation of a rather complex synapto-dendritic tree and a slight increase in spine density. Most importantly, Jacob formed intradendritic protrusions containing PSD-proteins. In previous studies of our lab and in this PhD thesis, the protein components of these PSD-like protrusions were analyzed in detail and it was found that several PSD proteins as well as Jacob binding partners are recruited to these protrusions (Zdobnova, PhD thesis, 2008). It was also addressed whether α -Internexin is recruited to these structures and if it has any influence on their formation. As stated above, at early stages of development the distribution of α -Internexin in dendrites of rat hippocampal primary neurons is fragmented. This in turn suggests that at these stages, α -Internexin is not present everywhere throughout the dendrites. Similarly, Jacob-induced PSD-like protrusions are formed mostly in transfected immature primary neurons, a time frame at which α -Internexin immunostaining is fragmented in dendrites of the primary neurons. In this PhD thesis, the immunohistochemistry and over-expression studies revealed that PSD-like protrusions are preferentially located at the discontinuities of α -Internexin immunostainings. Moreover, co-overexpression of hippocampal primary neurons with a GFP- α -Internexin-wt construct and an extra-nuclear Jacob-His-Myc construct showed that in most of the transfected neurons the PSD-like protrusions were not formed (~80% of transfected neurons) and in some of them the number and the size of the protrusions were decreased (~20% of transfected neurons) Since PSD-like protrusions in many respects resemble postsynaptic specialization, i.e. in recruiting many synaptic proteins but being formed before synaptogenesis takes place, here it was asked whether the presence of α -Internexin might have any influence on synapse formation. Co-immunostainings of hippocampal primary cultures performed with α -Internexin and ProSAP2 antibodies (to visualize synapses) at DIV11 revealed that the number of ProSAP2 puncta in a 10 μ m dendrite is the same no matter whether α -Internexin immunoreactivity is present or not. These data suggest that α -Internexin has no

influence on synapse formation. It can therefore be concluded that the presence of α -Internexin has a negative influence on the formation of Jacob-induced PSD-like protrusions in young hippocampal primary neurons (DIV5) but has no effect on synapse formation in older primary neurons (DIV11).

4.2 Identification of the Jacob dimerization sequence

It was mentioned above that PSD-like protrusions are formed when Jacob is over-expressed outside the nucleus. The region required for the formation of these structures includes the N-terminus of Jacob. It was previously shown that Jacob can form homo-dimers (Pöll, Diploma thesis, 2005). In this thesis it was asked whether Jacob homo-dimers could serve as a nucleation factor for the formation of PSD-like protrusions, and in conclusion induces the recruitment of many binding partners and PSD components into these structures. However, before addressing these questions it was crucial to characterize the dimerization of Jacob in detail using molecular and biochemical tools. Therefore in this PhD thesis, the Jacob dimer formation was confirmed by Co-IP and pull-down assays, and the dimerization sequence was identified using the Y2H system. Based on the data obtained, the minimal dimerization sequence consists of only 14 amino acids and is located between residues 173 and 186. This sequence includes the ERK kinase phosphorylation site of Jacob at serine 180. It has been also demonstrated that a point mutation (serine to alanine) interrupts the interaction in Y2H but not after over-expression in COS7 cells. The discrepancy in results might stem from one of two reasons. The first might be the length of the inserts used in these experiments. In Y2H interaction assays a small fragment of mutant- and wt- Jacob protein (residues 117-228) was used. On the other hand, full-length (residues 1-532) forms of the mutant- and wt- Jacob protein were used in the over-expression of COS7 cells. In the Y2H system the point mutation (serine to alanine) might result in a conformational change in the protein fragment, which in turn disturbs the interaction. In order to test this possibility, in future studies it is important to check whether full-length forms of mutant and wt-Jacob protein will show interaction in the Y2H system.

In addition to homo-dimers, Jacob can potentially form oligomers. In order to test this hypothesis, purified fusion proteins of Jacob can be used in analytical gel filtration and chemical cross-linking experiments. In fact, during this PhD thesis, an MBP fusion protein of N-terminal Jacob (MBP-Jacob₁₋₂₃₀) was purified and used in gel

filtration and chemical cross-linking experiments with glutaraldehyde used as a cross-linking agent (Jale Sahin, unpublished data). Western blot analysis of the samples of cross-linking experiments revealed that MBP alone can also form dimers. Moreover, the literature also states that MBP can form homo-dimers (Mockus *et al.*, 1997) which can be prevented by modifying the conditions (Wang *et al.*, 2003). Although the results of gel filtration experiments supported the possibility of Jacob-oligomer formation (Jale Sahin, unpublished data), this finding has to be confirmed by optimizing the conditions for MBP-Jacob₁₋₂₃₀ or using another fusion protein of Jacob with another tag or of an untagged Jacob protein. Along these lines, in this PhD thesis, a SUMO-tagged fusion protein of Jacob N-terminus was cloned. However, pilot protein expression studies showed that the fusion protein is expressed in far smaller amounts even under stimulated conditions. Therefore, in the future, conditions for the protein expression of SUMO-Jacob₁₁₆₋₂₂₃ should be optimized and then the resulting protein can be used in subsequent experiments as mentioned above to explore whether Jacob also forms oligomers.

4.2.1 The role of ERK kinase phosphorylation at serine 180 in Jacob homo-dimer formation

In order to further investigate the role of ERK kinase phosphorylation of Jacob in Jacob dimer formation, several Co-IP experiments were performed with the protein extracts of COS7 cells transfected with various combinations of wt-Jacob and non-phospho or phospho- mutant constructs of Jacob. Data revealed that both phospho and non-phospho forms of Jacob could be immunoprecipitated with wt-Jacob or with themselves. Additionally, differentially tagged wt-Jacob constructs were co-overexpressed in HEK 293 cells and stimulated with EGF in the presence and absence of ERK kinase inhibitor U-0126 and the protein extracts of transfected cells were used for Co-IP experiments. Analysis of the samples revealed that there was a slight increase of Jacob-Jacob interaction in the presence of EGF and decrease in the presence of the ERK kinase inhibitor. It has also been shown that after EGF stimulation levels of phosphorylated Jacob (pJacob) were higher than the non-phosphorylated form of the protein (Christina Spilker, unpublished data). These results suggest that the phosphorylation of Jacob by ERK kinase at serine 180 might have a role in Jacob homo-dimer formation. Since the role phosphorylation of Jacob at serine 180 are

contradictory, it is crucial to use pure fusion proteins of phospho and non-phospho forms of Jacob to reveal whether phosphorylation of Jacob is necessary for its homodimer formation.

4.3 N-terminal truncation of Jacob by Calpain is a prerequisite for its nuclear translocation after NMDA receptor activation in rat hippocampal primary neurons

It has been shown previously that N-mristoylation is required for extra-nuclear localization of Jacob (Dieterich *et al.*, 2008). Thus, prior to its nuclear translocation N-terminal truncation of Jacob is required. Calpain is a cysteine protease and is activated by Ca^{2+} influx generated upon NMDA receptor activation (Siman *et al.*, 1989; Wu *et al.*, 2005). It has been shown that Calpain cleaves its substrate protein in a limited manner and this limited proteolysis results in the modification of the function of the protein rather than abolishing its function completely (Sorimachi and Suzuki, 2001). In this PhD thesis, it has been revealed that Calpain activity is a prerequisite for NMDA-receptor induced nuclear translocation of Jacob from dendrites. Furthermore, *in vitro* experiments suggest that Calpain mediates proteolysis of endogenous Jacob after NMDA bath application and can also cleave a short N-terminal domain from Jacob fusion protein, thus enabling the rest of the protein to be accessible for nuclear import. Additionally, *in vivo* experiments have shown that the inhibition of Calpain activity completely abolishes NMDA-receptor mediated nuclear trafficking of Jacob. Taken together, these data indicates an irreversible removal of the N-terminus from the Jacob protein prior to its mobilization from dendrites. It has recently been shown that Jacob mRNA exhibits a prominent dendritic localization in the hippocampus (Kindler *et al.*, 2009). As a consequence of the nuclear translocation of Jacob, there might be a necessity to replenish the dendritic protein pool in hippocampal neurons. Moreover, this can induce a high protein turnover and possibly a requirement for a local extra-somatic synthesis of Jacob from dendritically localized mRNAs at sites where the protein was mobilized. In order to directly modulate synaptic function most of the proteins which are synthesized in dendrites are assumed to be recruited to postsynaptic sites. Similarly, Jacob dendritic mRNA and its assumed rapid turnover rate after synaptic activity can add a new cellular function to dendritic mRNA translation in the context of activity-dependent gene expression, and testing this hypothesis would be very interesting.

4.4 Concluding remarks

In this PhD thesis, the somato-dendritic docking site of Jacob and the mechanisms for its release from the docking site after NMDA stimulation were investigated (Fig. 32). α -Internexin, a neuronal intermediate filament, is characterized as a novel binding partner of Jacob, and it is proposed that α -Internexin serves as a docking site for Jacob in the dendrites and soma of neurons of rat brain. In addition, N-terminal truncation of Jacob by Calpain was shown. It was demonstrated that Calpain activity is a prerequisite for the nuclear import of Jacob after NMDA receptor activation and shown that Jacob is a novel Calpain substrate *in vitro*. Furthermore, it has been shown that Jacob forms dimers and the minimal dimerization region was narrowed down to 14 amino acids. Jacob dimers, potentially oligomers, might serve as a nucleation factor for PSD-like growth in immature primary neurons. As α -Internexin exerts a negative influence on these formations Jacob dimers/oligomers and/or other Jacob binding partners might have a positive influence on the formation of these PSD-like protrusions. Hence it would be very interesting to purify these structures and unravel their molecular composition.

In conclusion, data obtained during this PhD thesis reveals that α -Internexin serves as a docking site for Jacob at the somato-dendritic compartment of primary neurons of rat brain and that Calpain activity via NMDA receptor stimulation is important for its release and subsequent nuclear translocation. Moreover, it shows that phosphorylation of Jacob might be prevented by α -Internexin interaction and this in turn could affect Jacob dimer/oligomer formation.

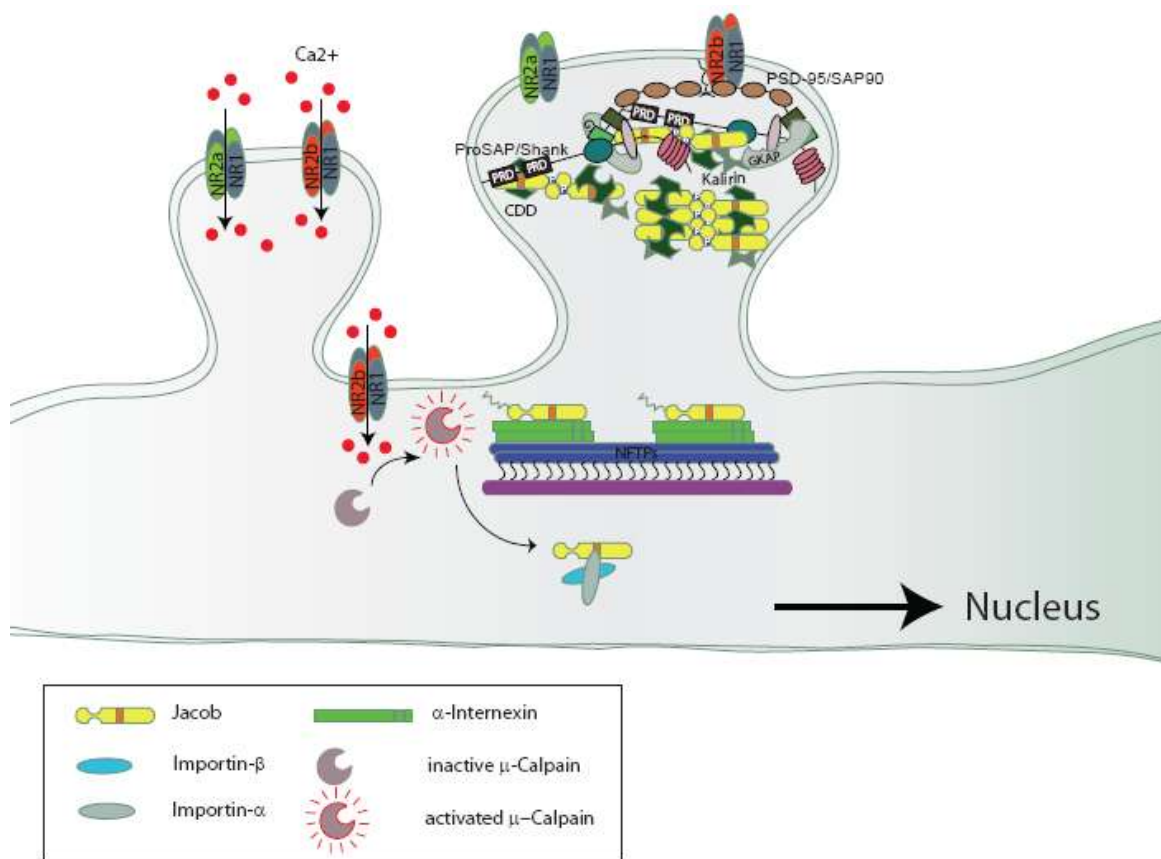


Figure 32. A model for the regulation of the subcellular distribution of Jacob after NMDA receptor activation. α -Internexin interacts with Jacob at two sites and serves as a docking site at the somato-dendritic compartments. μ -Calpain is activated by increases of free intracellular Ca^{2+} concentrations generated after NMDA receptor stimulation. Jacob is cleaved by active μ -Calpain at the N-terminus, released from the membrane and translocates to the nucleus via the classical Importin pathway. Erk kinase phosphorylation of Jacob at serine 180 might affect the Jacob dimer and potentially oligomer formation. Jacob dimers/ potentially oligomers could be responsible for the formation of Jacob induced PSD-like protrusions and together with other interaction partners various PSD components could be potentially recruited to these processes by recruiting various PSD proteins into these protrusions with the help of other Jacob interaction partners like Caldendrin. (CDD: Caldendrin; MT: Microtubules; NFTP: Neurofilament Triplet Proteins)

5. References

- Ahn S, Riccio A, Ginty DD (2000) Spatial considerations for stimulus dependent transcription in neurons. *Annu. Rev. Physiol.*, **62**, 803-823.
- Arthur JS, Elce JS, Hegadorn C, Williams K, Greer PA (2000) Disruption of the murine calpain small subunit gene, *capn4*: Calpain is essential for embryonic development but not for cell growth and division. *Mol Cell Biol*, **20**, 4474-4481.
- Azam M, Andrabi SS, Sahr KE, Kamath L, Kulipoulos A, Chisti AH (2001) Disruption of the mouse μ -calpain gene reveals an essential role in platelet function. *Mol Cell Biol*, **21**, 2213-2220.
- Ausubel FM, Brent R, Kingston RE (1999) Short Protocols in Molecular Biology. 4th ed.: Wiley John & Sons Inc.
- Bailey CH, Bartsch D, Kandel ER (1996) Toward a molecular definition of long-term memory storage. *Proc. Natl. Acad. Sci. USA*, **93**, 13445-13452.
- Benson DL, Mandell JW, Shaw G and Banker G (1996) Compartmentation of alpha-internexin and neurofilament triplet proteins in cultured hippocampal neurons. *J Neurocyt*, **25**, 181-196
- Birnboim HC, Doly J (1979) A rapid alkaline extraction procedure for screening recombinant plasmid DNA. *Nucleic Acids Res*, **7**, 1513-1523.
- Bito H, Takemoto-Kimura S (2003) Ca^{2+} /CREB/CBP-dependent gene regulation: a shared mechanism critical in long-term synaptic plasticity and neuronal survival. *Cell Calcium*, **34**, 425-30.
- Boutin JA (1997) Myristoylation. *Cellular Signalling*, **9**, 15-35.
- Burgoyne RD, Weiss JL (2001) The neuronal calcium sensor family of calcium-binding proteins. *Biochem J*, **353**, 1-12.
- Braunewell K, Gundelfinger ED (1999) Intracellular neuronal calcium sensor proteins: a family of EF-hand calcium-binding proteins in search of a function. *Cell Tissue Res*, **295**, 1-12.
- Burgoyne RD, O'Callaghan DW, Hasdemir B, Haynes LP, Tepikin AV (2004) Neuronal calcium-sensor proteins: multitasking regulators of neuronal function. *Trends Neurosci*, **27**, 203-209
- Chan SO, Runko E, Anyane-Yeboah K, Ko L, Chiu FC (1998) Calcium Ionophore-Induced Degradation of Neurofilament and Cell Death in MSN. *Neuroblast Cells Neurochem Research*, **23**, 393-400.
- Chang L, Goldman RD (2004) Intermediate Filaments Mediate Cytoskeletal Crosstalk. *Nature Reviews Mol Cell Biol*, **5**, 601-613.

- Chawla S, Hardingham GE, Quinn DR, Bading H (1998) CBP: a signal regulated transcriptional coactivator controlled by nuclear calcium and CaM kinase IV. *Science*, **281**, 1505-1509.
- Chiu FC, Barnes EA, Das K, Haley J, Socolow P, Macaluso FP, Fant J (1989) Characterization of a Novel 66 kd Subunit of Mammalian Neurofilaments. *Neuron*, **2**, 1435-1445.
- Ching GY, Liem RK (1993) Assembly of type IV neuronal intermediate filaments in nonneuronal cells in the absence of preexisting cytoplasmic intermediate filaments. *J Cell Biol*, **122**, 1323-1335.
- Ching GY, Chien CL, Flores R, Liem RK (1999) Overexpression of α -internexin causes abnormal neurofilamentous accumulations and motor coordination deficits in transgenic mice. *J Neurosci*, **19**, 2974-2986.
- Cochard P, Paulin D (1984) Initial expression of neurofilaments and vimentin in the central and peripheral nervous system of the mouse embryo in vivo. *J Neurosci*, **4**, 2080-2094.
- Croall DE, Ersfeld K (2007) The calpains: modular designs and functional diversity. *Genome Biology*, **8**, 218.
- Dresbach T, Hempelmann A, Spilker C, tom Dieck S, Altmann W, Zuschratter W, Garner C, Gundelfinger ED (2003) Functional regions of the presynaptic cytomatrix p protein Bassoon: significance for synaptic targeting and cytomatrix anchoring. *Mol Cell Neuroscience*, **23**, 279-291.
- Deisseroth K, Mermelstein PG, Xia H, Tsien RW (2003) Signaling from synapse to nucleus: The logic behind the mechanisms. *Curr Opin Neurobiol*, **13**, 354-365.
- Dieterich DC, Bockers TM, Gundelfinger ED, Kreutz MR (2002) Screening for differentially expressed genes in the rat inner retina and optic nerve after optic nerve crush. *Neurosci Lett*, **317**, 29-32.
- Dieterich DC, Karpova A, Mikhaylova M, Zdobnova I, König I, Landwehr M, Kreutz M, Smalla KH, Richter K, Landgraf P, Reissner C, Boeckers TM, Zuschratter W, Spilker C, Seidenbecher CI, Garner CC, Gundelfinger ED, Kreutz MR (2008) Caldendrin-Jacob: A Protein Liaison That Couples NMDA Receptor Signalling to the Nucleus. *PLoS Biol.*, **6**, e34.
- Evans J, Sumners C, Moore J, Huentelman MJ, Deng J, Gelband CH, Shaw G (2002) Characterization of mitotic neurons derived from adult rat hypothalamus and brain Stem. *J Neurophysiol*, **87**, 1076-1085.
- Fields S, Song O (1989) A novel genetic system to detect protein-protein interactions. *Nature*, **340**, 245-246.

- Fliegner KH, Ching GY, Liem RKH (1990) The predicted amino acid sequence of α -internexin is that of a novel neuronal intermediate filament protein. *The EMBO J*, **9**, 749-755.
- Franco SJ, Huttenlocher A (2005) Regulating cell migration: calpains make the cut. *J Cell Sci.* **118**, 3829-38.
- Gietz RD, Woods RA (2002) Transformation of yeast by lithium acetate/single-stranded carrier DNA/polyethylene glycol method. *Methods Enzymol*, **350**, 87-96
- Ginty DD, Bonni A, Greenberg ME (1994) Nerve growth factor activates a Ras-dependent protein kinase that stimulates c-fos transcription via phosphorylation of CREB. *Cell*, **77**, 713-725.
- Goll DE, Thompson VF, Li H, Wei Wand Cong J (2003) The Calpain System. *Physiol Rev*, **83**, 731-801.
- Goslin K, Asmussen H, Banker G (1998) Rat hippocampal neurons in low-density culture. In: Banker G, Goslin K. (eds). *Culturing nerve cells*, MIT Press: Cambridge, MA pp. 339-370.
- Guroff G (1964) A neutral calcium-activated proteinase from the soluble fraction of rat brain. *J. Biol. Chem.* **239**, 149-155.
- Guttmann RP, Baker DL, Seifert KM, Cohen AS, Coulter DA, Lynch DR (2001) Specific proteolysis of the NR2 subunit at multiple sites by calpain. *J Neurochem.* **78(5)**,1083-93.
- Guttmann RP, Sokol S, Baker DL, Simpkins KL, Dong Y, Lynch DR (2002) Proteolysis of the N-methyl-d-aspartate receptor by calpain in situ. *J Pharmacol Exp Ther.* **302(3)**,1023-30.
- Haeseleer F, Sokal I, Verlinde LMJ, Erdjumen-Bromage H, Tempst P, Pronin AN, Benovic JL, Fariss RN, Palczewski K (2000) Five members of a novel Ca²⁺-binding protein (CaBP) subfamily with similarity to calmodulin. *J Biol Chem*, **275**, 1247-60.
- Hajimohomadreza I, Raser KJ, Nath R, Nadimpalli R, Scott M, Wang KK (1997) Neuronal nitric oxide synthase and calmodulin-dependent protein kinase II alpha undergo neurotoxin-induced proteolysis. *J Neurochem*, **69**, 1006-1013.
- Han Y, Weinman S, Boldogh I, Walker RK and Braise AR (1999) Tumor necrosis factor- α -inducible I κ B α proteolysis mediated by cytosolic m-Calpain. *J Biol Chem*, **274**, 787-794.
- Hardingham GE, Arnold FJ, Bading H (2001) Nuclear calcium signaling controls CREB-mediated gene expression triggered by synaptic activity. *Nat Neurosci*, **4**, 261-267.

- Hardingham GE, Bading H (2002) Coupling of extrasynaptic NMDA-receptors to a CREB shut-off pathway is developmentally regulated. *Biochim Biophys Acta.*, **12**, 148-53.
- Hanz S (2003) Axoplasmic importins enable retrograde injury signaling in lesioned nerve. *Neuron*, **40**, 1095-1104.
- Helfand BT, Chang L, Goldman RD (2004) Intermediate filaments are dynamic and motile elements of cellular architecture. *Journal of Cell Science*, **117**, 133-141.
- Hell JW, Westenbroek RE, Warner C, Ahlijanian MK, Prystay W, Gilbert MM, Snutch TP, Catterall WA (1993) Identification and differential subcellular localization of the neuronal class C and class D L-type calcium channel alpha 1 subunits. *J Cell Biol.* **123(4)**:949-62.
- Heusner C, Martin KC (2008) Signaling from the synapse to the nucleus, In Structural and Functional Organization of the Synapse, eds Hell JW and Ehlers MD (*Springer, NY*), 601-620.
- Huston WA, Krebs EG (1968) Activation of skeletal muscle phosphorylase kinase by Ca^{2+} . II. Identification of the kinase activating factor as a proteolytic enzyme. *Biochemistry*, **7**, 2116-2122.
- Jordan BA, Kreutz MR (2009) Nucleocytoplasmic protein shuttling: the direct route in synapse-to-nucleus signaling. *Trends in Neurosciences*, **32**, 392-401.
- Impey S (1998) Cross talk between ERK and PKA is required for Ca^{2+} stimulation of CREB-dependent transcription and ERK nuclear translocation. *Neuron*, **21**, 869-883.
- Kaplan MP, Chin SSM, Fliegner KH, Liem RKH (1990) α -Internexin, a novel neuronal intermediate filament protein, precedes the low molecular weight neurofilament protein (NF-L) in the developing brain. *J Neurosci*, **10**, 2735-2748.
- Kaufmann WE, MacDonald SM, Altamura CR (2000) Dendritic cytoskeletal protein expression in mental retardation: an immunohistochemical study of the neocortex in rett syndrome. *Cerebral cortex*, **10**, 992-1004.
- Kim S, Coulombe PA (2007) Intermediate filament scaffolds fulfil mechanical, organizational, and signalling functions in the cytoplasm. *Genes & Development*, **21**, 1581-1597.
- Kindler S, Dieterich DC, Schutt J, Sahin J, Karpova A, Mikhaylova M, Schob C, Gundelfinger ED, Kreienkamp HJ, Kreutz MR (2009) Dendritic mRNA targeting of Jacob and N-methyl-d-aspartate-induced nuclear translocation after Calpain-mediated proteolysis. *J Biol Chem*, **284**, 25431-40.
- Kishimoto A, Mikawa K, Hashimoto K, Yasuda I, Tanaka S, Tominaga M, Kuroda T, Nishizuka Y (1989). Limited proteolysis of protein kinase C subspecies by calcium-dependent neutral protease (Calpain). *J Biol Chem*, **264**, 4088-4092.

- Kreutz MR, Seidenbecher CI, Gundelfinger ED (2006) Caldendrin - a neuronal calcium binding protein involved in synapto-dendritic Ca²⁺ signaling. *In: Neuronal Calcium Sensor Proteins (Phillipov P & Koch K-W eds) Nova Science Publishers*; 301-313.
- Laemmli UK (1970) Cleavage of structural proteins during the assembly of the head of bacteriophage T4. *Nature*, **227**, 680-685.
- Laube G, Seidenbecher CI, Richter K, Dieterich DC, Hoffmann B, Landwehr M, Smalla KH, Winter C, Böckers TM, Wolf G, Gundelfinger ED, Kreutz MR (2002) The neuron-specific Ca²⁺-binding protein caldendrin: gene structure, splice isoforms and expression in the rat central nervous system. *Mol Cell Neurosci*, **19**, 459-75.
- Lariviere RC, Julien JP (2003) Functions of Intermediate filaments in neuronal development and disease. *J Neurobiol*, **58**, 131-148.
- Lee MK, Xu Z, Wong PC, Cleveland DW (1993) Neurofilaments are obligate heteropolymers in vivo. *J Cell Biol*. **122(6)**:1337-50
- Levavasseur F, Zhu Q, Julien JP (1999) No requirement of alpha-Internexin for nervous system development and for radial growth of axons. *Brain Res Mol Brain Res*, **69**, 104-112.
- Lu T, Xu Y, Mericle MT, Mellgren RL (2002) Participation of the conventional calpains in apoptosis. *Biochim Biophys Acta*, **1590**, 16-26.
- Lynch DR, Gleichman AJ (2007) Picking up the pieces: the roles of functional remnants of Calpain-mediated proteolysis *Neuron*, **53**, 317-319.
- Magnusson A, HAug LS, Walaas SI, Ostvold AC (1993) Calcium-induced degradation of the inositol (1, 4, 5)-triphosphate receptor? Ca²⁺-channel. *FEBS Lett*, **323(3)**, 229-232.
- Matthews RP (1994) Calcium/calmodulin-dependent protein kinase types II and IV differentially regulate CREB-dependent gene expression. *Mol Cell Biol*, **14**, 6107-6116.
- Meriane M, Mary S, Comunale F, Vignal E, Fort P, Gauthier-Rouviere C (2000) Cdc42Hs and Rac1 GTPases induce the collapse of the vimentin intermediate filament network. *J Biol Chem*, **275**, 33046-33052.
- Murakami M, Naktani Y, Kuwata H, Kudo I (2000) Cellular components that functionally interact with signaling phospholipase A. *Biochim Biophys Acta*, **1488**, 159-166.
- Meyer WL, Fischer EH, Krebs EG (1964) Activation of skeletal muscle phosphorylase b kinase by Ca²⁺. *Biochemistry*, **3**, 1033-1039.
- Mockus SM, Kumer SC, Vrana KE (1997) Carboxyl terminal deletion analysis of tryptophan hydroxylase. *Biochimica et Biophysica Acta*, **1342**, 132-140

- Otis KO, Thompson KR, Martin KC (2006) Importin-mediated nuclear transport in neurons *Curr Op in Neurobiol*, **16**, 329–335.
- Paramio JM, Jorcano JL (2002) Beyond structure: do intermediate filaments modulate cell signalling? *BioEssays*, **24**, 836–844.
- Patcher JS, Liem RKH (1985) α -Internexin, a 66-kD intermediate filament-binding protein from mammalian central nervous tissues. *J Cell Biol*, **101**, 1316-1322.
- Perlson E, Hanz S, Yaakov KB, Ruder YS, Seger R, Fainzilber M (2005) Vimentin-dependent spatial translocation of an activated MAP kinase in injured nerve. *Neuron*, **45**, 715-726.
- Perlson E, Michaelevski I, Kowalsman N, Ben-Yaakov K, Shaked M, Seger R, Eisenstein M, Fainzilber M (2006) Vimentin Binding to Phosphorylated ERK Sterically Hinders Enzymatic Dephosphorylation of the Kinase. *J Mol Biol*, **364**, 938-944.
- Pinter M, Stierandova A, Friedrich P (1992) Purification and characterization of a Ca^{2+} -activated thiol protease from *Drosophila melanogaster*. *Biochemistry* **31**, 8201-8206.
- Rechsteiner M, Rogers SW (1996) PEST sequences and regulation by proteolysis. *TIBS*, **21**, 267-271.
- Sala C, Rudolph-Correia S, Sheng M. (2000) Developmentally Regulated NMDA Receptor-Dependent Dephosphorylation of cAMP Response Element-Binding Protein (CREB) in Hippocampal Neurons *The J of Neurosci*, **20**, 3529-3536.
- Sambrook J, Fritsch EF, Maniatis T (1989) Molecular cloning: a laboratory manual, 2nd edition. *Cold Spring Harbor Laboratory Press, Cold Spring Harbor, NY*.
- Sassone-Corsi P. (1995) Transcription factors responsive to cAMP. *Annu Rev Cell Dev Biol* **11**, 355-377.
- Sato K, Kawashima S (2001) Calpain Function in the Modulation of Signal Transduction Molecules. *Biol Chem*, **382**, 743-751.
- Seidenbecher CI, Langaese K, Sanmartí-Vila L, Boeckers TM, Smalla KH, Sabel BA, Garner CC, Gundelfinger ED, Kreutz MR (1998) Caldendrin, a novel neuronal calcium-binding protein confined to the somato-dendritic compartment. *J Biol Chem*, **273**, 21324-31.
- Seidenbecher CI, Reissner C, Kreutz MR (2002) Caldendrin s in the inner retina. *Adv Exp Med Biol*, **514**, 451-463.
- Shaw G, Yanga C, Zhang L, Cook P, Pike B, Hill WD (2004) Characterization of the bovine neurofilament NF-M protein and cDNA sequence, and identification of *in vitro* and *in vivo* calpain cleavage sites. *Biochem and Biophys Research Comm*, **325**, 619-625

- Sheng M, Thompson MA, Greenberg ME (1991) CREB: a Ca^{2+} -regulated transcription factor phosphorylated by calmodulin-dependent kinases. *Science*, **252**, 1427-1430.
- Shields DC, Leblanc C, Banik NL (1997) Calcium-Mediated Neurofilament Protein Degradation in Rat Optic Nerve In Vitro: Activity and Autolysis of Calpain Proenzyme. *Exp Eye Res*, **65**, 15-21.
- Shieh PB, Hu SC, Bobb K, Timmusk T, Ghosh A (1998) Identification of a signalling pathway involved in calcium regulation of BDNF expression. *Neuron*, **20**, 727-740.
- Siddiqui AA, Zhou Y, Podesta RB, Karcz SR, Clarke MW, Strejan GH, Dekaban GA, Tognon CE (1993) Characterization of Ca^{2+} -dependent neutral protease (calpain) from human blood flukes, *Schistosoma mansoni*. *Biochim Biophys Acta*, **1181**, 37-44.
- Silva AJ, Kogan JH, Frankland PW, Kida S (1998) CREB and memory. *Annu. Rev. Neurosci*, **21**, 127-148.
- Siman R, Noszek JC, Kegerise C (1989) Calpain I Activation Is Specifically Related to Excitatory Amino Acid Induction of Hippocampal Damage. *J Neurosci*, **5**, 1579-1590.
- Sorimachi H, Suzuki K (2001) The structure of Calpain. *J Biochem*, **129**, 653-664.
- Smalla KH, Seidenbecher CI, Tischmeyer W, Schicknick H, Wyneken U, Böckers TM, Gundelfinger ED, Kreutz MR (2003) Kainate-induced epileptic seizures induce a recruitment of caldendrin to the postsynaptic density in rat brain. *Brain Res Mol Brain Res*, **116**, 159-62.
- Styers ML, Salazar G, Love R, Peden AA, Kowalczyk AP, Faundez V (2004) The endo-lysosomal sorting machinery interacts with the intermediate filament cytoskeleton. *Mol. Biol. Cell*, **15**, 5369-5382.
- Steinert PM, Marekov LN, Parry DA (1999) Molecular parameters of type IV alpha-Internexin and type IV-type III alpha-Internexin-Vimentin copolymer intermediate filaments. *J Biol Chem*, **274**, 1657-1666.
- Steinert PM, Liem RKH (1990) Intermediate filament dynamics. *Cell*, **60**, 521-523.
- Suzuki T, Mitake S, Okumura-Noji K, Shimizu H, Tada T, Fujii T (1997) Excitable membranes and synaptic transmission: postsynaptic mechanisms. Localization of alpha-Internexin in the postsynaptic density of the rat brain. *Brain Res*, **765**, 74-80.
- Tao X, Finkbeiner S, Arnold DB, Shaywitz AJ, Greenberg ME (1998) Ca^{2+} influx regulates BDNF transcription by a CREB family transcription factor-dependent mechanism. *Neuron*, **20**, 709-726.
- Thompson KR (2004) Synapse to nucleus signaling during long-term synaptic plasticity; a role for the classical active nuclear import pathway. *Neuron*, **44**, 997-1009.

- Towbin H, Staehelin T, Gordon J (1979) Electrophoretic transfer of proteins from polyacrylamide gels to nitrocellulose sheets: procedure and some applications. *Proc Natl Acad Sci USA*, **76**, 4350-4354.
- Undamatla J, Szaro BG (2001) Differential expression and localization of neuronal intermediate filament proteins within newly developing neurites in dissociated cultures of *Xenopus laevis* embryonic spinal cord. *Cell Motil Cytoskeleton*, **49**, 16-32.
- Wang Y, Guo HC (2003) Two-step Dimerization for Autoproteolysis to Activate Glycosylasparaginase. *J Biol Chem*, **278**, 3210–3219.
- Wu HA, Yuen EY, Lu YF, Matsushita M, Matsui H, Yan Z, Tomizawa K (2005) Regulation of *N*-Methyl-D-aspartate receptors by Calpain in cortical neurons. *J Biol Chem*, **280**, 21588-21593.
- Wu HY, Lynch DR (2006) Calpain and synaptic function. *Mol Neurobiol*, **33**, 215-36.
- Xiao S, McLean J, Robertson J (2006) Neuronal intermediate filaments and ALS: A new look at an old question. *Biochim Biophys Acta*, **1762 (11-12)**, 1001-12.
- Xu W, Wong TP, Chery N, Gaertner T, Wang YT, Baudry M (2007) Calpain-mediated mGluR1- α truncation: a key step in excitotoxicity. *Neuron*, **53**, 399-412
- Yeckel MF, Sleeper AA, Fitzpatrick JS, Hertle DN, Hagenston AM, Garner RT (2007) Intracellular calcium waves transmit synaptic information to the nucleus in hippocampal pyramidal neurons. In: *Transcriptional Regulation by Neuronal Activity. To the Nucleus and Back*. (Dudek SM, ed); SpringerLink, 73-89.
- Yuan A, Rao MV, Sasaki T, Chen Y, Kumar A, Veeranna, Liem RK, Eyer J, Peterson AC, Julien JP, Nixon RA (2006) α -internexin is structurally and functionally associated with the neurofilament triplet proteins in the mature CNS, *J. Neurosci*, **26**, 10006-10019.
- Zdobnova I (2008) Jacob – an activity-regulated morphogenetic factor for synapto-dendritic cytoarchitecture. *PhD thesis*, Otto-von-Guericke-Universität Magdeburg.

6. Suplemantery information

6.1 List of primers

| Number | Name | Position (bp) | Sequence (from 5' to 3') | RE site | Tm (°C) |
|--------|--------------------------|---------------|-----------------------------------|--------------|---------|
| 1 | Jb 167-188-for | 633-653 | GGAATTCAAAGAATGCCCCG GATGTGCC | <i>EcoRI</i> | 58 |
| 2 | Jb 167-188-rev | 698-678 | CGGGATCCCTGTTCCAACCCG AAGGCCCG | <i>BamHI</i> | 65 |
| 3 | Jb 229-249-for | 819-839 | GGAATTCAGACGGCAACCA CAACTATG | <i>EcoRI</i> | 56 |
| 4 | Jb 203-249 – for | 741-761 | GGAATTCAGGATGTATAGTGT TGATGGA | <i>EcoRI</i> | 52 |
| 5 | Jb 203-249 – rev | 881-861 | CGGGATCCACGCTTCCTCTCC GCGTAGCC | <i>BamHI</i> | 65 |
| 6 | α -Internexin-for | 32-55 | ATGAGCTTCGGATCAGAGCAC TAC | | 55 |
| 7 | α -Internexin-rev | 1534-1511 | ACCAGTTCAGCCAAAAAATG TAA | | 52 |
| 8 | IN-Short-for | 1430-1454 | GGGAAAGTTTCGAAGAAAC ACTGG | | 53 |
| 9 | IN-Short-rev | 1534-1509 | TTACATTTTTGGCTGGAAC GGTGG | | 51 |
| 10 | IN-Long-rev | 1406-1429 | TACCTTGGATGTTTCTTAGTG AC | | 47 |
| 11 | IN- SF-2-for | 1250-1273 | GGGTTAAGCATCTCAGGGCTG AAT | | 52 |
| 12 | IN-LF-2-rev | 1249-1226 | GCTGGTGCTAAATCGTGTCTC TTC | | 52 |
| 13 | IN-Tail-for | 1241-1264 | AGCACCAGCGGGTTAAGCATC TCA | | 54 |
| 14 | IN- Coil-2-for | 806-829 | TCGGCGCTGAGGGAGATCCGC GCC | | 63 |
| 15 | IN-Coil-2-rev | 1240-1217 | AAATCGTGTCTCTCGCCTTC CAG | | 52 |

| Number | Name | Position (bp) | Sequence (from 5' to 3') | RE site | Tm (°C) |
|--------|---------------------------------|---------------|------------------------------------|--------------|---------|
| 16 | IN-half Coil 2-half Tail-for | 1010-1033 | GGAGCCAATGAATCCCTG GAGAGG | | 56 |
| 17 | IN-half Coil 2-half Tail-rev | 1357-1334 | CAGGGACAGCCCAGCGGA TGAGAC | | 59 |
| 18 | IN-407-466-for | 1250-1270 | GGAATTCGGGTAAAGCATC TCAGGGCTG | <i>EcoRI</i> | 58 |
| 19 | IN-407-466-rev | 1429-1409 | CGGGATCCTACCTTGGATG TTTTCTTAGT | <i>BamHI</i> | 55 |
| 20 | IN-407-442-rev | 1357-1337 | CGGGATCCCAGGGACAGC CCAGCGGATGA | <i>BamHI</i> | 65 |
| 21 | GFP-In-wt-Myc- for | *613-631 | GCGGCCGCTTTAATGGTGA GCAAGGGCGAG | <i>Not I</i> | 63 |
| 22 | GFP-In-wt-Myc- rev | 1534-1511 | CGGGATCCCATTTTTTGGC TGGAAGCTGG | <i>BamHI</i> | 58 |
| 23 | SUMO-Jacob-116-223-for | 352-375 | ATGGCCATTGAGCTAGCAG TGGTGAAA | | 55 |
| 24 | SUMO-Jacob-116-223-rev | 669-645 | TTATTCCTTGGGGAACCAG GTACGGAT | | 59 |
| 25 | SUMO-IN-408-442-for | 1250-1292 | ATGGGGTTAAGCATCTCAG GGCTGA | | 54 |
| 26 | SUMO-IN-408-442-rev | 1357-1337 | TTACAGGGACAGCCCAGC GGATGAG | | 58 |
| 27 | pIVEX -2.3 MCS-Jacob bt2-for | 135-153 | GCTCGAGGATGGGTGCCG CCGCCTCC | <i>XhoI</i> | 65 |
| 28 | pIVEX -2.3 MCS-Jacob bt2-rev | 818-800 | TCCCCCGGGGAGAAGCT GAAAGGGTT | <i>SmaI</i> | 61 |
| 29 | pIVEX -2.3 MCS-Jacob Part C-for | 484-502 | GCTCGAGGGAAGCCATTG AGCTAGCA | <i>XhoI</i> | 58 |

* cDNA sequence of GFP- α -Internexin-wt construct was used for cloning. To get the Myc tag in the end the GFP- α -Internexin sequence was inserted into pcDNA 3.1/ myc-His A (-).

6.2 List of oligonucleotides

| Number | Name | Position (bp) | Sequence (from 5' to 3') | RE site |
|--------|-----------------------|---------------|--|--------------|
| 1 | Jb 167-179 sense | 633-671 | P-AATTCAAAGAATGCCCCGGATG TGCCAAGCTGGTCCCTGGTCCCG | <i>EcoRI</i> |
| 2 | Jb 167-179 anti-sense | 671-633 | P-GATCCGGGACCAGGGACCAGC TTGGCACATCCGGGGCATTCTTTG | <i>BamHI</i> |
| 3 | Jb 169-179 sense | 639-671 | P-AATTCTGCCCCGGATGTGCCAAG CTGGTCCCTGGTCCCG | <i>EcoRI</i> |
| 4 | Jb 169-179 anti-sense | 671-639 | P-GATCCGGGACCAGGGACCAGCT TGGCACATCCGGGGCAG | <i>BamHI</i> |
| 5 | Jb 173-186 sense | 660-692 | P-AATTCGCCAAGCTGGTCCCTGG TCCCTCCCCTCGGGCCTTCGGGTTG G | <i>EcoRI</i> |
| 6 | Jb 173-186 anti-sense | 692-660 | P-GATCCAACCCGAAGGCCCGAGG GGAGGGACCAGGGACCAGCTTGGCG | <i>BamHI</i> |
| 7 | Jb 169-186 sense | 639-692 | P-AATTCTGCCCCGGATGTGCCAAG CTGGTCCCTGGTCCCTCCCCTCGGG CCTTCGGGTTGG | <i>EcoRI</i> |
| 8 | Jb 169-186 anti-sense | 692-639 | P-GATCCAACCCGAAGGCCCGAG GGGAGGGACCAGGGACCAGCTTGG CACATCCGGGGCAG | <i>BamHI</i> |

6.3 List of constructs

| Clone name | Insert | RE sites | Vector | Application | Obtained from |
|--|-------------------|-----------------------------|--------|-------------------------|----------------------|
| wt-Jacob-pAS2-1 | bp 135-1730 | <i>EcoRI</i> / <i>XhoI</i> | pAS2-1 | YTH-System | Daniela C. Dieterich |
| wt-Jacob-pGBKT7 | bp 135-1730 | <i>EcoRI</i> / <i>BamHI</i> | pGBKT7 | YTH-System | Daniela C. Dieterich |
| Jacob-N ₁₋₂₃₀ - pGADT7 | bp 135-819 | <i>EcoRI</i> / <i>BamHI</i> | pGADT7 | YTH-System | Jale Sahin |
| Jacob-N ₁₋₂₃₀ - pGBKT7 | bp 135-819 | <i>EcoRI</i> / <i>BamHI</i> | pGBKT7 | YTH-System | Imbrit König |
| Jacob ₂₆₂₋₅₃₂ - pGADT7 | bp 918-1730 | <i>EcoRI</i> / <i>BamHI</i> | pGADT7 | YTH-System | Jale Sahin |
| Jacob ₂₆₂₋₅₃₂ - pGBKT7 | bp 918-1730 | <i>EcoRI</i> / <i>BamHI</i> | pGBKT7 | YTH-System | Daniela C. Dieterich |
| Jacob PartA ₁₋₁₁₆ - pGBKT7 | bp 135-482 | <i>EcoRI</i> / <i>BamHI</i> | pGBKT7 | YTH-System | Imbrit König |
| Jacob PartB ₅₉₋₁₇₉ - pGBKT7 | bp 310-656 | <i>EcoRI</i> / <i>BamHI</i> | pGBKT7 | YTH-System | Imbrit König |
| Jacob PartC ₁₁₇₋₂₂₈ - pGBKT7 | bp 484-818 + stop | <i>EcoRI</i> / <i>BamHI</i> | pGBKT7 | YTH-System | Imbrit König |
| Jacob PartC ₁₁₇₋₂₂₈ S180D -pGADT7 | bp 484-818 + stop | <i>EcoRI</i> / <i>BamHI</i> | pGADT7 | YTH-System, mutagenesis | Jale Sahin |
| Jacob PartC ₁₁₇₋₂₂₈ S180D -pGBKT7 | bp 484-818 + stop | <i>EcoRI</i> / <i>BamHI</i> | pGBKT7 | YTH-System, mutagenesis | Imbrit König |
| Jacob PartC ₁₁₇₋₂₂₈ S180A -pGADT7 | bp 484-818 + stop | <i>EcoRI</i> / <i>BamHI</i> | pGADT7 | YTH-System, mutagenesis | Jale Sahin |
| Jacob PartC ₁₁₇₋₂₂₈ S180A -pGBKT7 | bp 484-818 + stop | <i>EcoRI</i> / <i>BamHI</i> | pGBKT7 | YTH-System, mutagenesis | Imbrit König |
| Jacob PartC ₁₁₇₋₂₂₈ S180E -pGBKT7 | bp 484-818 + stop | <i>EcoRI</i> / <i>BamHI</i> | pGBKT7 | YTH-System, mutagenesis | Imbrit König |
| Jacob PartC C1 ₁₆₇₋₁₉₃ -pGADT7 | bp 634-713 | <i>EcoRI</i> / <i>BamHI</i> | pGADT7 | YTH-System | Jale Sahin |

| Clone name | Insert | RE sites | Vector | Application | Obtained from |
|---|---------------------------------------|-----------------------------|---------------|--------------------|----------------------|
| Jacob PartC C1 ₁₆₇₋₁₉₃ -pGBKT7 | bp 634-713 | <i>EcoRI</i> / <i>BamHI</i> | pGBKT7 | YTH-System | Imbrit König |
| Jacob PartC C2 ₁₇₅₋₂₀₁ -pGADT7 | bp 658-737 | <i>EcoRI</i> / <i>BamHI</i> | pGADT7 | YTH-System | Jale Sahin |
| Jacob PartC C2 ₁₇₅₋₂₀₁ -pGBKT7 | bp 658-737 | <i>EcoRI</i> / <i>BamHI</i> | pGBKT7 | YTH-System | Imbrit König |
| Jacob PartC C3 ₂₀₂₋₂₂₈ -pGADT7 | bp 738-818 | <i>EcoRI</i> / <i>BamHI</i> | pGADT7 | YTH-System | Jale Sahin |
| Jacob PartC C3 ₂₀₂₋₂₂₈ -pGBKT7 | bp 738-818 | <i>EcoRI</i> / <i>BamHI</i> | pGBKT7 | YTH-System | Imbrit König |
| Jacob 203 ₂₀₃₋₂₄₉ -pGADT7 | bp 741-881, with primer 4, 5 | <i>EcoRI</i> / <i>BamHI</i> | pGBKT7 | YTH-System | Jale Sahin |
| Jacob PartC C4 ₁₁₇₋₂₀₁ -pGBKT7 | bp 484-737 | <i>EcoRI</i> / <i>BamHI</i> | pGBKT7 | YTH-System | Imbrit König |
| Jacob PartC C5 ₁₆₇₋₂₂₈ -pGADT7 | bp 634-818 | <i>EcoRI</i> / <i>BamHI</i> | pGADT7 | YTH-System | Jale Sahin |
| Jacob PartC C5 ₁₆₇₋₂₂₈ -pGBKT7 | bp 634-818 | <i>EcoRI</i> / <i>BamHI</i> | pGBKT7 | YTH-System | Imbrit König |
| Jacob 229 ₂₂₉₋₂₄₉ -pGADT7 | bp 819-881, with primer 3, 4 | <i>EcoRI</i> / <i>BamHI</i> | pGADT7 | YTH-System | Jale Sahin |
| Jacob 188 ₁₆₇₋₁₈₈ -pGADT7 | bp 633-698, with primer 1, 2 | <i>EcoRI</i> / <i>BamHI</i> | pGADT7 | YTH-System | Jale Sahin |
| Jacob 188 ₁₆₇₋₁₈₈ -pGBKT7 | bp 633-698, with primer 1, 2 | <i>EcoRI</i> / <i>BamHI</i> | pGBKT7 | YTH-System | Jale Sahin |
| Jacob ₁₆₇₋₁₇₉ -pGBKT7 | bp 633-671, with oligonuc. 1, 2 | <i>EcoRI</i> / <i>BamHI</i> | pGBKT7 | YTH-System | Jale Sahin |
| Jacob ₁₆₉₋₁₇₉ -pGADT7 | bp 639-671, with oligonuc.1, 2 | <i>EcoRI</i> / <i>BamHI</i> | pGADT7 | YTH-System | Jale Sahin |
| Jacob ₁₆₉₋₁₇₉ -pGBKT7 | bp 639-671, with oligonuc. 3, 4 | <i>EcoRI</i> / <i>BamHI</i> | pGBKT7 | YTH-System | Jale Sahin |

| Clone name | Insert | RE sites | Vector | Application | Obtained from |
|--|--|-----------------------------|--------|-------------|---------------|
| Jacob 173 ¹⁷³⁻¹⁸⁶ - pGADT7 | bp 660-692, with oligonuc. 5, 6 | <i>EcoRI</i> / <i>BamHI</i> | pGADT7 | YTH-System | Jale Sahin |
| Jacob 173 ¹⁷³⁻¹⁸⁶ - pGBKT7 | bp 660-692, with oligonuc. 5, 6 | <i>EcoRI</i> / <i>BamHI</i> | pGBKT7 | YTH-System | Jale Sahin |
| Jacob 186 ¹⁶⁹⁻¹⁸⁶ - pGADT7 | bp 639-692, with oligonuc. 7, 8 | <i>EcoRI</i> / <i>BamHI</i> | pGADT7 | YTH-System | Jale Sahin |
| Jacob 186 ¹⁶⁹⁻¹⁸⁶ - pGBKT7 | bp 639-692, with oligonuc. 7, 8 | <i>EcoRI</i> / <i>BamHI</i> | pGBKT7 | YTH-System | Jale Sahin |
| α -Internexin-wt - pGBKT7 | bp 32-1534, with primer 6, 7 | <i>EcoRI</i> | pGBKT7 | YTH-System | Jale Sahin |
| α -Internexin-wt - pGADT7 | bp 32-1534, with primer 6, 7 | <i>EcoRI</i> | pGADT7 | YTH-System | Jale Sahin |
| α -Internexin LF ¹⁻ 465 -pGBKT7 | bp 32-1429, with primer 6, 10 | <i>EcoRI</i> | pGBKT7 | YTH-System | Jale Sahin |
| α -Internexin LF ¹⁻ 465 -pGADT7 | bp 32-1429, with primer 6, 10 | <i>EcoRI</i> | pGADT7 | YTH-System | Jale Sahin |
| α -Internexin SF ⁴⁶⁶⁻ 500 -pGBK T7 | bp 1430-1534, with primer 8, 9 | <i>EcoRI</i> | pGBKT7 | YTH-System | Jale Sahin |
| α -Internexin SF ⁴⁶⁶⁻ 500 -pGAD T7 | bp 1430-1534, with primer 8, 9 | <i>EcoRI</i> | pGADT7 | YTH-System | Jale Sahin |
| α -Internexin SLF ¹⁻ 407 -pGBKT7 | bp 32-1249, with primer 6, 12 | <i>EcoRI</i> | pGBKT7 | YTH-System | Jale Sahin |
| α -Internexin LSF ⁴⁰⁸⁻⁵⁰⁰ -pGBKT7 | bp 1250-1534, with primer 11, 9 | <i>EcoRI</i> | pGBKT7 | YTH-System | Jale Sahin |
| α -Internexin Coil2 ²⁵⁸⁻⁴⁰² -pGADT7 | bp 806-1240, with primer 14, 15 | <i>EcoRI</i> | pGADT7 | YTH-System | Jale Sahin |
| α -Internexin half Coil2 + half Tail D ³²⁶⁻⁴⁴² -pGBKT7 | bp 1010-1357, with primer 16, 17 | <i>EcoRI</i> | pGBKT7 | YTH-System | Jale Sahin |
| α -Internexin half Coil2 + half Tail D ³²⁶⁻⁴⁴² -pGADT7 | bp 1010-1357, with primer 16, 17 | <i>EcoRI</i> | pGADT7 | YTH-System | Jale Sahin |

| Clone name | Insert | RE sites | Vector | Application | Obtained from |
|--|--|---------------------------------|---------------------------------|--|-------------------------|
| α -Internexin Tail D 403-500 -pGADT7 | bp 1241-1534, with primer 7, 13 | <i>EcoRI</i> | pGADT7 | YTH-System | Jale Sahin |
| α -Internexin 407 408-466 -pGADT7 | bp 1250-1429, with primer 18, 19 | <i>EcoRI</i> / <i>BamHI</i> | pGADT7 | YTH-System | Jale Sahin |
| α -Internexin 442 408-442 -pGBKT7 | bp 1250-1357, with primer 18, 20 | <i>EcoRI</i> / <i>BamHI</i> | pGBKT7 | YTH-System | Jale Sahin |
| α -Internexin 442 408-442 -pGADT7 | bp 1250-1357, with primer 18, 20 | <i>EcoRI</i> / <i>BamHI</i> | pGADT7 | YTH-System | Jale Sahin |
| Wt-Jacob-GFP | bp 135-1730 | <i>EcoRI</i> / <i>BamHI</i> | pEGFP-N1 | expression, Co- IP | Daniela C. Dieterich |
| GFP- α -Internexin- wt | bp 32-1534 with primer 6, 7 | <i>EcoRI</i> with STOP codon | pEGFP-C1 | expression, Co- IP | Jale Sahin |
| GFP- α -Internexin- wt-myc | bp 32-1534, with primer 21, 22 | <i>NotI</i> / <i>BamHI</i> | pcDNA 3.1 / Myc-His A (-) | Expression, Calpain cleavage assay | Jale Sahin |
| wt-Jacob-His-Myc | bp 135-1730 | <i>EcoRI</i> / <i>BamHI</i> | pcDNA 3.1 / Myc-His B (-) | expression, Co- IP | Daniela C. Dieterich |
| Δ NLS-Jacob-His- Myc | bp 135-1730 | <i>EcoRI</i> / <i>BamHI</i> | pcDNA 3.1 / Myc-His B (-) | expression, Co- IP | Daniela C. Dieterich |
| Δ exon9-Jacob-GFP | bp 135-1152 | <i>EcoRI</i> / <i>BamHI</i> | pEGFP-N3 | expression, Co- IP | Daniela C. Dieterich |
| Δ exon9-Jacob-His- Myc | bp 135-1152 | <i>EcoRI</i> / <i>BamHI</i> | pcDNA 3.1 / Myc-His A (-) | expression, Co- IP | Daniela C. Dieterich |

| Clone name | Insert | RE sites | Vector | Application | Obtained from |
|--|--|----------------|-----------------------|--|---------------|
| *SUMO-Jacob-116-223 | bp 481-803 + stop, with primer 23, 24 | | Champion™ pET SUMO | pull-down, chemical cross-linking, gel filtration | Jale Sahin |
| *SUMO- α -Internexin-408-442 | bp 1250-1357+ stop, with primer 25, 26 | | Champion™ pET SUMO | pull-down, Calpain cleavage assay | Jale Sahin |
| *pIVEX 2.3-MCS Jacob bt2 (aa 1-228) | bp 135-819 with primer 27, 28 | XhoI / SmaI | pIVEX 2.3-MCS | pull-down, chemical cross-linking, gel filtration | Jale Sahin |
| *pIVEX 2.3-MCS Jacob Part C ₁₁₇₋₂₂₈ | bp 484-818 with primer 28, 29 | XhoI / SmaI | pIVEX 2.3-MCS | pull-down, chemical cross-linking, gel filtration | Jale Sahin |

* These constructs were produced for the applications mentioned above. However, the expression conditions of the proteins are needed to be optimized. For details please look at the discussion chapter.

7. Abbreviations

The single or triple letter code was used for amino acids

| | |
|------------------|--|
| aa | amino acid(s) |
| AMPA | α -amino-3-hydroxy-5-methyl-4-isoxazole propionic acid |
| ATP | adenosine triphosphate |
| BDNF | brain derived neurotrophic factor |
| bp | base pair(s) |
| BSA | bovine serum albumin |
| Ca ²⁺ | calcium ion |
| CaBPs | Ca ²⁺ -binding proteins |
| CaM | Calmodulin |
| CaMKIV | Calcium/calmodulin-dependent protein kinase IV |
| CaMKII | Calcium/calmodulin-dependent protein kinase II |
| cAMP | Cyclic adenosine monophosphate |
| cDNA | complementary DNA |
| CIP | calf intestine phosphatase |
| COS7 | african green monkey kidney cell line |
| CRE | Ca ²⁺ /cAMP-responsive element |
| CREB | cyclic-AMP response element binding protein |
| C-terminus | carboxy terminus |
| DAPI | 4'-6-Diamidino-2-phenylindole |
| DIV | day in vitro |
| DMEM | Dulbecco's modified Eagle's medium |
| DMSO | dimethylsulfoxide |
| DNA | deoxyribonucleic acid |
| dNTPs | deoxy-nucleotide-triphosphates |
| DTT | dithiothreitol |
| E | embryonic day |
| <i>E.coli</i> | <i>Escherichia coli</i> |
| EDTA | ethylenediaminetetraacetic acid |
| EGF | epidermal growth factor |
| EGTA | ethylene glycol-bis(beta-aminoethyl-ether)-N,N,N',N'-tetra acetate |
| ER | endoplasmic reticulum |
| ERK1/2 | extracellular signal-regulated protein kinases 1/2 |
| Fig. | figure |
| GluR | glutamate receptor subunit |
| GFP | green fluorescent protein |
| gp | guinea pig |
| GTP | guanosine triphosphate |
| HEPES | 4-(2-hydroxyethyl)-1-piperazineethanesulfonic acid |
| h | hours |
| IFAP | intermediate filament-associated protein |
| IFs | Intermedite filaments |
| IgG | immunoglobulin G |
| IP | immunoprecipitations |
| IP3 | Inositol 1,4,5-triphosphate |

| | |
|----------------|---|
| IR | immunoreactivity |
| kb | kilo bases |
| kDa | kilo Dalton |
| KO | knockout |
| LB | Luria-Bertani |
| LM | light membranes |
| MAP2 | microtubule associated protein |
| MAPK | mitogen-activated protein kinase |
| MBP | maltose binding protein |
| MeOH | methanol |
| MF | microfilament |
| min | minutes |
| mRNA | messenger RNA |
| ms | mouse |
| MT | microtubule |
| n | number of scored cells/samples |
| NCS | neuronal calcium sensor |
| NF | neurofilament |
| NFATc4 | nuclear factor of activated T-cells c4 |
| NF-H | neurofilament heavy chain |
| NF- κ B | nuclear factor-kappa b |
| NF-L | neurofilament light chain |
| NF-M | neurofilament medium chain |
| NFTP | neurofilament triplet protein |
| NLS | nuclear localization signal |
| NMDA | N-methyl D-aspartate |
| N-terminus | amino terminus |
| PBS | phosphate buffered saline |
| pCREB | phosphorylated CREB |
| PCR | polymerase chain reaction |
| pERK | phosphorylated ERK |
| PD | pull-down |
| PFA | paraformaldehyde |
| pH | potentium hydrogenii |
| PKC | protein kinase C |
| ProSAP | Proline rich synapse-associated protein |
| PSD | the postsynaptic density |
| PSD95 | postsynaptic density protein 95 |
| RanGTP | GTP-binding protein Ran |
| rb | rabbit |
| RE | restriction enzyme |
| RNA | ribonucleic acid |
| ROI | region of interest |
| rpm | rounds per minute |
| RT | room temperature |
| SDS | sodium dodecyl sulfate |
| SDS-PAGE | sodium dodecyl sulfate polyacrylamide gel |
| SEM | standard error mean |

| | |
|----------|--|
| TAE | tris acetate-EDTA |
| TBS | tris buffered saline |
| Tris | Tris (hydroxymethyl)-aminoethane |
| Tris-HCl | Tris (hydroxymethyl)-aminoethane hydrochloride |
| U | unit |
| VDCC | voltage-dependent calcium channel |
| WB | western blot |
| wt | wild type |
| Y2H | yeast two-hybrid |
| Δ | deletion |

Curriculum Vitae

Name: Jale Sahin
Date of birth: 30.04.1979
Place of birth: Ankara, Turkey
Nationality: Turkish

Education and experience:

- 2005-2009** Ph.D student in the Project Group 'Neuroplasticity' ((Leibniz-Institute for Neurobiology, Magdeburg, Germany; P.I.: Dr. Michael R. Kreutz).
- 2004-2005** Application specialist in Roche Applied Sciences and Roche Molecular Diagnostics groups, Ankara, Turkey.
- 2002-2004** Master of Science degree in Molecular Biology and Genetics, Bilkent University, GPA: 3,48 /4,0.
Master thesis title: Molecular Characterization of ATPase component of an ABC type transporter in *Moraxella catarrhalis*.
Teaching assistant for Microbiology laboratory course given to third year students at the Department of Molecular Biology and Genetics, Bilkent University, Ankara.
Content developer/instructional designer in Simens e-Learning & RtB Educational Solutions Co., Ankara.
- 2001-2002** Bachelor of Science Minor Degree in Chemistry, Middle East Technical University (METU).
Senior project on optimization of *Acetylxylane esterase* used in pulp Industry from an aqua bacterium isolated from Lake Eymir, Ankara, Department of Biology, METU.
- 1997-2002** Bachelor of Science Major Degree in Biology, Middle East Technical University (METU), GPA: 3,5/4,0.
- 2001** Summer internship in Genetic Engineering and Biotechnology Research Institute, Marmara Research Center, The Scientific and Technical Research Council of Turkey (TUBITAK).

Awards, honours and scholarships:

- 2009** Student of 9th ISN advanced school of neurochemistry held in Gyeongju, S.Korea. "Cellular communication in the nervous system".
- 2005-2008** DFG (Deutsche Forschungsgemeinschaft) scholarship, member of GRK 1167, "Cell-Cell-Communication in Neural and Immune Systems: Topological Organisation of Signal Transduction".
- 2002-2004** Full scholarship for master program in Department of Molecular Biology and Genetics, Bilkent University, Ankara.
- 1999-2002** Undergraduate scholarship from BAYG (Young Scientists Support Group), TUBITAK.
- 2002** BSc. High honour degree, Department of Biology, METU.

Scientific publications

- 1) Bernstein HG, **Sahin J**, Smalla KH, Gundelfinger ED, Bogerts B, Kreutz MR (2007) A reduced number of cortical neurons show increased Calbindin protein levels in chronic schizophrenia. *Schizophr Res*, **84**, 246-256.
- 2) Smalla KH, Mikhaylova M, **Sahin J**, Bernstein HG, Bogerts B, Schmitt A, van der Schors R, Smit AB, Li KW, Gundelfinger ED, Kreutz MR (2008) A comparison of the synaptic proteome in human chronic schizophrenia and rat ketamine psychosis suggest that prohibitin is involved in the synaptic pathology of schizophrenia. *Mol Psychiatry*, **13(9)**, 878-96.
- 3) Smalla KH, **Sahin J**, Putzke J, Tischmeyer W, Gundelfinger ED, Kreutz MR. (2009) Altered postsynaptic-density-levels of Calbindin in the para-chloroamphetamine-induced serotonin syndrome but not in the rat ketamine model of psychosis. *Neurochem Res*, **34**, 1405-1409.
- 4) Kindler S, Dieterich DC, Schutt J, **Sahin J**, Karpova A, Mikhaylova M, Gundelfinger ED, Kreienkamp HJ, Kreutz MR (2009). Dendritic mRNA targeting can replenish the synaptodendritic Jacob after Calpain-mediated proteolysis and NMDA-induced nuclear translocation. *J Biol Chem*, **284(37)**, 25431-40.